DASA – 1355

INVESTIGATION OF LONG WAVES AND THEIR EFFECTS ON THE COASTAL AND HARBOR ENVIRONMENT OF THE LOWER CHESAPEAKE BAY

VOLUME II

CONTRACT NO. DA-49-146-XZ-151

APRIL, 1963

NATIONAL ENGINEERING SCIENCE

PREPARED FOR

HEADQUARTERS, DEFENSE ATOMIC SUPPORT AGENCY

WASHINGTON, D.C.

INVESTIGATION OF LONG WAVES AND THEIR EFFECTS ON THE COASTAL AND HARBOR ENVIRONMENT OF THE LOWER CHESAPEAKE BAY

VOLUME II

Prepared by

NESCO Staff

Research Conducted for:

Headquarters, Defense Atomic Support Agency
Washington 25, D. C.

Contract No. DA-49-146-XZ-151
as a contribution to its Research
and Development Program

NESCO Technical Report No. SN-93
April 1963

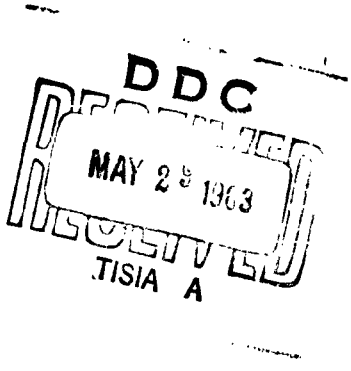

FOREWORD

Volume I of this study on the effect of long waves in the lower Chesapeake Bay dealt particularly with the practical and engineering aspects of this problem and was based in part on new theoretical investigations. These theoretical investigations are presented in this Volume II as various appendices. Most of them are original contributions to the science of hydrodynamics of long waves. They may have other applications than those presented in Volume I of this study.

Volume II is made up of the following studies:

Appendix I: Long Waves Generated by Nuclear Explosions. Types of Waves and Initial Decay in Deep Water. (Dr. Basil Wilson)

Appendix II: Theoretical Considerations and Computations for Water Waves produced by Explosion. (Dr. Larry Armijo and Miss Mary Ann Noser)

Apperdix III: Surface Waves Generated by Disturbance on Sea Bed in Constant Depth Open Sea. (Dr. J. A. Hendrickson)

Appendix IV: The Principle of Superposition and Theory of Cauchy-Poisson.(Dr. B. Le Mehaute)

Appendix V: The Shoaling, Damping, Breaking and Run-up of Long Waves over the Continental Shelf. On Saturated and Nonsaturated Breakers. (Dr. B. Le Mehaute)

Appendix VI: The Wave Run-up by the Method of Characteristics. (Dr. B. Le Mehaute. Dr. J. Freeman was scientific advisor and Mr. R. Grewal did the numerical computations.)

Appendix VII: Two-Dimensional Nonlinear Wave Motion in an Estuary. (Drs. J. C. Freeman and Larry Armijo and Miss Mary Ann Noser)

TABLE OF CONTENTS

VOLUME II

LIST OF FIGURES

LIST OF TABLES

ABSTRACT

This volume assembles a number of theoretical studies relevant to the field of hydrodynamics of long waves. They are:

1. Literature survey on theoretical and experimental information on the problem of cylindrical waves generated by a local disturbance, with application.

2. Application of the theory of Kranzer and Keller on cylindrical waves generated by explosion to three magnitudes of power.

3. Theoretical study of cylindrical waves generated by a cylindrical upthrust on the sea bottom.

4. The principle of superposition is applied to the Cauchy-Poisson solution for determining the cylindrical wave motion due to a finite sea surface disturbance.

5. Wave deformation on a very gentle slope, wave damping by bottom friction. Saturated and nonsaturated breakers. A survey on experimental data on the wave run-up.

6. A method of characteristics is presented for analyzing the wave deformation over a gentle slope, wave breaking, spilling breakers, bore, and run-up on a dry bed.

7. A numerical procedure for calculating the penetration of a bore and nonlinear long wave into estuaries is given and applied in the case of a bore.

INDEX TO APPENDICES

APPENDIX I

LONG WAVES GENERATED BY NUCLEAR EXPLOSIONS

TYPE OF WAVES AND INITIAL DECAY IN DEEP WATER

By

Basil W. Wilson

1. INTRODUCTION

The literature on the effects of surface and sub-surface disturbances of water both theoretical and experimental is quite extensive and this tentative survey of available results makes no claim to being exhaustive. Satisfactory treatment of the initial conditions prevailing in a thermo-nuclear underwater explosion has not yet been achieved, to the writer's knowledge, in any theoretical analysis or laboratory experiment. Both mathematical and experimental models remain relatively crude, though they can nonetheless provide useful guidelines to the natural behavior of the archetype event. The hydrodynamical difficulties of achieving an effective theoretical simulation of the explosion are considerable, though progress in this direction undoubtedly will come. In the end, however, the most reliable information on the effects of nuclear explosions in water will be that secured from actual prototype experiments. In this report an attempt will be made to examine the problem of wave propagation from a nuclear explosion in the deep ocean (water depth circa 16,000 ft.) up to the point that the waves encounter the submerged continental slope of the nearest land mass. In accomplishing this, recourse is made to such theoretical, laboratory and field studies of impulsive water waves as it has been possible to analyze within the time available.

2. THEORIES OF RADIALLY SYMMETRIC DISPERSIVE WAVES

The great pioneering theoretical treatment of disturbances in water resulting from initial elevations or depressions of localized extent came from Cauchy (1815) and Poisson (1816). Their combined achievement, now made classic through the elegant presentation and extension of it by Lamb (1904), examined the effects in water of infinite depth of certain shapes of paraboloidal and ellipsoidal depressions or elevations. Lamb generalized the solution in the two-dimensional case for both initial elevation and initial impulse by making use of the Fourier Integral Theorem and in the three-dimensional case by use of Neumann's (1862) Theorem. As our present interest lies really in the three-dimensional problem, having cylindrical symmetry, we shall give only passing consideration to two-dimensional solutions.

Within the limits of the assumption of a concentrated point impulse or elevation applied to the surface, Lamb derives an exact hydrodynamical solution. The solution of the free surface, in the form of an infinite series (Lamb, 1932, § 255), has, however, rather limited physical significance because the input energy is implanted on an area of infinitely small extent. Kelvin's method of stationary phase (1887), applied by Lamb, nevertheless serves to show that at large distances from the source the wave forms η_e (initial elevation) and η_i (initial impulse) will be given by

$$
\left.
\begin{aligned}
&\text{(i)} \quad \eta_e \simeq \frac{Q_0 k}{\sqrt{2}\cdot\pi\cdot r}\cos kr \\
&\text{(ii)} \quad \eta_e \simeq \frac{-I_0 k \sigma}{\sqrt{2}\cdot\pi\cdot\rho\cdot g\cdot r}\sin kr \\
&\text{(iii)} \quad k = g t^2 / 4 r^2 \\
&\text{(iv)} \quad \sigma = g t / 2 r
\end{aligned}
\right\} \qquad \text{(I-1)}
$$

wherein Q_o and I_o are respectively the concentrated elevation and impulsive pressure at the point source per unit area, r is radial distance from the source, t is variable time and ρ and g have their usual meanings of fluid density and gravitational acceleration.

The period T of these waves, if $t \gg T$, is

$$T = \frac{2\pi}{\sigma} = \frac{4\pi r}{g t} \qquad \text{(I-2)}$$

and their wave length λ, provided $r \gg \lambda$, is

$$\lambda = \frac{2\pi}{k} = \frac{8\pi r^2}{g t^2} \qquad \text{(I-3)}$$

making the wave velocity c,

$$c = \frac{\lambda}{T} = 2\frac{r}{t} = 2V \qquad \text{(I-4)}$$

or twice the group velocity, V.

Since the wave length and period of the waves at considerable distance from the source tend to change very slowly with result that r/t (the group velocity) varies only gradually, Eqs. (I-1) tend to show that wave amplitude will decline approximately as r^{-1}.

Terazawa (1915) applied Lamb's methods to the case of an initial disturbance spread over a finite extent of the free surface in infinitely deep water, and likewise found the amplitude decay to be proportional to r^{-1}. Terazawa also investigated the effect of an impulsive explosion at a finite depth h below the surface and found the initial amplitude of the wave disturbance at surface zero to be proportional to $h^{-3/2}$. The same result is deduced by Lamb (1922) for a rather different model of explosion in which an abrupt pressure rise is followed immediately by a gradual fall. If the initial pressure rise is more gradual the amplitude of surface elevation tends to vary as h^{-2}.

The high frequency of occurrence of tsunami-generating earthquakes off the Japanese islands has led Japanese scientists to pay considerable attention to the problems of waves generated by impulsive movements of the sea bed and ocean surface. Prominent among authors who have contributed to analyses of these problems have been Sano and Hasegawa, Syono, Homma, Nakamura, Sezawa and Kanai, Takahasi, Ichiye, Matzawa, Miyoshi and Unoki and Nakano.

We shall commence by considering briefly the remarkable series of papers of Unoki and Nakano (1953, (i), (ii), (iii)), which extend the work of Lamb and Terazawa for a surface disturbance or impulse of finite amount spread over a finite area in deep water and

compare the results with observed waves from a volcanic explosion. For the case where the initial elevation is a uniform piston-like rise Q of the surface over a circle of radius R at the origin, the wave disturbance is described by

$$\eta_e \simeq \frac{\sqrt{2}\,QR}{r} e^{-\mu t} J_1(kR) \cos(kr) \qquad \text{(I-5)}$$

provided $r \gg R$, this being the asymptotic solution of the problem using Kelvin's powerful method of stationary phase. In Eq. (I-5) μ is a coefficient of "virtual viscosity" or friction coefficient in the exponential time decay arising from the assumption that friction from eddy viscosity is proportional to fluid velocity; J_1 is a Bessel function of the first order which modulates the last cosine term.

The equivalent result for a piston-like impulse of uniform amount I imposed on the surface over a circle of radius R at the origin is

$$\eta_i \simeq -\frac{\sqrt{2}\,I\sigma R}{\rho g r} e^{-\mu t} J_1(kR) \sin(kr) \qquad \text{(I-6)}$$

again under the condition $r \gg R$.

In both Eqs. (I-5) and (I-6), since the group velocity $V\ (=r/t)$ changes only slowly for large values of r, wave amplitude decay, discounting the exponential decay with time, is proportional to r^{-1}. The system of waves that arise in these two instances have beats whose modes are determined by zero values of the Bessel functions $J_1(kR)$.

Unoki and Nakano successfully applied these results to the case of the Myojinsho reef submarine volcanic explosions and concluded that the wave system described by Eq. (I-6) best fitted the observational data. The volcanic explosions (which have been described as not dissimilar to small nuclear explosions) thus accorded reasonably well with the mathematical model of a uniform cylindrical surface impulse. The authors estimated the energy of the explosions as being from 3 to 8 x 10^{19} ergs (about the equal of a 1 kiloton nuclear blast), and concluded that most of the energy went into wave formation. From a comparison of observations with theory, they concluded that R had the value 2.2 km.

In some cases the volcanic explosions gave rise to wave trains which showed no beat effects. Unoki and Nakano explain this on the basis that the initiating impulse was sometimes probably of Gaussian form. Thus by assuming the instantaneous impulse to have the form

$$I(r) = I_0 e^{-\frac{r^2}{4R^2}} \qquad \text{(I-7)}$$

These authors show that the resulting asymptotic approximation to the wave form, η_i , for $r \gg R$ is

$$\eta_i \simeq -\frac{2\sqrt{2}\, I_0 k \sigma R^2}{\rho g r} e^{-\mu t} e^{-(kR)^2} \sin(kr) \qquad \text{(I-8)}$$

In this case there is an absence of beating and wave amplitude merely decays monotonicly.

We may note that Unoki and Nakano also elaborated the two-dimensional case of wave disturbances originating from finite source disturbances and showed that wave amplitude decay in deep water in these circumstances, remote from the source, is proportional to $x^{-1/2}$, where x in this case defines the horizontal distance. Both Jeffreys and Jeffreys (1956 Edn., p. 517) and Eckart (1948, p. 409), however, independently show that for this two-dimensional case the wave amplitude near the front of the train, where group velocity approaches the value $\sqrt{gd}$, d being the water depth, declines as $r^{-1/3}$, so that the front of the wave train becomes increasingly more prominent with lapse of time and distance in the dispersion of the system. Eckart's solution shows that this wave front is an amplitude modulation of a sinusoidal carrier system of waves whose wave length is infinite (at least for the usual assumed incompressible water medium). Effective wave length near the front of the train is thus dictated by the modes of the modulating Airy integral, while towards the rear the sinusoidal carrier waves increasingly assume dominance in defining the wave length.

Reverting again to the three-dimensional problem, we find that Kranzer and Keller (1959), again confining attention to initial surface elevation or impulse, but introducing the influences of water depth, d, and finite areal disturbance, derive for the case of initial elevation

$$\eta_e \simeq \frac{\overline{Q}(k)}{rd} \psi_e (kd) \cos (kr - \sigma t) \qquad \text{(I-9)}$$

where $\bar{Q}(k)$ is the Hankel transform of the function $Q(r)$ describing the initial elevation as a function of r and $\psi_e(kd)$ is a continuous function of kd which varies in value from about 1 when kd is less than $\pi/10$ (shallow water) to an asymptotic value ($\sqrt{2kd}$) when $kd > \pi$ (deep water).

For the comparable case of initial impulse Kranzer and Keller's result is

$$\eta_i \simeq \frac{k\bar{I}(k)}{\rho r\sqrt{gd}}\ \psi_i(kd)\sin(kr-\sigma t) \qquad \text{(I-10)}$$

in which $\bar{I}(k)$ is the Hankel transform of the function $I(r)$ describing the initial impulse as a function of r and $\psi_i(kd)$ is a continuous function of kd which approaches the value unity for $kd < \pi/10$ (shallow water) and becomes asymptotic to the value $\sqrt{2kd}$ when $kd > \pi$ (deep water).

Kranzer and Keller's derivations are the asymptotic solutions of the surface disturbance problems, applicable only for large values of kr which justify the use of Kelvin's method of stationary phase. They follow the transform techniques applied first, apparently, by Sneddon (1951), and elaborated by Stoker (1957). The Hankel transforms $\bar{Q}(k)$ and $\bar{I}(k)$ are defined as

$$\left.\begin{aligned} &\text{(i)} \quad \bar{Q}(k) = \int_0^\infty Q(r)\, r\, J_0(kr)\, dr \\ &\text{(ii)} \quad \bar{I}(k) = \int_0^\infty I(r)\, r\, J_0(kr)\, dr \end{aligned}\right\} \qquad \text{(I-11)}$$

in which J_o is a Bessel function of zero order.

In Eqs. (I-9) and (I-10) a distinction has now to be recognized in the values of k and σ over those given by Eqs. (I-1 iii) and (I-1 iv). Here k is defined by the root of an equation:

$$\phi(kd) = r/(t\sqrt{gd}) \tag{I-12}$$

while σ is given by

$$\sigma^2 = gk \tanh(kd) \tag{I-13}$$

The function ϕ (kd) varies between asymptotic values of 1 for $kd < \pi/10$ (shallow water) and $1/(2\sqrt{kd})$ for $kd > \pi$ (deep water). Thus for the deep water case with $\phi(kd) = 1/(2\sqrt{kd})$, k and σ assume the values specified in Eq. (I-1).

If in (I-9) we introduce the deep water value $\psi_e \simeq \sqrt{2kd}$, and take $Q(r) = Q$ for $0 < r < R$ with $Q(r) = 0$ for $r \geq R$, then we obtain exactly the same amplitude result as Unoki and Nakano in Eq. (I-5), from the special property (in this case) that

$$\int_o^\infty Q(r)\, kr\, J_o(kr)\, dr \equiv QRJ_1(kR), \tag{I-14}$$

the only difference residing in the absence of the friction term $e^{-\mu t}$. In like manner the amplitude terms of Eq. (I-10) reduce identically to those of Eq. (I-6) when the deep water value $\psi_i = \sqrt{2kd}$ is taken along with the special case $I(r) = I$ for $0 < r < R$ and $I(r) = 0$ for $r \geq R$.

Again for the special case treated by Unoki and Nakano in Eq. (I-7) we find that Kranzer and Keller's generalized solution applied to

deep water ($\psi_i = \sqrt{2\,kd}$) gives identically the same amplitude result as Eq. (I-8) ($e^{-\mu t}$ excepted) in virtue of the fact that the Hankel transform of (I-7) is

$$\bar{I}(k) = 2\, I_0 R^2\, e^{-(kR)^2} \tag{I-15}$$

If now we apply Eqs. (I-9) and (I-10) to shallow water, for which $kd < \pi/10$ and $\psi_e \simeq 1 \simeq \psi_i$, the wave disturbances at a long distance from the source for the cases of piston-like surface elevation Q and impulse I applied at the origin over a radius R, become, respectively:

$$\left.\begin{aligned} &\text{(i)} \qquad \eta_e \simeq Q \cdot \frac{R}{r} \cdot \frac{J_1(kR)}{kd} \cos(kr - \sigma t) \\ &\text{(ii)} \qquad \eta_i \simeq \frac{I}{\rho} \cdot \frac{R}{r} \cdot \frac{J_1(kR)}{\sqrt{gd}} \sin(kr - \sigma t) \end{aligned}\right\} \tag{I-16}$$

Dependence of η_e upon depth is thus as d^{-1} and η_i as $d^{-1/2}$; dependence on distance in both cases is as r^{-1}.

All this discussion of the three-dimensional form of the Cauchy-Poisson-Lamb problem suggests that wave amplitude decay at distances remote from the source is proportional to r^{-1}. We might infer, however, from analogy to the two-dimensional problem of Jeffreys and Eckart, that wave amplitude near the head of the wave train will follow another law. As pointed out by Munk (1952) this in fact conforms to $r^{-5/6}$. The reason for this is given by Takahasi (1961)

who points out that the method of stationary phase is no longer valid in the neighborhood of the wave front. For there the third term in the Taylor expansion of $(kr - \sigma t)$ (cf. Lamb, § 241) is indeterminate because $d^2\sigma/dk^2$ is zero, in virtue of the fact that $d\sigma/dk (= r/t = \sqrt{gd})$ is a constant. Takahasi shows that wave height at the front is proportional to $r^{-5/6}$ for the case of waves resulting from a piston-like upthrust of the sea-bed over a radius R. Since the behavior of dispersive waves at a large distance from the source is practically independent of the nature of the source disturbance, the $r^{-5/6}$ law may be considered to prevail in general at the front of the wave train and the r^{-1} law in the main body of the waves. Takahasi (1961) has demonstrated experimentally that the $r^{-5/6}$ amplitude decay law does in fact prevail at the leading crest and trough of wave trains generated by the sudden upthrust of a circular portion of sea-bed in shallow water.

In all the theoretical results presented above, the nature of the wave disturbance near the source is undefined because of the mathematical difficulties of describing the fluid motions near the moving boundaries. Theoretically complete solutions have, however, been obtained by Lamb (1932, § 238, 239) in series form for the rather hypothetical cases of concentrated elevation and impulsive pressure within the limits of linear theory. Recently, the near-source disturbances generated by various forms of sea-bed movement which could simulate earthquake displacements, have been examined in a number of mathematical treatments by Takahasi, Ichiye, Honda,

Nakamura, Keller and others. Many of these are two-dimensional in scope and are therefore not of direct interest or application to this study. In other respects, however, it is doubtful whether any of their models can be considered to simulate an underwater nuclear explosion to a degree which could justify reliance on the mathematical prediction of the wave forms generated near the source. More satisfactory mathematical models of underwater explosions have been developed by Penny (1950), Kirkwood and Seeger (1950) and Fuchs (1952), but in one way or another these are rather poor approximations to the nuclear underwater burst near its source, some of the features of which have been illustrated by Snay (1957) and discussed by Cole (1948) and by Lane and Green (1956).

We note in passing that the theoretical result obtained by Hendrickson (see Appendix III) for a piston-like upthrust of the bottom gives a wave-amplitude decay law proportional to r^{-1}. The result is quite similar to that of Takahasi (1961) for large values of kr in which the method of stationary phase is applicable for deriving an asymptotic solution.

In regard to the input data supplied to this project from the analysis of Kaplan, Wallace and Goodale (1962) (Fig. 1), a question really needing investigation is whether the application of the asymptotic solution of Kranzer and Keller (1959), as given in Eq. (I-9), is valid at the relatively small values of kr pertaining when r is only 20 miles from surface zero, and whether full reliance can therefore be placed on the results of such an application.

3. EXPERIMENTS ON DISPERSIVE WAVE BEHAVIOR

In Fig. I-1 are assembled such results of observations on explosion waves as are readily available in "Effects of Nuclear Weapons" (Glasstone, 1957, 1962) from the underwater nuclear explosion tests in the Pacific.

Shot BAKER of a 20 Kiloton nuclear charge at Bikini in 1946, in a water depth approximating 200 feet, set up trains of waves whose maximum height, H, at various distances shows a decay proportional to r^{-1} to a distance of about 1 mile from surface zero (Fig.I-1) and a decay thereafter proportional to $r^{-5/6}$.

In Fig. I-1 we also plot the standard results for a 1 kiloton nuclear underwater burst as presented in "Effects of Nuclear Weapons." The earlier version of this publication (Glasstone, 1957) suggests a decay law of wave height proportional to r^{-1} in a water depth of 85 ft. The 1962 version on the other hand gives the decay law as $r^{-5/6}$ over a range of distance r from 1 to 100 miles. For explosions in deep water (> 400 ft.) the decay law conforms to r^{-1}.

An attempt has been made in Fig. I-2 to represent the Bikini field data in a dimensionless plot for comparision with certain laboratory experiments of Johnson and Bermel (1949). Crest elevation, above still water, of the maximum waves, as a ratio of the diameter D_c of the crater or cylinder of the burst at the surface, has been plotted against dimensionless distance r/d, in which d is the water depth. In Fig. I-2 the first part of the BAKER test results (for $r/d < 35$), no longer subscribes to

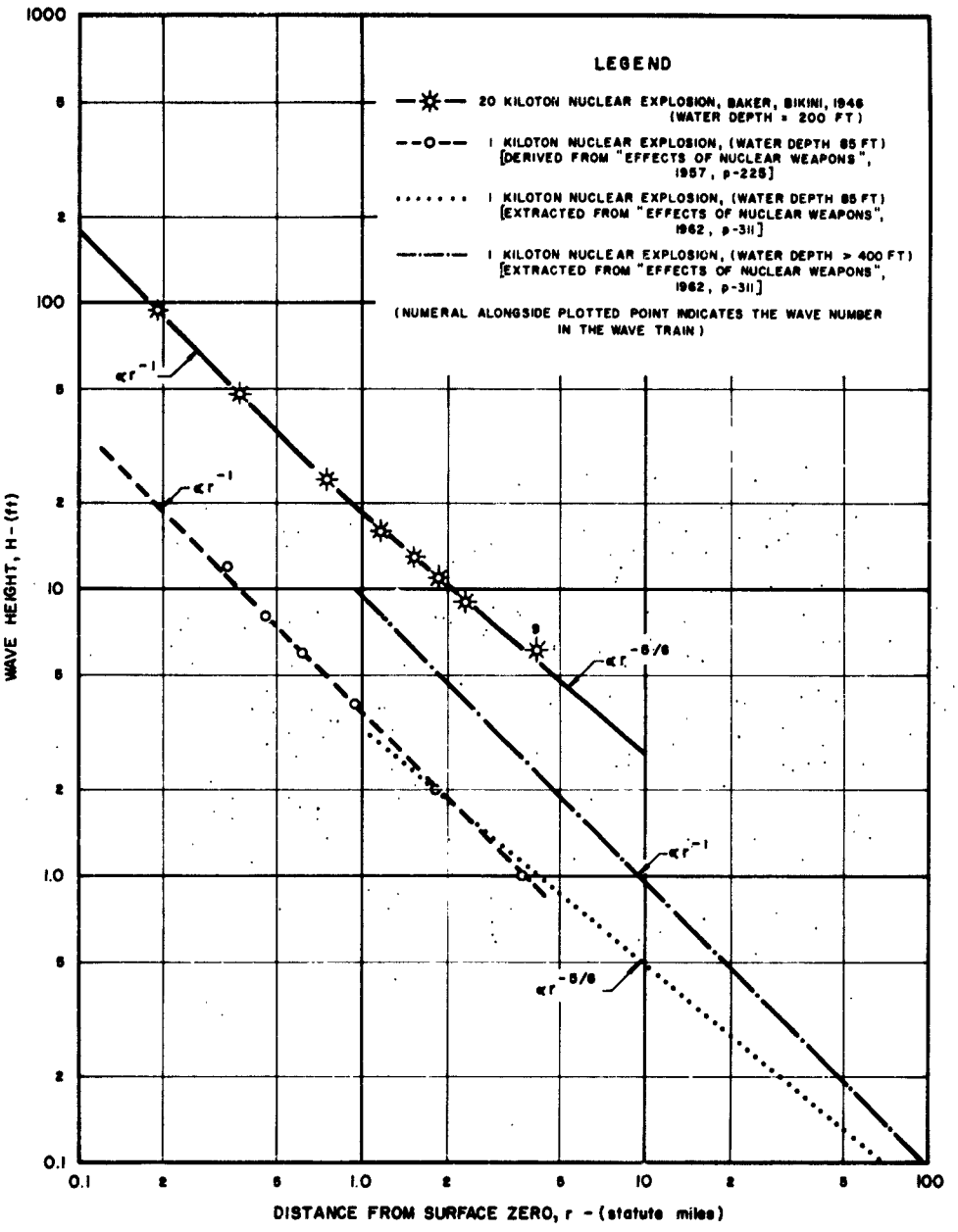

FIGURE I-1

MAXIMUM WAVE HEIGHT DECAY WITH DISTANCE; UNDERWATER NUCLEAR EXPLOSIONS

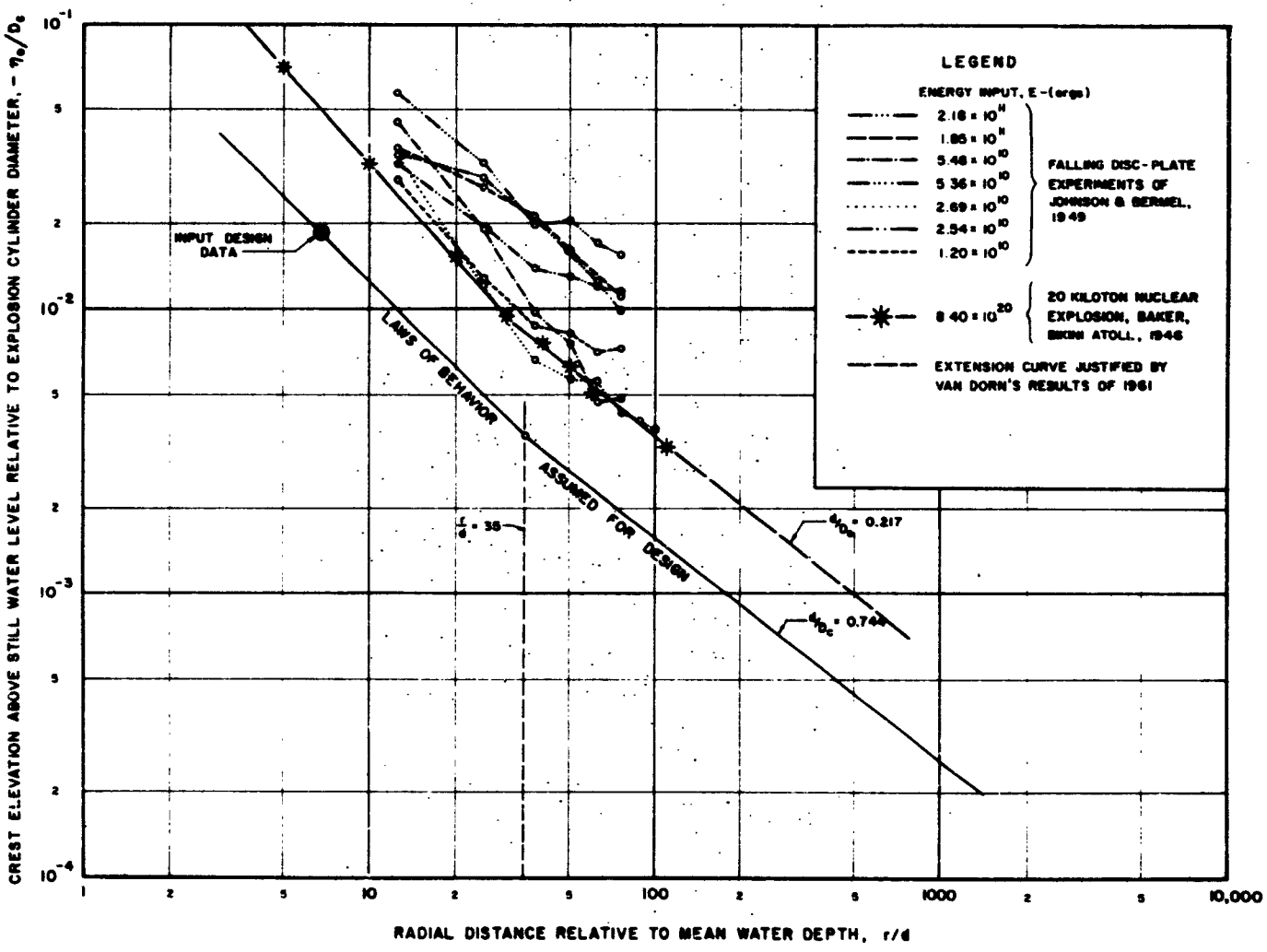

FIGURE I-2

MAXIMUM CREST ELEVATION OF DISPERSIVE IMPULSIVELY GENERATED WAVES AS A FUNCTION OF RADIAL DISTANCE FROM THE ORIGIN

$$\eta_0 / D_c \propto (r/d)^{-1}$$

because η_0 in the initial stages of the wave propagation in shallow water was in general greater than half the wave height H. It was necessary to infer the appropriate value of η_0 from Fig. I-3 which was originally compiled by Reid and Bretschneider (1953) and subsequently modified slightly by Rechtin, Steele and Scales (1957), by Bretschneider (1958) and currently by the present writer. For this application it was necessary to know the wave period T, which was calculated from Eq. (I-13) in terms of the known distance r and elapsed time t. We may point out here that Unoki and Nakano (1953, i, ii, iii) had demonstrated the accuracy of this formula (Eq. (I-2), for deep water) in their analysis of the volcanic explosions of the Myojinsho reef.

The slope of the latter part of the curve representing the BAKER test in Fig. I-2 accords with the decay law $r^{-5/6}$ because the waves for $r/d > 35$ are largely oscillatory with $\eta_0/H \simeq 0.5$. The field experiments of Van Dorn (1961), related to nuclear underwater explosions in the Pacific in 1956, show that relative wave amplitude declines as $(r/d)^{-5/6}$ over a range of values of the latter parameter from 100 to 1000. Although the standard of reference of relative amplitude is not given by Van Dorn, it seems reasonable to infer from his results that the BAKER test results of Fig. I-2 which extend to about $r/d = 100$ could be projected at the same slope ($\propto r^{-5/6}$) as far as $r/d = 1000$. The validity of this step, however,

may be open to question, on grounds that different values of d/D_c (alternatively d/λ) are involved.

The experiments of Johnson and Bermel (1949) measured the characteristics of waves generated impulsively by horizontal circular discs falling vertically from different heights into still water. The data of their Fig. I-3 has been recalculated and adapted to the requirements of our Fig. I-2. Although individual test results show considerable variability there is a remarkable overall parallelism with the Bikini data even to the extent of an indicated slope change at $r/d \simeq 35$. For values of $r/d < 35$ particular test results show higher than average and some lower than average rates. The fact that initial decay rates greater than r^{-1} were found in particular instances lends emphasis to the need for knowing more about the special conditions that may lead to energy dissipation which could detract from the energy available for wave formation.

Generally speaking, the experimental results on wave amplitude decay satisfactorily confirm the theoretical predictions of Section 2. The experiments tend to show that in a dispersive system of linear waves, with beat characteristics, the decay law r^{-1} prevails until the distance becomes sufficiently great to give greater prominence to the front of the wave train and render invalid the theoretical approximation of stationary phase, thus causing the decay law to change to one proportional to $r^{-5/6}$. The transition is probably gradual even though the experiments suggest quite a sharp change at $r/d \simeq 35$.

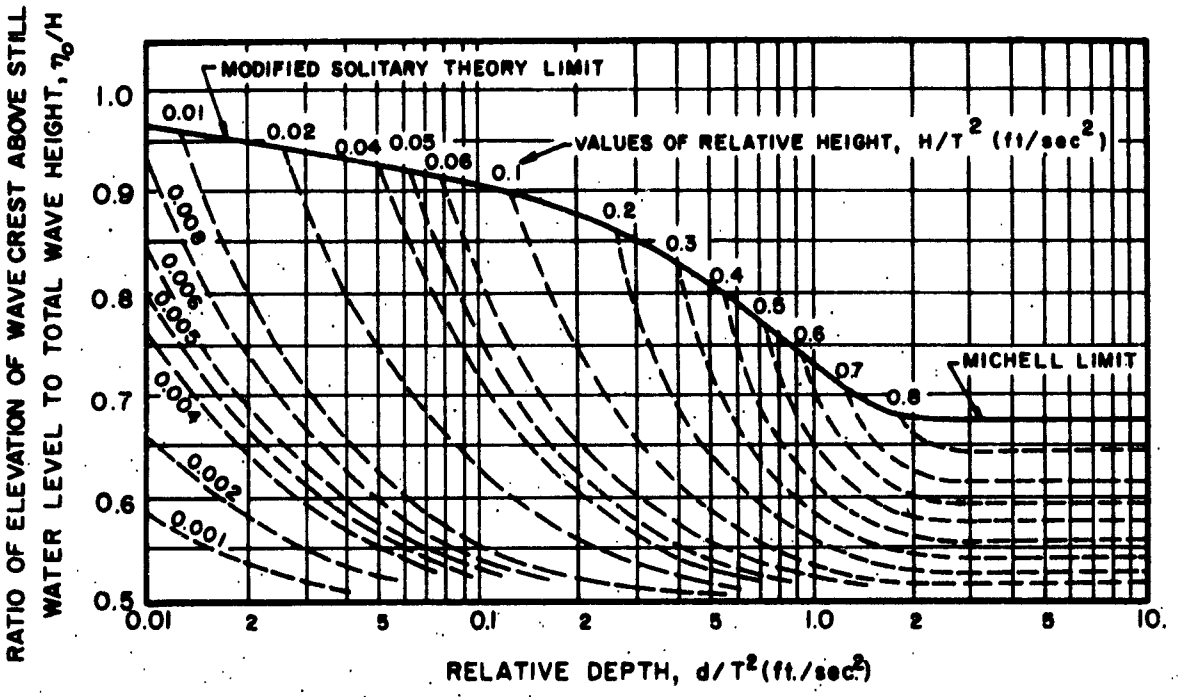

FIGURE I-3

RATIO OF ELEVATION OF WAVE CREST ABOVE STILL WATER LEVEL TO TOTAL WAVE HEIGHT, η_o/H, AS A FUNCTION OF RELATIVE DEPTH d/T^2, AND RELATIVE HEIGHT H/T^2

4. TYPES OF WAVES IN INPULSIVELY GENERATED SYSTEMS

The data of Figs. I-1 and I-2 all pertain to long waves in shallow water. In Eqs. (I-9) and (I-10) we have already noted that the Fourier transforms $\overline{Q}$ and $\overline{\Gamma}$ and the functions ψ_e and ψ_i are dependent on kd, or alternatively, d/λ, the relative depth referred to wave length. In consequence, the type of wave that will result from any given initiating disturbance will be a function of the relative depth d/λ. Eqs. (I-9) and (I-10) show however that the carrier waves at a great distance from the source (large kr) are simply sinusoidal. This obviously is not necessarily true in general of the waves near the source. To investigate this aspect we have recourse to Fig. I-4 (adapted from Wilson (1962)). This portrays the area of existence of waves of different types in a plot of H/λ_o versus d/λ_o, in which λ_o is the equivalent deep-water wave length of any given wave type. Waves are theoretically unable to exist outside of the shaded areas, which are bounded by the breaking wave criteria of McCowan (long waves) and Michell (short waves), and an intermediate limit largely defined by experiment and interpolation. Short waves are normally defined as those for which the relative depth d/λ $(=d/\lambda_o) > 0.5$. Long waves are usually interpreted as those for which $d/\lambda < 0.05$ $(d/\lambda_o < 0.015)$.

In Fig. I-4 a set of isolines of the dimensionless parameter $(\eta_o \lambda^2/d^3)$, in which η_o is wave crest elevation above still water level, is shown crossing the diagram in diagonal fashion. The significance of this parameter has been stressed by Ursell (1953) who

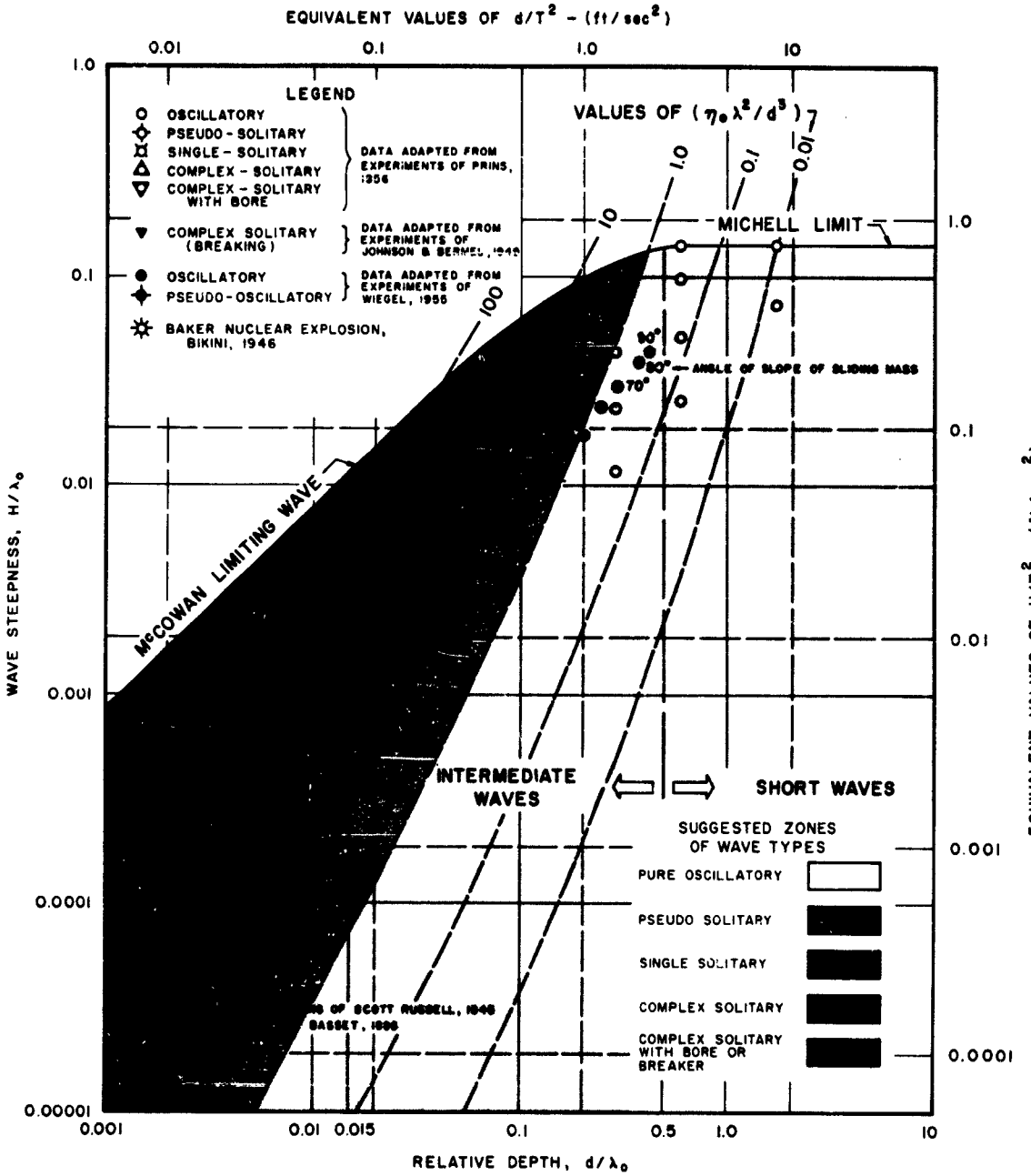

FIGURE I-4

CHARACTERISTICS OF IMPULSIVELY GENERATED WAVES AS DETERMINED EXPERIMENTALLY, IN RELATION TO THEIR THEORETICAL PREDICTION

points out that linear wave theory, such as that of Airy, is normally applicable only if $(\eta_o \lambda^2/d^3) << 1$ and H/λ_o is also small.

Ursell's analysis showed that long waves are inevitably non-permanent when $(\eta_o \lambda^2/d^3) >> 1$. The crests of such waves advance more rapidly than the troughs and finally reach a condition of instability which manifests itself in breaking or bore-formation. Ursell was disposed to consider that the solitary wave of permanent type could exist at or near $(\eta_o \lambda^2/d^3) = 1$. The present writer, however, has compiled evidence (Wilson, 1962) to show that the most favored range for the existence of solitary waves is in the belt shown hatched, or more broadly, between isolines of $(\eta_o \lambda^2/d^3)$ from 10 to 35. In the zone of $(\eta_o \lambda^2/d^3)$ from 1 to 10 cnoidal waves of permanent type are possible, which overlap permanent waves derived from Stokes theory of second or higher orders. Beyond $(\eta_o \lambda^2/d^3) > 35$, waves are likely to be non-permanent.

Since dispersive waves are composite of the interference effect of a broad spectrum of frequency components, the relevance of Fig. I-4 may at first seem questionable, as Fig. I-4 really has application to uniform wave trains. However, the theory of Cauchy-Poisson-Lamb, as elaborated by Unoki and Nakano and by Kranzer and Keller, clearly shows that the resultant type of wave in a dispersive wave train has all the characteristics of an equivalent wave in a non-dispersive system at any particular moment of its existence, before influences of distances and time bring about change. Consequently it is of importance to recognize the type of wave likely to exist in a dispersive system, particularly in regions close to the source

where available theories are difficult to evaluate.

Here we resort to a consideration of the experiments of Prins (1956, 1958) who generated waves in a laboratory flume from suddenly released initial elevations or depressions of finite extent in water of constant depth. The initial waves, near the source, generated under different conditions of water depth d, height of elevation and length of initial elevation, have been plotted in Fig. I-4, each plotted point referring to a different test. Prins gave valuable information on the type of wave initiated, shown in the legend of Fig. I-4. It is therefore of considerable interest to find that his types lie within specific belts of the parameter $(\eta_o \lambda^2/d^3)$ and that the occurrence of single solitary waves (followed usually by a trailing train of small oscillatory waves) agrees remarkably well with the zone of existence for solitary waves that we have already specified. For $(\eta_o \lambda^2/d^3) > 40$ Prins found waves of "complex-solitary" type, and under conditions which brought the leading wave characteristics close to the McCowan limiting criteria, the wave was inevitably a type of bore.

Also shown plotted in Fig. I-4 are some experimental results of Wiegel (1955), who generated waves under laboratory conditions by causing submerged block masses to slide down slopes of varying steepness, thereby simulating submarine landsliding in earthquakes. Most of these waves were of oscillatory character and plot in a region of Fig. I-4 which would identify them as Stokes waves.

The experimental results of Johnson and Bermel (1949) have

also been plotted in Fig. I-4 on the assumption that the effective initial wavelength λ of the primary wave near the source was four times the radius of the circular plate dropped on the water surface. The data are found to fall in a zone which would classify the waves as breaking complex solitary or single solitary waves.

Finally, the initial waves of the nuclear underwater explosion test BAKER has been located in Fig. I-4 by determining the applicable values of H/T^2 and d/T^2 and this plotted point is found to lie in the unstable (breaking) complex-solitary or single-solitary zone for which $(\eta_o \lambda^2/d^3)$ is from about 30 to 40. The BAKER test result accords remarkably well with Johnson and Bermel's laboratory data which were scaled to produce results approximately equivalent to the field explosion of 1946. That the initial waves from the BAKER test were actually of solitary type is confirmed by the following quotation from Glasstone (1962):

> "Observations of the properties of the waves indicated that the first wave behaved differently from succeeding ones in that it was apparently a long solitary wave generated directly by the explosion, receiving its initial energy from the high velocity outward motion of the water accompanying the expansion of the gas bubble."

Assuming that the primary wave form near the explosion source in a nuclear underwater burst is solitary or complex-solitary, as suggested by Fig. I-4, the extent to which the wave form will change will obviously be dictated by the prevailing value of $(\eta_o \lambda^2/d^3)$ in

which each of the variables of this parameter is a function of r, the radial distance of progression. If the depth is constant the parameter will depend only on the product $\eta_o(r) \left[\lambda(r)\right]^2$. Since $\eta_o(r)$ is a decaying function, and $\lambda(r)$ an increasing function, of the distance r, the value of the product will be dictated by whichever of these variables prevails. If the product should remain constant, Fig. I-4 shows that wave form will remain unchanged. Thus the wave could propagate as a distended and flattened solitary wave. If the product declined in value, the wave form would become cnoidal and eventually oscillatory. On the other hand, if it increased in value, the wave form would become complex and unstable, finally leading to bore formation. Since depth is seldom constant in wave propagation, this variable (d) obviously will have a powerful influence on the value of the parameter $(\eta_o \lambda^2/d^3)$ and hence on the ultimate wave form. As the depth decreases towards the coast the parameter must inevitably increase and cause the wave form to assume the unstable shape that finally leads to bore or breaker.

The nature of the decay of η_o with distance r has already received considerable attention in Sections 2 and 3 of this appendix. There remains to consider how the wave length λ and period T of the waves are modified by the dispersion.

Before leaving this section it may be noted that the input data originally supplied to this project gave the maximum wave height at r = 20 miles as $\eta_o = H/2 = 388$ ft. (calculated from Kranzer-Keller theory for d = 18,000 ft.), with a corresponding period T = 1.2

minutes. This gives us $H/T^2 = 0.15$ and $d/T^2 = 3.47$ (ft./sec.^{2} units). When this point is located in Fig. I-4 (not actually shown) it falls in a region which would not seem to justify the use of linear theory (the premise upon which Kranzer-Keller, Unoki-Nakano, and Cauchy-Poisson-Lamb theories are all founded). About the highest value that H/T^2 could have, in order not to violate the necessary conditions of linear theory, would be 0.042 (cf. Wilson, 1962, Fig. 28). This is an additional reason, perhaps, beyond that expressed earlier, for questioning the use of Kranzer-Keller theory in derivation of the input data.

5. INCREASE OF WAVE PERIOD WITH DISPERSION

From Eq. (I-9) it is clear that a wave crest will be encountered whenever $\cos(kr - \sigma t) = 1$. This will happen whenever

$$\text{(i)} \qquad kr - \sigma t = \pm 2\pi m$$

$$\text{(ii)} \qquad m = 0, 1, 2, 3, \ldots \qquad \text{(I-17)}$$

Eq. (I-17 i) may be written in the form

$$kr\left(1 - \frac{\sigma}{k}\cdot\frac{t}{r}\right) = \pm 2\pi m \qquad \text{(I-18}$$

and since by definition

$$\text{(i)} \qquad c = \lambda/T = \sigma/k$$

$$\text{(ii)} \qquad V = \frac{d\sigma}{dk} = r/t, \qquad \text{(I-19)}$$

V being the group velocity, or rate of progression of the wave groups, Eq. (I-18) is adaptable to the form

$$kd\left(1-\frac{c}{V}\right)=\pm\frac{2\pi m}{(r/d)} \qquad \text{(I-20)}$$

We have already noted that waves generated from an initial disturbance, although composite of a spectrum of frequencies, tend through interference effects to assume momentarily the form of waves of non-dispersive type, subject to the same conditions under which the latter can exist. Thus, as the linear theory of Kranzer-Keller predicts

$$\text{(i)} \qquad c=\sqrt{gd}\left[\frac{\tanh kd}{kd}\right]^{\frac{1}{2}} \qquad \text{(I-21)}$$

$$\text{(ii)} \qquad V=\frac{c}{2}\left[1+\frac{2kd}{\sinh 2kd}\right]$$

Since V in general is less than c, we must take the negative sign with the right hand side of (I-20). Eq. (I-20) thus transforms to

$$kd\left[\frac{\sinh 2kd-2kd}{\sinh 2kd+2kd}\right]=\frac{2\pi m}{(r/d)} \qquad \text{(I-22)}$$

Van Dorn (1961) has evaluated the function of (kd) forming the left hand side of Eq. I-22). It is sufficient to note here the two extremes of its values.

First, for deep water conditions ($kd > \pi$), (I-22) becomes

$$kd \simeq \frac{2\pi m}{(r/d)} \tag{I-23}$$

and since for the same conditions $c^2 = g/k$ or $\sigma = \sqrt{gk}$ from Eq. (I-13), elimination of k in (I-22) in favor of σ ($= 2\pi/T$) yields

$$T\sqrt{\frac{g}{d}} = \sqrt{\frac{2\pi}{m}}\,(\frac{r}{d})^{\frac{1}{2}} \tag{I-24}$$

Eq. (I-24) shows that the period of those waves for which $d/\lambda > \frac{1}{2}$, which would inevitably include most of the trailing waves in the dispersive system and possibly the bulk of the waves if the depth is great and the explosion small, will increase as the square root of the distance $(r^{1/2})$.

For the opposite extreme the function (kd) of Eq. (I-22) assumes the asymptotic value of $[\,(kd)^3/3]\,/[\,1 + (kd)^2/3]$ when $kd < \pi/10$, applicable to shallow water conditions. In this case then Eq. (I-22) reduces to

$$\frac{(kd)^3}{3} \simeq \frac{2\pi m}{(r/d)} \tag{I-25}$$

For this condition Eq. (I-13) yields $\sigma^2 = gdk^2$ so that (I-25) reduces to the form

$$T\sqrt{\frac{g}{d}} \simeq (\frac{4\pi^2}{3m})^{\frac{1}{3}}\,(\frac{r}{d})^{\frac{1}{3}} \tag{I-26}$$

and the inference is that wave period increases as the cube root of the distance ($r^{1/3}$) when depth conditions are such that $d/\lambda < 1/20$. This result agrees with Van Dorn (1961) and accords with the two-dimensional theory of Eckart (1948, p. 409).

In Eqs. (I-24) and (I-26) an anomaly arises for $m = 0$ at the front of the wave train for which the wave period and wave length are theoretically infinite, for here from Eq. (I-17 i), $(kr - \sigma t) = 0$ or

$$\text{(i)} \qquad c = \sigma/k = r/t = \frac{d\sigma}{dk} = V$$

$$\text{(ii)} \qquad c = \sqrt{gd} \qquad \text{(I-27)}$$

The anomaly is implicit in the Kranzer-Keller theory since Eq. (I-27) is in agreement with (I-12), provided $\phi(kd) = 1$ with $kd = 0$. It brings to focus the statement made earlier in reference to Eckart's (1948) solution of a two-dimensional dispersive wave system, that the modulating factor apparently becomes the criterion determining the wave length. It is of interest to quote Eckart in this regard:

> "The situation near this front is very peculiar. It may be described as a carrier wave which is amplitude modulated. However, contrary to the customary case, the carrier has a longer (infinitely longer!) wave length than the modulation. Consequently, the empirically determined "wave length" bears no relation whatever to the spectrum of the disturbance. Such wave fronts are of considerable importance as they constitute the seismic sea waves, commonly called 'tidal waves'."

To resolve this problem we shall attempt an approximate analysis based on Eq. (I-16i), which gives the wave form for shallow water conditions (applicable to the wave front) for a piston-like surface elevation Q applied over a radius R at the origin. If, in conformity with Eckart, the modulator, $J_1(kR)/kd$ in this case, becomes conditional in prescribing the effective wave length and period at the front of the dispersive system, then it can be seen that for small values of kR the above term approximates to

$$\frac{J_1(kR)}{kd} \simeq \frac{R}{2d}\left[1 - \frac{(kR)^2}{8} + \frac{(kR)^4}{192}\right] = \Psi \qquad (I\text{-}28)$$

so that, approximately

$$kR \simeq 4\left[\frac{1}{2} - \frac{d}{R}\Psi\right]^{1/2} \qquad (I\text{-}29)$$

if Ψ represents the function $J_1(kR)/kd$.

Crests of the carrier waves near the front, however, occur whenever $\cos(kr - \sigma t) = 1$, so that the same condition (I-25) prevails as before, giving

$$kd = \left[\frac{2\pi m}{3(r/d)}\right]^{1/3} \qquad (I\text{-}30)$$

On multiplying Eqs. (I-29) and (I-30) and noting that $k^2 = \sigma^2/gd$

for small values of kd, as pertain to the wave front, we find

$$T_i \sqrt{\frac{g}{d}} \simeq \left(\frac{3\pi^5}{2m}\right)^{1/6} \left(\frac{R}{d}\right)^{3/4} \left[\frac{R}{2d} - \Psi\right]^{1/4} \left(\frac{r}{d}\right)^{1/6} \tag{I-31}$$

The series approximation, Eq. (I-28), is valid so long as kR is less than about 2.0 and since the Bessel function $J_1(kR)$ reaches its first maximum value at kR = 1.84, it may be concluded that Eq. (I-31) is pertinent for values of m (= 1, 2, 3....) up to the maximum waves in the first group so long as kd < 1/20. For kR = 2.0, Eq. (I-29) gives

$$\Psi = \frac{R}{4d} \tag{I-32}$$

resulting in a simplification of Eq. (I-31) to

$$T_i \sqrt{\frac{g}{d}} \simeq \left(\frac{12\pi^5}{m}\right)^{1/6} \left(\frac{R}{d}\right)^{1/2} \left(\frac{r}{d}\right)^{1/6} \tag{I-33}$$

If the p-th wave is the highest in the first beat then its period will be given approximately by Eq. (I-32) for m = p.

The general picture we gain of increase of wave period with distance on dispersion from the source is now as follows: first, the size of the initial waves set up by an underwater explosion or other disturbance is a function of the magnitude of the disturbance, R. Wave length and period would appear to increase very slowly with distance according to $r^{1/6}$ with long waves some

distance behind the front the period increase would conform to $r^{1/3}$ and with short waves near the rear of the train, or in otherwise exceptionally deep water, the period increase would follow the law $r^{1/2}$.

6. EXPERIMENTAL EVIDENCE FOR WAVE PERIOD INCREASE

In a classic paper on the subject of wave period increase, Munk (1947) had indicated that the wave period of tsunamis must bear some relationship to the original disturbance, because of an indeterminateness of the function in the general solution of the governing differential equation:

$$\frac{\delta T}{\delta t} + V \frac{\delta T}{\delta x} = 0 \qquad \text{(I-34)}$$

This is patent from the data drawn from his paper and plotted in Fig. I-5, which relates the dimensionless quantities $T\sqrt{g/d}$ and r/d. Clearly the tsunamis of April 1, 1946 (Aleutian Trench), April 13, 1923 (Kamchatka), and November 10, 1922 (Chile), obey different laws of period increase with distance, as also the tsunami originating from the submarine volcanic eruption at Myojinsho Reef, on March 11, 1953 (Unoki and Nakano, 1953).

For the tsunami of April 1, 1946, we have extracted from the data given by Munk, the periods of the waves 20 mins. behind the wave front, as recorded at Valparaiso, Matarani, La Jolla and Honolulu. Also assembled in Fig. I-5 are period data for the leading waves obtained from Takahasi's (1961) model experiments on a

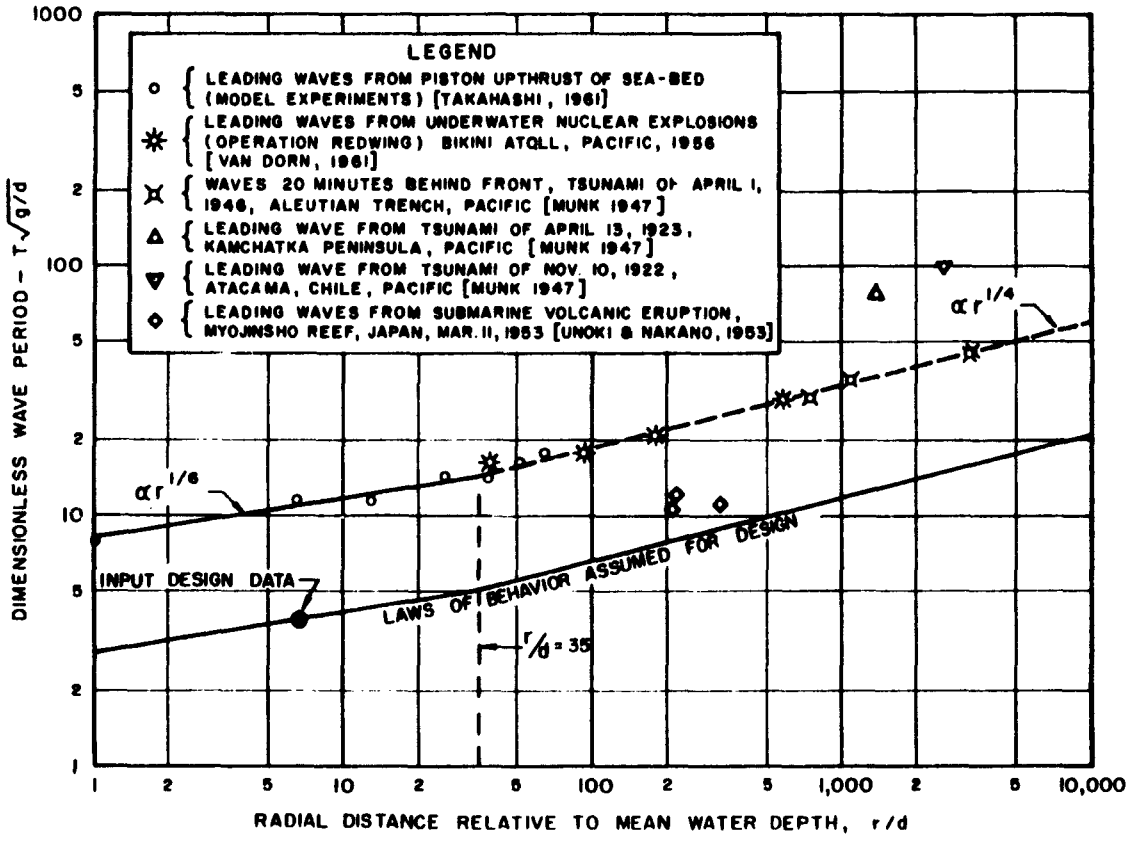

FIGURE I-5

PERIOD OF THE LEADING WAVE IN A DISPERSIVE, IMPULSIVELY GENERATED SYSTEM AS A FUNCTION OF RADIAL DISTANCE FROM THE ORIGIN

piston-like upheaval of sea bed and from Van Dorn's (1961) measurements of underwater nuclear explosion waves from Bikini Atoll, as measured at Ailinginae, Eniwetok, Wake and Johnston Islands in the Pacific. It is quite fortuitous that all these last mentioned data are in virtual alignment in Fig. I-5, suggesting that from a dimensional standpoint the source disturbances in each case must have been quite similar. What is of special interest is that for small values of r/d Takahasi's data show $T \propto r^{1/6}$, in agreement with Eq. (I-33) while Van Dorn's and Munk's data conform almost exactly to a law $T \propto r^{1/4}$. What is further of extraordinary interest is that the change from $r^{1/6}$ to $r^{1/4}$ occurs at $r/d \simeq 35$, suggesting some parallel with the height-change law of Fig. I-2. We may recall too that the experimental height-change law ($\propto r^{-1}$) for small r/d was in accordance with the prediction of the theoretical stationary-phase asymptotic approximation and note the similarity here that the experimental period-change law ($\propto r^{1/6}$) for small r/d is also in accord with the theoretical stationary-phase asymptotic approximation (Eq. (I-33)). Beyond $r/d \simeq 35$, the height change law ($\propto r^{-5/6}$) exhibited the invalidity of the approximation. It seems evident therefore that the same invalidity is responsible for the period-change law following a new pattern ($r^{1/4}$). Data from the two-dimensional experiments of Prins (1956, 1958) have not been invoked in Fig. I-5, as they would be inappropriate.

Eq. (I-33) can be expressed alternatively as

$$\text{(i)} \qquad T_i \sqrt{\frac{g}{d}} = K \left(\frac{r}{d}\right)^{\frac{1}{6}}$$

$$\text{(ii)} \qquad K \simeq \left(\frac{12\pi^5}{3p}\right)^{\frac{1}{6}} \left(\frac{R}{d}\right)^{\frac{1}{2}} \qquad \text{(I-35)}$$

It is of interest to compare the theoretical value of K given by (I-35 ii) with the value K (= 8.2), found from Fig. I-5 as applicable to Takahasi's experiments. For this purpose we take p = 1 for the first wave and insert R = 6 ins, d = 1.875 ins, the dimensions of piston radius and water depth respectively in the model experiments. Eq. (I-35 ii) then yields K = 7.03 which is of the correct order of magnitude. Since R should really be the radius of the initial surface disturbance which probably exceeded 6 ins., the congruency could probably be improved. Eqs. (I-33) or (I-35) thus appear to be a reliable prediction of initial wave period increase.

From the alignment of the April 1, 1946 tsunami and the 1956 REDWING nuclear explosion data with that of Takahasi's (Fig. I-5), we conclude that the same R/d value of about 3.2 prevailed. For the tsunami this would imply an initial radius of surface disturbance R ≃ 52,200 ft. (d ≃ 16,320 ft.) or 8.60 n. mi. Interpreting this as related to an earthquake fault-length of 19.2 n. mi. or 35.6 km, the equivalent earthquake magnitude would be about 7.40 (cf. Wilson, 1962 (Fig. 8)), whereas the actual earthquake magnitude was in fact 7.4. For the REDWING explosion series, the implication is

that if the waves had emanated from an explosion, unobstructed by atolls or reefs, the bubble crater diameter D_c (= 2R) would have been 6.4d, or about 6 times the water depth. For d $\simeq$ 200 ft, D_c would thus have been of the order of 1280 ft.

7. CALCULATION OF DESIGN WAVE HEIGHT AND PERIOD AT THE CONTINENTAL SLOPE

Despite any reservations made regarding the input design data, we proceed to use them in conjunction with the laws of height and period change with radial distance of dispersion, justified in this appendix, in determining the wave height and period that would prevail at the continental slope off Chesapeake Bay.

The law of maximum wave height change, following the discussions of Sections 2 and 3, may be generalized as

$$\frac{\eta_o}{D_c} = \alpha_n \left(\frac{r}{d}\right)^{-n} \tag{I-36}$$

in which n is a numerical exponent and α_n the corresponding proportionality constant. It is convenient to write this in the form

$$Y = \alpha_n X^{-n} \tag{I-37}$$

where

$$\text{(i)} \qquad Y = \eta_o / D_c$$

$$\text{(ii)} \qquad X = r/d \tag{I-38}$$

In order to apply Eq. (I-36) derived for constant depth, to conditions under which the depth is a function of r, namely d = d(r), it is necessary to integrate $d\eta_0/dr$ as a function from which X has been eliminated, (cf. Wilson, 1961). Thus by differentiating Eq. (I-37), regarding d as constant, and eliminating X in favor of Y by use of (I-37), we arrive at the expressions

$$\text{(i)} \qquad \frac{d\eta_0}{dr} = \frac{D_c}{d(r)} Y' \tag{I-39}$$

$$\text{(ii)} \qquad Y' = -n a_n^{-\frac{1}{n}} Y^{\frac{n+1}{n}}$$

The law of period increase, following the discussions of Sections 5 and 6, may be generalized in a similar way as

$$T\sqrt{\frac{g}{d}} = \beta_m \left(\frac{r}{d}\right)^m \tag{I-40}$$

with m a numerical exponent and β_m the corresponding constant of proportionality. Writing this as

$$Z = \beta_m X^m \tag{I-41}$$

in which

$$\text{(i)} \qquad Z = T\sqrt{\frac{g}{d}} \tag{I-42}$$

$$\text{(ii)} \qquad X = r/d$$

we may follow the same general procedure as for wave height in deriving

$$\text{(i)} \qquad \frac{dT}{dr} = g^{-\frac{1}{2}} \left[d(r)\right]^{-\frac{1}{2}} Z' \tag{I-43}$$

$$\text{(ii)} \qquad Z' = m \beta_m^{\frac{1}{m}} Z^{\frac{m-1}{m}}$$

In case III, the given data prescribes a half-wave amplitude $\eta_o = 388$ ft. at $r = 20$ miles resulting from a bubble crater diameter $D_c = 20,800$ ft. For an assumed point of detonation at latitude $35^o\ 30'$, longitude $65^o\ 27'$, * off the east coast the water depth profiles along great circle paths directed towards Chesapeake and New York Bays are as shown in Fig. I-6, with depth at the detonation point $d \simeq 15,500$ ft. The leading wave period is given as $T_1 = 2.75$ mins. and that of the highest wave (crest No. 4 or trough No. 5) as $T_4 = 1.2$ mins.

With this information we find $\eta_o/D_c = 1.87 \times 10^{-2}$ and $T_1 \sqrt{g/d} = 3.87$ at $r/d = 6.77$. These points are located on Figs. I-2 and I-5 and design curves have been constructed through them parallel to the theoretical empirical relationships found to correspond with observations. The same indicated change of slope at $r/d = 35$ has been adopted in both cases.

---

* This location was the first originally prescribed for the project but was later amended to one closer to the shore (see Chapter V - Vol. I Part B). The calculation here given is left unchanged, however, on grounds that general deductions are still pertinent.

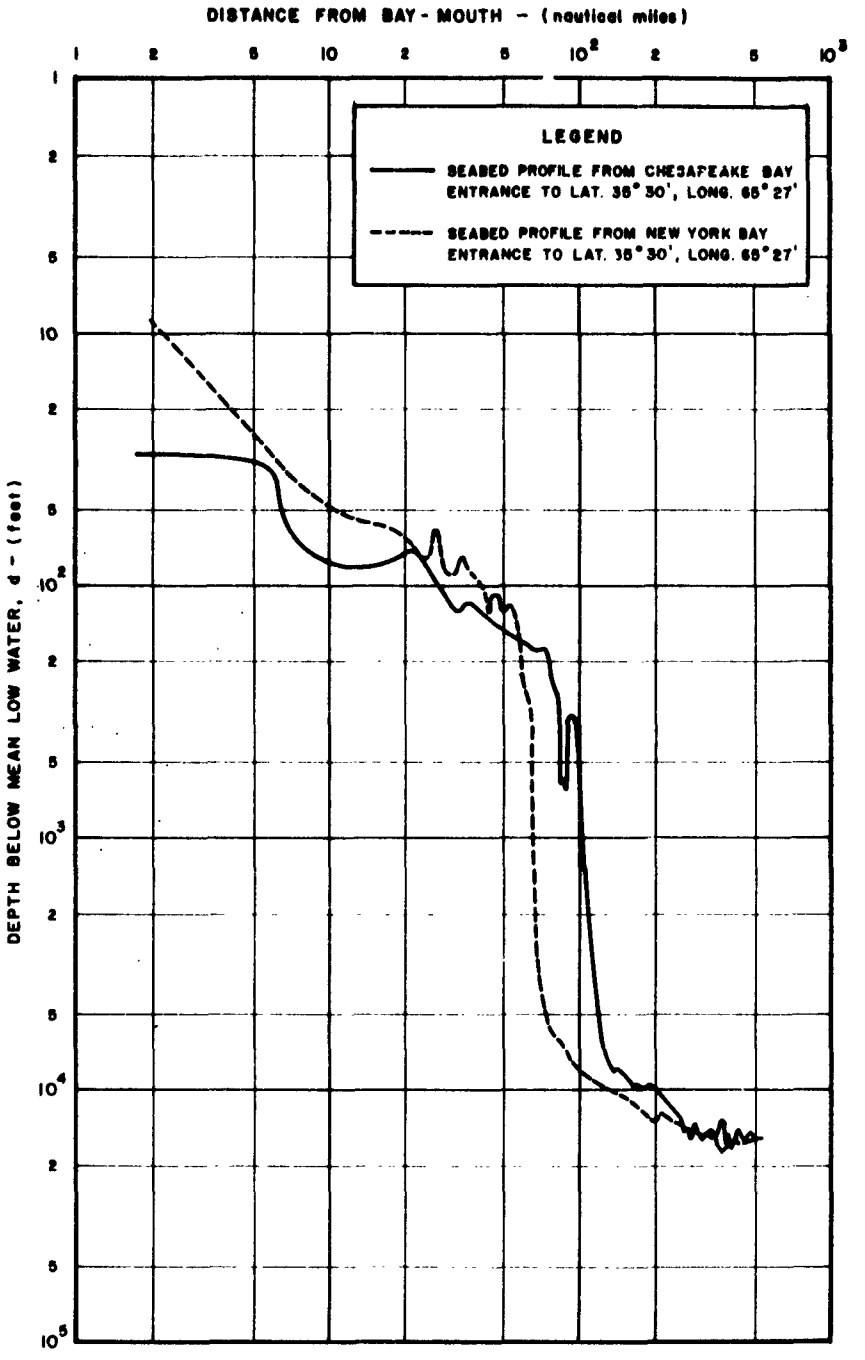

FIGURE I-6

PROFILES OF SEA-BED ALONG GREAT CIRCLE PATHS FROM MOUTHS OF CHESAPEAKE AND NEW YORK BAYS TO OCEAN STATION AT LAT. 35° 30', LONG. 65° 27'

Applicable values of n, α_n, m, β_m, now readily evaluated from the design curves of Figs. I-2 and I-5 are recorded in Table I-1.

TABLE I-1

DESIGN CONSTANTS GOVERNING WAVE HEIGHT AND PERIOD

Relative Distance	Wave Height Decay		Wave Period Increase	
r/d	n	α_n	m	β_m
<35	1	0.127	1/6	2.90
>35	5/6	0.0734	1/4	2.12

Eqs. (I-39) and (I-43) have been used in conjunction with the parameters of Table I-1 in a stepwise numerical integration procedure for computing η_o and T over the (full-line) depth profile shown in Fig. I-6, carried as far as the foot of the continental slope. The results of the calculations are portrayed in Fig. I-7.

The highest wave, without regard to its position in the wave groups, will decline from an initial elevation η_o = 388 ft. at r = 19 n. mi. to η_o = 17.3 ft. at r = 428 n. mi. from the origin. Over this distance the water depth decreases from 15,420 ft. to 7800 ft. Maximum water depth of 17,760 ft. is encountered at the intermediate distance r = 155.5 n. mi. The further history of wave height has not been pursued beyond r = 428 n. mi. because

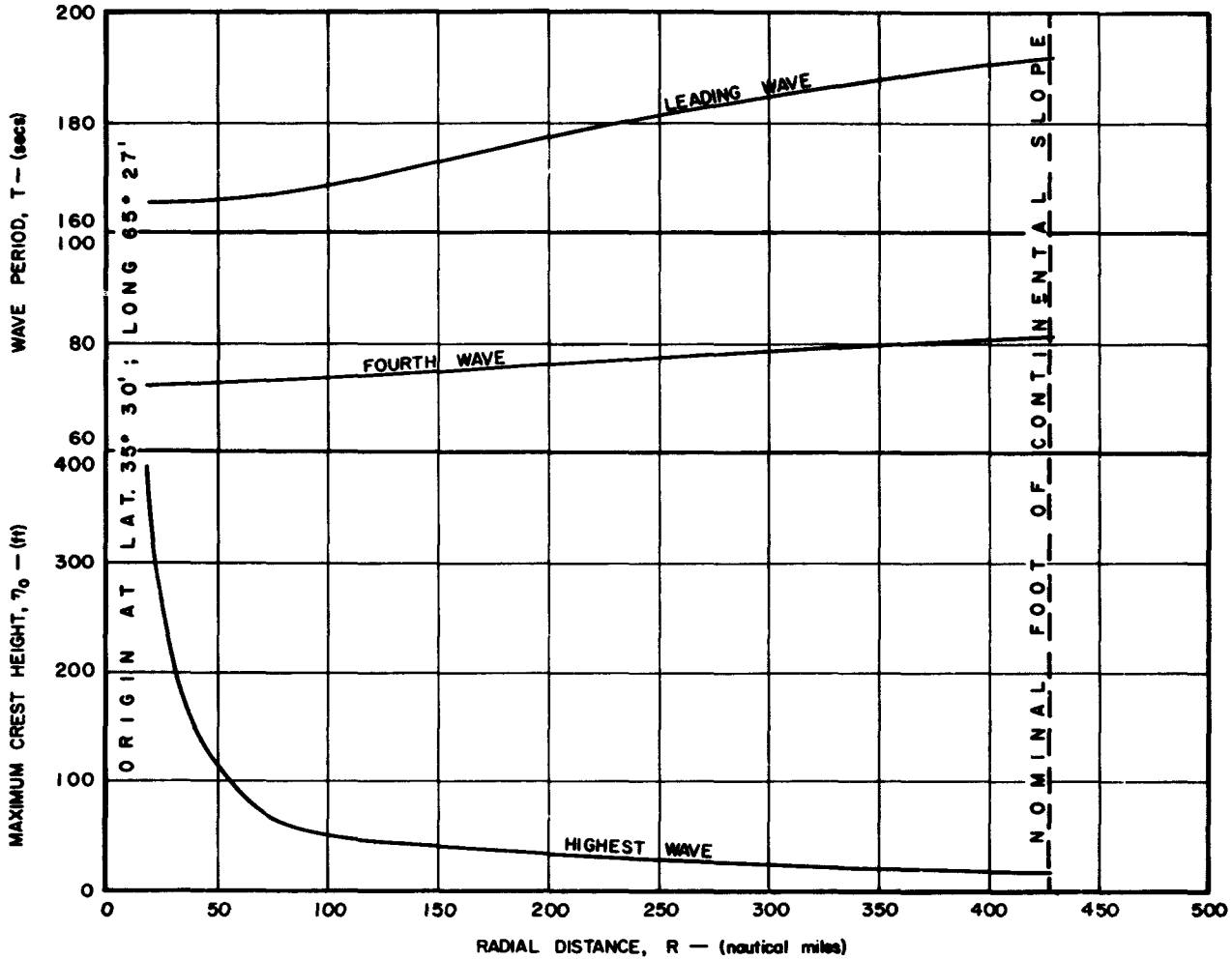

FIGURE I-7

OVERALL MAXIMUM CREST ELEVATION AND PERIODS (first and fourth waves) FOLLOWING DISPERSION OF DESIGN EXPLOSION-GENERATED WAVES, COMPUTED AS FAR AS THE CONTINENTAL SLOPE

of the complications of reflection at the continental slope, which require separate study (as given in Chapter IV, Part B, Vol. I).

Over the same wave path the period of the leading wave, T_1 = 165 secs. at r = 19 n. mi. is found to increase to T_1 = 192 secs. at r = 428 n. mi. On the assumption that the fourth wave in the leading group of waves follows the same laws of period increase as the actual wave front, its period of T_4 = 72 secs. at r = 19 n. mi. is found to increase to 81 secs. at r = 428 n. mi. The legitimacy of this calculation may be open to question as the governing law may be more in accord with Eq. (I-26). For the initial values of d = 15,500 ft. at r = 19 n. mi. the latter equation gives T_4 = 70.5 secs. for m = 3 (the fourth wave) which is in surprising agreement with T_4 = 72 secs. of the given data. Since Eq. (I-26) is valid only for constant d, we must take a mean value of depth over the distance to estimate T_4 at r = 428 n. mi. For d = 15,000 ft. then, T_4 is found to be 197 secs. at r = 428 n. mi. on this basis. This value exceeds the computed value of T_1 = 192 secs. and is therefore not likely to be correct. The inference must be that Eq. (I-26) is only applicable much further back in the body of the waves for larger values of m.

8. CONCLUSIONS

On the basis of the arguments evolved in this appendix, and on the assumption that a nuclear explosion with a bubble crater diameter D_c = 20,800 ft. produces maximum waves of a height

η_o = 388 ft. above still water at a distance of r = 20 miles from surface zero in a water depth of 15,420 ft., it is found that over the shelving depth to the base of the continental shelf (d $\simeq$ 7800 ft.) the maximum waves will have decreased to η_o = 17.3 ft. at r = 428 n. mi. The period of the leading wave (which will be of much lower height) will approximate 192 secs. (3.2 mins.), but the period of the highest wave will very likely be in the neighborhood of 80 secs. at this distance.

At a radius of 300 n. mi. from surface zero (d $\simeq$ 10,000 ft.) Fig. I-7 shows that the probable maximum height above still water of the highest wave will be about η_o = 25 ft. and its corresponding period about T = 78 secs., which is in very good agreement with what has been found in Appendix II.

A question as yet unanswered is whether the Kranzer-Keller theory and the asymptotic solution which it invokes is legitimately applicable to a system of high waves which, in the initial stages at least, are likely to be extremely non-linear. However, an encouraging aspect of this query is that experimental results of wave height and period-change, even for comparatively small values of r/d, do confirm the theoretical predictions based on the asymptotic solutions of the linearized theory. Since the Kranzer-Keller theory is merely an adaptation of the more fundamental Cauchy-Poisson-Lamb linear theory which conceives the emergent waves as the sum of an infinite number of small amplitude waves distributed over a continuous spectrum of frequencies, there is the possibility that the aggregate

outcome of its legitimate linear processes, applied to the spectral elements, is a very close approximation (if not an exact solution) to the characteristics of large waves, which as entities must otherwise be considered as obeying non-linear laws.

REFERENCES

Cauchy, A. L. (1815); Mem. acad. roy. sci., I, 1827; also Oeuvres Completes (Paris, 1822), Premier serie v. I, p. 38.

Cole, R. H. (1948); Underwater explosions; (Princeton Univ. Press, Princeton, N. H.), 1948.

Eckart, C. (1948); The approximate solution of one-dimensional wave-equations; Review of Modern Physics, v. 20 (1), April 1948, pp. 399-417.

Fuchs, R. A. (1952); Theory of surface waves produced by underwater explosions; Tech. Rept. ser. 3, Iss. 335, Inst. Eng. Res., Univ. Calif., Berkeley, 1952.

Glasstone, S. (1957) (1962); The effects of nuclear weapons; U. S. Department of Defense and U. S. Atomic Energy Commission, 1957; reprinted and enlarged April 1962.

Jeffreys, H. and Jeffreys, B. S. (1956 Edn.); Methods of mathematical physics, (Cambridge Press, Cambridge, England), 1956.

Johnson, J. W. and Bermel, K. J. (1949); Impulsive waves in shallow water as generated by falling weights; Trans. Am. Geophs. Union, v. 30, 1949, pp. 223-230.

Kaplan, K., Wallace, N. R., and Goodale, T. C. (1962); Studies and analysis of explosion generated surface water waves; Tech. Report, U. R. S. B 192-2, United Research Services, Burlingame, California.

Kirkwood, J. G. and Seeger, R. T. (1950); Surface waves from an underwater explosion; Underwater Explosion Research, v. II, Office of Naval Research, U. S. Navy, 1950, pp. 707-760.

Kranzer, H. C. and Keller, J. B. (1950); Water waves produced by explosions; J. Appl. Phys., v. 30(3), Mar. 1959, pp. 398-407.

Lamb, H. (1904); On deep-water waves; Proc. London Math Soc.; (Presidential address), 1904, pp. 371-400.

Lamb, H. (1922); On water waves due to a disturbance beneath the surface; Proc. London Math. Soc., v. 21(2), 1922, pp. 359-372.

Lamb, H. (1932 Edn.); Hydrodynamics (Cambridge Univ. Press, England), 1932 Edn. (1st Edn., 1879).

Lane, W. R. and Green, H. L. (1956); The mechanics of drops and bubbles; Surveys in Mechanics, (Cambridge Univ. Press, Cambridge, England), 1956, pp. 162-215.

Munk, W. H. (1947); Increase in the period of waves travelling over large distances; with applications to tsunamis, swell, and seismic surface waves. Trans. Am. Geophys. Union, v. 28(2), 1947, pp. 198-217.

Munk, W. H. (1953); Small tsunami waves reaching California from the Japanese earthquake of Mar. 4, 1952; Bulln. Seismol. Soc. Am., v. 43(3), July 1953, pp. 219-222.

Penny, W. C. (1950); Gravity waves produced by surface and underwater explosions; Underwater Explosion Research, v. II, Office of Naval Research, U. S. Navy, 1950, pp. 679-700.

Poisson, S. D. (1816); Mem. Acad. Roy. Sci., I, 1816.

Prins, J. E. (1956); Characteristics of waves generated by a local surface disturbance; Tech. Report Ser. 99(1), Inst. Eng. Res., Univ. Calif., Berkeley, Aug. 1956.

Snay, H. G. (1957); Hydrodynamics of underwater explosions; Symposium on Naval Hydrodynamics, Nat. Acad. Sci. Nat. Res. Counc., Pub. 515, 1957, pp. 325-352.

Sneddon, I. N. (1951); Fourier transforms, (McGraw-Hill Book Co., New York), 1951

Stoker, J. H. (1957); Water waves (Interscience Publishers Inc., New York), Chapter 6.

Takahasi, R. (1961); On the spectra and the mechanism of generation of tsunamis; Proc. Tsunami Hydrodynamics Conf., Univ. Hawaii, Aug. 1961, (publication pending).

Terazawa, K. (1915); On deep sea water waves caused by a local disturbance on or beneath the surface; Proc. Roy. Soc. London, v. 92(A), 1915, pp. 57-81.

Unoki, S. and Nakano, M. (1953); On the Cauchy-Poisson waves caused by the eruption of a submarine volcano, Paper I; Oceanographical Magazine (Japan), and 4(4), 1953, pp. 119-141.

Unoki, S. and Nakano, M. (1953); On the Cauchy-Poisson waves caused by the eruption of a submarine volcano, Paper II, Ocn. Mag. (Japan), v. 5(1), 1953, pp. 1-13.

Unoki, S. and Nakano, M. (1953); On the Cauchy-Poisson waves caused by the eruption of a submarine volcano, Paper III, Met. Res. Inst., Papers in Met. and Geophys., v. 4(3-4) 1953, pp. 139-150.

Ursell, F. (1953); The long wave paradox in the theory of gravity waves; Proc. Cambr. Phil. Soc., v. 49(4), 1953, pp. 685-694.

Van Dorn, W. G. (1961, i); Some characteristics of surface gravity waves in the sea produced by nuclear explosions; Journ. Geophys. Res., v. 66(11), Nov. 1961, pp. 3845-3862.

Van Dorn, W. G. (1961, ii); The source motion of the tsunami of March 9, 1957, as deduced from measurements at Wake Island; Proc. Tsunami Hydrodynamics Conf., Honolulu, Hawaii, 1961 (publication pending).

Wiegel, R. L. (1955); Laboratory studies of gravity waves generated by the movements of a submerged body; Trans. Am. Geophys. Union, v. 36(5), Oct. 1955, pp. 759-774.

Wilson, B. W. (1961); Deep water wave generation by moving wind systems; Proc. ASCE, v. 87(WW2), May 1961, pp. 113-141.

Wilson, B. W. (1962); The nature of tsunamis; their generation and dispersion in water of finite depth; Technical Report (Contract No. CGS-801(2442), National Engineering Science Co., August 1962.

LIST OF SYMBOLS
FOR APPENDIX I

c	phase velocity of water waves
d	water depth
D_c	diameter of bubble crater at the water surface in underwater explosions
e	universal constant (2.718...)
g	acceleration due to gravity
h	depth below the surface of an underwater explosion
H	wave height, crest to trough
I	uniform impulse (per unit area) over source area
$I(r)$	function describing the initial impulse as a function of r
$\bar{I}(k)$	Hankel transform of $I(r)$ (Eqs. (I-11))
I_o	concentrated impulse at the point source (per unit area)
J_o	Bessel function of zero order
J_1	Bessel function of first order
k	wave number ($= \frac{2\pi}{\lambda}$)
K	constant of proportionality, function of R/d, (Eqs. (I-36 ii)
m	(1) numerical exponent; (2) corresponding subscript
n	(1) numerical exponent; (2) corresponding subscript
p	integer number representing the wave with greatest height counted from the front of the train
Q	vertical surface elevation over a circle of radius R
$Q(r)$	initial surface elevation as a function of r

$\overline{Q}(k)$	Hankel transform of $Q(r)$, (Eqs. I-11))
Q_o	initial surface elevation of point source disturbance at the origin (per unit area)
r	variable horizontal radial distance in cylindrical symmetry
R	radius of a cylindrically symmetrical surface or bottom disturbance
t	variable time
T	wave period
T_i	period of the initial or leading wave in a dispersive system
V	group velocity of water waves
W	charge-weight of nuclear explosion
W_w	that part of the total energy W which is responsible for the generation of waves
x	variable horizontal distance
X	dimensionless variable, (Eq. (I-43 ii))
Y	dimensionless variable (Eq. I-39 i))
Y'	differential coefficient of Y with respect to X (Eq. I-40 ii))
Z	dimensionless variable (Eq. (I-43 i))
Z'	differential coefficient of Z with respect to X, (Eq. (I-44 ii))
α_n	constant of proportionality, (Eq. (I-38))
β_m	constant of proportionality, (Eq. (I-42))
η	elevation of wave surface above still water level
η_0	maximum value of η at the wave crest
η_e	value of η deriving from an initial elevation over a limited source region

η_i	value of η deriving from an initial impulse applied over a limited source region
λ	wave length of a wave in water of any depth
λ_o	deep-water wave length of any given wave type
λ_i	wave length of the leading wave in a dispersive system
μ	coefficient of virtual viscosity (sec.$^{-1}$ units), (Eq. (I-5))
π	universal constant (3.14159...)
ρ	mass density of (sea) water
σ	angular frequency (= 2 π/T)
ϕ	function of (kd) in Kranzer-Keller theory, common to cases of initial elevation and initial impulse
ψ_e	function of kd in Kranzer-Keller theory, case of initial elevation
ψ_i	function of kd in Kranzer-Keller theory, case of initial impulse
Ψ	function of kR and kd (Eq. (I-28))

APPENDIX II

THEORETICAL CONSIDERATIONS AND COMPUTATIONS FOR WATER WAVES PRODUCED BY EXPLOSIONS

By

Larry Armijo

and

Mary Ann Noser

1. INTRODUCTION

A critical literature survey on the various theories for studying gravity waves generated by underwater explosion has been given in Appendix I. It is recalled that a description of the motion of the free surface of a body of water of constant depth following an arbitrary initial distribution of impulse applied to the surface, or an initial elevation or depression of the surface of arbitrary shape, is given by the Kranzer-Keller theory (1955) for the radially symmetric case. Kaplan, Wallace and Goodale (1962) have carried out computations of the Kranzer-Keller equations for three cases of initial paraboloidal depressions of the surface for a point on the surface twenty miles from the center of the initial disturbance. These results have been presented in Fig. 1 (Vol. I) of this report. The primary object of this appendix is to present a similar set of computations for the same three cases considered by Kaplan, Wallace and Goodale, but at a point on the surface 300 miles from the center of the initial disturbance. For the cases under consideration, certain theoretical results have been obtained by the authors and these results are also presented.

2. PRINCIPAL EQUATIONS

The displacement η (r, t) of the free surface is given by

$$\eta(r,t) = \frac{\eta_0 R}{r} B \cos\left[2\pi\left(\frac{t}{T} - \frac{r}{\lambda}\right)\right] \qquad \text{(II-1)}$$

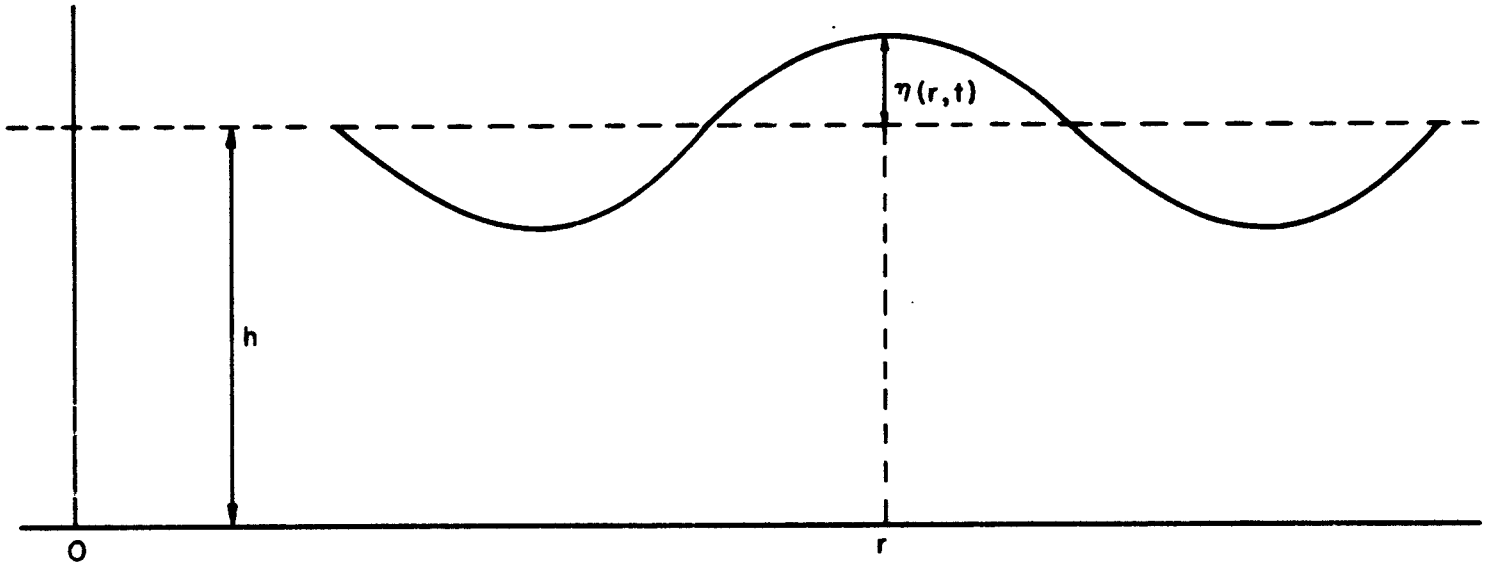

FIGURE II-1
NOTATION

where

$$B = \frac{1}{\eta_0 R h}\ \bar{E}\left(\frac{\sigma}{h}\right)\left[-\frac{\sigma\phi(\sigma)}{\phi'(\sigma)}\right]^{\frac{1}{2}} \qquad \text{(II-2)}$$

and $\sigma = \frac{2\pi h}{\lambda}$

λ = wave length

T = wave period

h = fluid depth

R = effective radius of disturbance

r = distance from center of disturbance

η_0 = depth of disturbance at r = 0

t = time

The function $\bar{E}(s)$ is the Hankel transform of the function $E(r)$, the initial paraboloidal depression, which is assumed to be of the form

$$E(r) = \begin{cases} Ar^2 - \eta_0, & 0 \le r \le \gamma, \\ 0, & \gamma \le r, \end{cases} \qquad \text{(II-3)}$$

where

$$A = \frac{\eta_0}{\gamma^2} \qquad \text{(II-4)}$$

See Figure II-2.

It follows that

$$\bar{E}(s) = -\frac{2\eta_0}{s^2}\ J_2(\gamma s) \qquad \text{(II-5)}$$

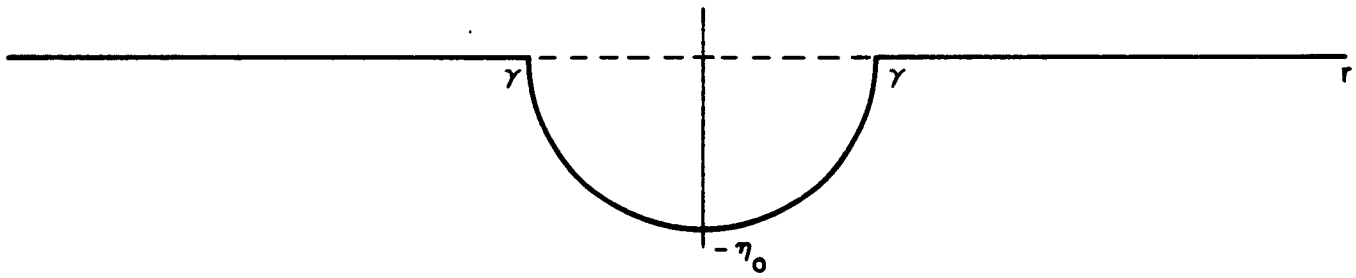

FIGURE II-2
NOTATION FOR THE ORIGIN

where $J_2(x)$ is the Bessel function order 2.

The function $\phi(\sigma)$ is given by

$$\phi(\sigma) = \frac{1}{2}\left(\frac{\tanh \sigma}{\sigma}\right)^{\frac{1}{2}} + \frac{1}{2(\cosh \sigma)^{\frac{3}{2}}}\left(\frac{\sigma}{\sinh \sigma}\right)^{\frac{1}{2}}, \quad \sigma \geq 0 \qquad \text{(II-6)}$$

The function $\phi(\sigma)$ is a positive monotone decreasing function of σ and $\lim_{\sigma \to 0} \phi(\sigma) = 1$, i.e. $\phi(0) = 1$.

The parameter σ is related to the quantities r and t by the equation

$$\phi(\sigma) = \frac{r}{\sqrt{g h}\ t}, \qquad t \geq \frac{r}{\sqrt{g h}} \qquad \text{(II-7)}$$

so that

$$\sigma = \phi^{-1}\left(\frac{r}{\sqrt{g h}\ t}\right), \qquad t \geq \frac{r}{\sqrt{g h}} \qquad \text{(II-8)}$$

where ϕ^{-1} is the inverse of ϕ and g is the gravitational acceleration constant.

The period T is given by the equation

$$T = \frac{2\pi}{\sqrt{\frac{g}{h}\ \sigma \tanh \sigma}} \qquad \text{(II-9)}$$

The effective radius R is related to the quantity γ by the equation

$$R = \frac{\gamma}{\sqrt{2}} \qquad \text{(II-10)}$$

It follows from (II-2), (II-5) and (II-10) that

$$B = -\frac{2\sqrt{2}\,h}{\gamma\sigma^2}\, J_2\left(\frac{\gamma\sigma}{h}\right)\xi(\sigma) \tag{II-11}$$

where

$$\xi(\sigma) \equiv \left[-\sigma\,\frac{\phi(\sigma)}{\phi'(\sigma)}\right]^{\frac{1}{2}} \tag{II-12}$$

For convenience, we have defined

$$B^*(r,t) \equiv \frac{\eta_0 R}{r}\, B = -\frac{2\eta_0 h}{r\sigma^2}\, J_2\left(\frac{\gamma\sigma}{h}\right)\xi(\sigma) \tag{II-13}$$

and

$$\theta^*(r,t) \equiv 2\pi\left(\frac{t}{T} - \frac{r}{\lambda}\right), \quad t \geq \frac{r}{\sqrt{g\,h}} \tag{II-14}$$

so that by (II-1), (II-13) and (II-14)

$$\eta(r,t) = B^*(r,t)\,\cos\theta^*(r,t) \tag{II-15}$$

The quantity $B^*(r, t)$ therefore represents the displacement of the amplitude of the wave envelope. The quantity $\theta^*(r, t)$ given by (II-14) may be shown to be a monotone increasing function of t for $t \geq \frac{r}{\sqrt{g\,h}}$. Moreover, $\lim_{t \searrow \frac{r}{\sqrt{gh}}} \theta(r,t) = 0$ and $\lim_{t \nearrow \infty} \theta(r,t) = \infty$

The times of arrival of crests and troughs are given by the solutions t_m of the equations

$$\theta^*(r,t_n) = n\pi, \quad n = 1,2,.. \tag{II-16}$$

3. APPROXIMATIONS

Following the example set by Kaplan, Wallace and Goodale, we have replaced the functions $\phi(\sigma)$ and $\xi(\sigma)$ in the above equations by their asymptotic expressions $\frac{1}{2\sqrt{\sigma}}$ and $\sqrt{2\sigma}$, respectively, for values $\sigma \geq 4$. The parameter σ may be eliminated from the preceding equations and the following simplifications occur:

$$B^*(r,t) = -\frac{8\sqrt{2}\,\eta_0\, r}{gt^2}\, J_2\left(\frac{\gamma g t^2}{4r^2}\right), \quad t \geq \frac{4r}{\sqrt{gh}} \tag{II-17}$$

and

$$\theta^*(r,t) = \frac{gt^2}{4r}, \quad T = \frac{4\pi r}{gt}, \quad \lambda = \frac{8\pi r^2}{gt^2}, \quad t \geq \frac{4r}{\sqrt{gh}} \tag{II-18}$$

The times of arrival t_m of crests and troughs may be computed from the equations

$$t_n = \sqrt{\frac{4\pi r n}{g}} \quad \text{for positive integers} \quad n \geq \frac{4r}{\pi h} \tag{II-19}$$

The following theoretical results have been noted by the authors of this report. The zeros of $B^*(r, t)$ occur at the times t^*_k given by

$$t_k^* = \sqrt{\frac{4r^2 x_k^*}{\gamma g}} \qquad \text{(II-20)}$$

where x_k^* is the k^{th} positive zero of $J_2(x)$.

If $\frac{h}{\gamma} \geq 1.739$, the maximum values of $|B^*(r, t)|$ occur at the times t_k^{**} given by

$$t_k^* = \sqrt{\frac{4r^2 x_k^{**}}{\gamma g}} \qquad \text{(II-21)}$$

where x_k^{**} is the k^{th} positive zero of $J_2(x) - x J_3(x)$.

To compute the first two packets of waves, we have made use of the values

k	x_k^*	x_k^{**}
1	5.136	2.300
2	8.417	6.541

The restriction $\frac{h}{\gamma} \geq 1.739$, is satisfied for Cases I and II considered by Kaplan, Wallace and Goodale. For their Case III, $\frac{h}{\gamma} = 1.731$ and the restriction is very nearly satisfied. Eq. (II-20) follows from (II-13), and Eq. (II-21) follows from (II-17), which follows the asymptotic expressions for $\phi(\sigma)$ and $\xi(\sigma)$.

It should be emphasized that the value $t_1^{**} = \sqrt{\frac{4r^2 x_1^{**}}{\gamma g}}$ is the time of arrival of the maximum value of the absolute value of the amplitude of the wave envelope. This maximum

value is equal to $|B^*(r, t_1^{**})|$. The value t_1^{**} will be very nearly equal to the time of arrival of the highest crest and the value $|B^*(r, t_1^{**})|$ will be very nearly equal to the displacement of the highest crest.

4. DESCRIPTION OF COMPUTATIONS

In calculating the displacement η (r, t), it is first necessary to compute the functions $\phi(\sigma)$ and $\xi(\sigma)$. A table of these functions has been prepared, using a Bendix G-15 computer, with σ incremented by 0.01 in the interval from 0 to 4, in order to simplify any future hand computations. These results are found in Table II-4. Also, the following numerical values were used to compute η (r, t) and $B^*(r, t)$:

r = 300 miles = 1,584,000 feet

h = 18,000 feet

g = 1.1592×10^5 ft./min.^{2}

These computations were carried out for the following three cases

Dimensions of Initial Displacement		
	Depth (feet)	Radius (feet)
Case I	3,380	4,440
Case II	6,010	7,900
Case III	7,920	10,400

TABLE II-1

The time t_o at which disturbances begin at a distance r from the center of the initial depression is the same for all three cases and is given by

$$t_0 = \frac{r}{\sqrt{gh}} = 34.67 \text{ min.}$$

The times of arrival t_1^* and t_2^* of the first two zeros of the displacement of the wave envelope $B^*(r, t)$ were computed from Eq. (II-20) and are listed in Table II-2.

Times of Arrival of the First Two Zeros of the Displacement of the Wave Envelope		
	k	t_k^* (min.)
Case I	1	316.4
	2	405.0
Case II	1	237.2
	2	303.6
Case III	1	206.7
	2	264.6

TABLE II-2

The times of arrival t_1^{**} and t_2^{**} of the first two maxima of the absolute value of the displacement of the wave envelope $|B^*(r, t)|$ as well as the maximum values $|B^*(r, t_1^{**})|$, $|B^*(r, t_2^{**})|$, and the periods and wave lengths at times t_1^{**}

and t_2^{**} were computed from Eqs. (II-21) and (II-17), and are listed below.

Times of Arrival of the First Two Maxima of the Absolute Value of the Displacement of the Wave Envelope and the Corresponding Maximum Values, Periods, and Wave Lengths

Case	k	t_k^{**} (min)	$B^*(r, t_k^{**})$ (feet)	T (min)	λ (feet)
I	1	211.7	4.826	0.811	12,140
	2	357.0	1.270	0.481	4,270
II	1	158.7	15.268	1.082	21,600
	2	267.6	4.018	0.642	7,600
III	1	138.3(?)	26,488(?)	1,242	28,440
	2	233.3	6.971	0.736	10,010

TABLE II-3

The values followed by (?) are doubtful because the restriction $\frac{h}{\gamma} \geq 1.739$ is not satisfied.

In the range $34.67 \leq t \leq 138.01$, which corresponds to the range $0 \leq \sigma \leq 4$, the values of the displacement of the wave envelope $B^*(r, t)$ were computed from Eq. (II-13) using the Bendix G-15 computer. For values $138.01 < t \leq t_2^*$, the values of $B^*(r, t)$ were computed by hand using Eq. (II-17).*

* The tables of the Bessel Functions of the First Kind of Orders 2 and 3 by the Staff of the Computation Laboratory, published in Cambridge by the Harvard Press, were used in these computations.

TABLE II-4 THE FUNCTIONS $\phi(\sigma)$ AND $\xi(\sigma)$

σ	$\phi(\sigma)$	$\xi(\sigma)$
0.01	.9999500	1.0000277
0.02	.9998000	1.0001111
0.03	.9995502	1.0002500
0.04	.9992006	1.0004444
0.05	.9987516	1.0006944
0.06	.9982034	1.0010000
0.07	.9975563	1.0013612
0.08	.9968107	1.0017779
0.09	.9959672	1.0022503
0.10	.9950262	1.0027782
0.11	.9939884	1.0033617
0.12	.9928543	1.0040009
0.13	.9916247	1.0046957
0.14	.9903004	1.0054462
0.15	.9888821	1.0062523
0.16	.9873708	1.0071141
0.17	.9857673	1.0080317
0.18	.9840727	1.0090049
0.19	.9822880	1.0100339
0.20	.9804142	1.0111186
0.21	.9784525	1.0122592
0.22	.9764040	1.0134556
0.23	.9742700	1.0147078
0.24	.9720518	1.0160158
0.25	.9697506	1.0173798
0.26	.9673677	1.0187997
0.27	.9649046	1.0202756
0.28	.9623627	1.0218075
0.29	.9597435	1.0233954
0.30	.9570483	1.0250395
0.31	.9542788	1.0267396
0.32	.9514365	1.0284959
0.33	.9485229	1.0303084
0.34	.9455397	1.0321771
0.35	.9424884	1.0341022
0.36	.9393708	1.0360836
0.37	.9361884	1.0381214
0.38	.9329430	1.0402157
0.39	.9296362	1.0423665
0.40	.9262699	1.0445739

TABLE II-4 (continued)

σ	$\phi(\sigma)$	$\xi(\sigma)$
0.41	.9228456	1.0468379
0.42	.9193651	1.0491586
0.43	.9158302	1.0515361
0.44	.9122427	1.0539704
0.45	.9086042	1.0564617
0.46	.9049165	1.0590099
0.47	.9011815	1.0616151
0.48	.8974008	1.0642775
0.49	.8935762	1.0669972
0.50	.8897095	1.0697741
0.51	.8858000	1.0726000
0.52	.8818600	1.0755000
0.53	.8778800	1.0784000
0.54	.8738600	1.0815000
0.55	.8698100	1.0845000
0.56	.8657200	1.0876000
0.57	.8616100	1.0908000
0.58	.8574700	1.0941000
0.59	.8533000	1.0974000
0.60	.8491100	1.1007000
0.61	.8448900	1.1041000
0.62	.8406500	1.1076000
0.63	.8363900	1.1111000
0.64	.8321200	1.1147000
0.65	.8278200	1.1184000
0.66	.8235100	1.1221000
0.67	.8191900	1.1258000
0.68	.8148500	1.1297000
0.69	.8105100	1.1336000
0.70	.8061500	1.1375000
0.71	.8017900	1.1415000
0.72	.7974100	1.1456000
0.73	.7930300	1.1497000
0.74	.7886500	1.1539000
0.75	.7842700	1.1581000
0.76	.7798800	1.1624000
0.77	.7755000	1.1668000
0.78	.7711100	1.1712000
0.79	.7667300	1.1757000
0.80	.7623500	1.1803000

TABLE II-4 (continued)

σ	$\phi(\sigma)$	$\xi(\sigma)$
0.81	.7579700	1.1849000
0.82	.7536000	1.1895000
0.83	.7492400	1.1943000
0.84	.7448800	1.1991000
0.85	.7405300	1.2039000
0.86	.7362000	1.2088000
0.87	.7318700	1.2138000
0.88	.7275500	1.2189000
0.89	.7232500	1.2240000
0.90	.7189600	1.2291000
0.91	.7146900	1.2344000
0.92	.7104200	1.2397000
0.93	.7061800	1.2450000
0.94	.7019500	1.2504000
0.95	.6977400	1.2559000
0.96	.6935500	1.2615000
0.97	.6893700	1.2671000
0.98	.6852200	1.2728000
0.99	.6810800	1.2785000
1.00	.6769700	1.2843000
1.01	.6728700	1.2902000
1.02	.6688000	1.2961000
1.03	.6647500	1.3021000
1.04	.6607300	1.3082000
1.05	.6567200	1.3144000
1.06	.6527400	1.3206000
1.07	.6487900	1.3268000
1.08	.6448600	1.3332000
1.09	.6409500	1.3396000
1.10	.6370700	1.3460000
1.11	.6332100	1.3526000
1.12	.6293900	1.3592000
1.13	.6255800	1.3658000
1.14	.6218100	1.3726000
1.15	.6180600	1.3794000
1.16	.6143400	1.3863000
1.17	.6106400	1.3932000
1.18	.6069700	1.4002000
1.19	.6033300	1.4073000
1.20	.5997200	1.4144000

TABLE II-4 (continued)

σ	$\phi(\sigma)$	$\xi(\sigma)$
1.21	.5961400	1.4217000
1.22	.5925900	1.4290000
1.23	.5890600	1.4363000
1.24	.5855600	1.4437000
1.25	.5820900	1.4512000
1.26	.5786500	1.4588000
1.27	.5752400	1.4664000
1.28	.5718600	1.4741000
1.29	.5685000	1.4819000
1.30	.5651800	1.4898000
1.31	.5618800	1.4977000
1.32	.5586200	1.5057000
1.33	.5553800	1.5138000
1.34	.5521700	1.5219000
1.35	.5489900	1.5301000
1.36	.5458400	1.5384000
1.37	.5427200	1.5467000
1.38	.5396200	1.5552000
1.39	.5365600	1.5637000
1.40	.5335200	1.5722000
1.41	.5305100	1.5809000
1.42	.5275400	1.5896000
1.43	.5245900	1.5984000
1.44	.5216600	1.6072000
1.45	.5187700	1.6162000
1.46	.5159000	1.6252000
1.47	.5130600	1.6343000
1.48	.5102600	1.6434000
1.49	.5074700	1.6526000
1.50	.5047200	1.6619000
1.51	.5019900	1.6713000
1.52	.4992900	1.6808000
1.53	.4966200	1.6903000
1.54	.4939700	1.6999000
1.55	.4913500	1.7096000
1.56	.4887600	1.7193000
1.57	.4861900	1.7291000
1.58	.4836500	1.7390000
1.59	.4811400	1.7490000
1.60	.4786500	1.7591000

TABLE II-4 (continued)

σ	$\phi(\sigma)$	$\xi(\sigma)$
1.61	.4761900	1.7692000
1.62	.4737500	1.7794000
1.63	.4713400	1.7896000
1.64	.4689600	1.8000000
1.65	.4665900	1.8104000
1.66	.4642600	1.8209000
1.67	.4619500	1.8315000
1.68	.4596600	1.8421000
1.69	.4573900	1.8528000
1.70	.4551500	1.8636000
1.71	.4529400	1.8745000
1.72	.4507400	1.8854000
1.73	.4485800	1.8964000
1.74	.4464300	1.9075000
1.75	.4443100	1.9187000
1.76	.4422000	1.9299000
1.77	.4401300	1.9412000
1.78	.4380700	1.9526000
1.79	.4360400	1.9641000
1.80	.4340200	1.9756000
1.81	.4320300	1.9872000
1.82	.4300600	1.9989000
1.83	.4281100	2.0106000
1.84	.4261900	2.0225000
1.85	.4242800	2.0344000
1.86	.4223900	2.0463000
1.87	.4205300	2.0584000
1.88	.4186800	2.0705000
1.89	.4168600	2.0827000
1.90	.4150500	2.0949000
1.91	.4132600	2.1073000
1.92	.4114900	2.1197000
1.93	.4097400	2.1322000
1.94	.4080100	2.1447000
1.95	.4063000	2.1573000
1.96	.4046100	2.1700000
1.97	.4029400	2.1828000
1.98	.4012800	2.1956000
1.99	.3996400	2.2085000
2.00	.3980200	2.2214000

TABLE II-4 (continued)

σ	$\phi(\sigma)$	$\xi(\sigma)$
2.01	.3964100	2.2345000
2.02	.3948300	2.2476000
2.03	.3932500	2.2608000
2.04	.3917000	2.2740000
2.05	.3901600	2.2873000
2.06	.3886400	2.3007000
2.07	.3871400	2.3141000
2.08	.3856500	2.3276000
2.09	.3841800	2.3412000
2.10	.3827200	2.3548000
2.11	.3812800	2.3685000
2.12	.3798500	2.3823000
2.13	.3784400	2.3961000
2.14	.3770400	2.4100000
2.15	.3756600	2.4240000
2.16	.3742900	2.4380000
2.17	.3729400	2.4521000
2.18	.3716000	2.4663000
2.19	.3702800	2.4805000
2.20	.3689700	2.4947000
2.21	.3676700	2.5091000
2.22	.3663900	2.5235000
2.23	.3651100	2.5379000
2.24	.3638600	2.5524000
2.25	.3626100	2.5670000
2.26	.3613800	2.5816000
2.27	.3601600	2.5963000
2.28	.3589600	2.6111000
2.29	.3577600	2.6259000
2.30	.3565800	2.6407000
2.31	.3554100	2.6556000
2.32	.3542500	2.6706000
2.33	.3531000	2.6856000
2.34	.3519700	2.7007000
2.35	.3508500	2.7158000
2.36	.3497300	2.7310000
2.37	.3486300	2.7462000
2.38	.3475400	2.7615000
2.39	.3464600	2.7768000
2.40	.3453900	2.7922000

TABLE II-4 (continued)

σ	$\phi(\sigma)$	$\xi(\sigma)$
2.41	.3443400	2.8076000
2.42	.3432900	2.8231000
2.43	.3422500	2.8386000
2.44	.3412200	2.8542000
2.45	.3402100	2.8698000
2.46	.3392000	2.8855000
2.47	.3382000	2.9012000
2.48	.3372200	2.9170000
2.49	.3362400	2.9328000
2.50	.3352700	2.9486000
2.51	.3343100	2.9645000
2.52	.3333600	2.9804000
2.53	.3324200	2.9964000
2.54	.3314900	3.0124000
2.55	.3305600	3.0285000
2.56	.3296500	3.0446000
2.57	.3287400	3.0607000
2.58	.3278400	3.0769000
2.59	.3269500	3.0931000
2.60	.3260700	3.1093000
2.61	.3252000	3.1256000
2.62	.3243400	3.1419000
2.63	.3234800	3.1583000
2.64	.3226300	3.1746000
2.65	.3217900	3.1910000
2.66	.3209500	3.2075000
2.67	.3201300	3.2240000
2.68	.3193100	3.2405000
2.69	.3185000	3.2570000
2.70	.3177000	3.2736000
2.71	.3169000	3.2902000
2.72	.3161100	3.3068000
2.73	.3153300	3.3235000
2.74	.3145500	3.3401000
2.75	.3137800	3.3568000
2.76	.3130200	3.3736000
2.77	.3122600	3.3903000
2.78	.3115100	3.4071000
2.79	.3107700	3.4239000
2.80	.3100300	3.4407000

TABLE II-4 (continued)

σ	$\phi(\sigma)$	$\xi(\sigma)$
2.81	.3093000	3.4576000
2.82	.3085800	3.4745000
2.83	.3078600	3.4913000
2.84	.3071500	3.5082000
2.85	.3064400	3.5252000
2.86	.3057400	3.5421000
2.87	.3050500	3.5591000
2.88	.3043600	3.5761000
2.89	.3036800	3.5931000
2.90	.3030000	3.6101000
2.91	.3023300	3.6271000
2.92	.3016700	3.6442000
2.93	.3010000	3.6612000
2.94	.3003500	3.6783000
2.95	.2997000	3.6954000
2.96	.2990500	3.7125000
2.97	.2984100	3.7296000
2.98	.2977800	3.7467000
2.99	.2971500	3.7638000
3.00	.2965300	3.7810000
3.01	.2959100	3.7981000
3.02	.2952900	3.8153000
3.03	.2946800	3.8324000
3.04	.2940700	3.8496000
3.05	.2934700	3.8668000
3.06	.2928800	3.8840000
3.07	.2922800	3.9012000
3.08	.2917000	3.9184000
3.09	.2911200	3.9356000
3.10	.2905400	3.9528000
3.11	.2899600	3.9700000
3.12	.2893900	3.9872000
3.13	.2888300	4.0044000
3.14	.2882600	4.0216000
3.15	.2877100	4.0388000
3.16	.2871500	4.0560000
3.17	.2866000	4.0733000
3.18	.2860600	4.0905000
3.19	.2855200	4.1077000
3.20	.2849800	4.1249000

TABLE II-4 (continued)

σ	$\phi(\sigma)$	$\xi(\sigma)$
3.21	.2844400	4.1421000
3.22	.2839100	4.1594000
3.23	.2833900	4.1766000
3.24	.2828700	4.1938000
3.25	.2823500	4.2110000
3.26	.2818300	4.2282000
3.27	.2813200	4.2454000
3.28	.2808100	4.2626000
3.29	.2803000	4.2798000
3.30	.2798000	4.2969000
3.31	.2793000	4.3141000
3.32	.2788100	4.3313000
3.33	.2783200	4.3484000
3.34	.2778300	4.3656000
3.35	.2773400	4.3828000
3.36	.2768600	4.3999000
3.37	.2763800	4.4170000
3.38	.2759100	4.4342000
3.39	.2754300	4.4513000
3.40	.2749600	4.4684000
3.41	.2745000	4.4855000
3.42	.2740300	4.5026000
3.43	.2735700	4.5197000
3.44	.2731100	4.5367000
3.45	.2726600	4.5538000
3.46	.2722100	4.5708000
3.47	.2717600	4.5879000
3.48	.2713100	4.6049000
3.49	.2708700	4.6219000
3.50	.2704300	4.6389000
3.51	.2699900	4.6559000
3.52	.2695500	4.6729000
3.53	.2691200	4.6899000
3.54	.2686900	4.7068000
3.55	.2682600	4.7238000
3.56	.2678300	4.7407000
3.57	.2674100	4.7576000
3.58	.2669900	4.7745000
3.59	.2665700	4.7914000
3.60	.2661600	4.8082000

TABLE II-4 (continued)

σ	$\phi(\sigma)$	$\xi(\sigma)$
3.61	.2657400	4.8251000
3.62	.2653300	4.8420000
3.63	.2649200	4.8588000
3.64	.2645200	4.8756000
3.65	.2641100	4.8924000
3.66	.2637100	4.9092000
3.67	.2633100	4.9260000
3.68	.2629200	4.9427000
3.69	.2625200	4.9595000
3.70	.2621300	4.9762000
3.71	.2617400	4.9929000
3.72	.2613500	5.0096000
3.73	.2609600	5.0263000
3.74	.2605800	5.0429000
3.75	.2602000	5.0596000
3.76	.2598200	5.0762000
3.77	.2594400	5.0928000
3.78	.2590600	5.1094000
3.79	.2586900	5.1260000
3.80	.2583200	5.1425000
3.81	.2579500	5.1591000
3.82	.2575800	5.1756000
3.83	.2572100	5.1921000
3.84	.2568500	5.2086000
3.85	.2564800	5.2251000
3.86	.2561200	5.2416000
3.87	.2557600	5.2580000
3.88	.2554100	5.2745000
3.89	.2550500	5.2909000
3.90	.2547000	5.3073000
3.91	.2543500	5.3236000
3.92	.2540000	5.3400000
3.93	.2536500	5.3563000
3.94	.2533000	5.3727000
3.95	.2529600	5.3890000
3.96	.2526100	5.4053000
3.97	.2522700	5.4216000
3.98	.2519300	5.4378000
3.99	.2515900	5.4541000
4.00	.2512600	5.4703000

These results are displayed in Figs. II-3, II-4 and II-5.

In the range $34.67 \leq t \leq 138.01$, the values of the displacement of the free surface η (r, t) have also been computed from Eq. (II-1) using the Bendix G-15 computer. However, because of their bulk and the fact that they do not have the general interest of Table II-4, these results have not been presented in this report. Also, only the wave envelopes $B^*(r, t)$ and wave period distribution are used for practical purposes. The values of η (r, t) have been plotted only for Case I in Fig. II-6 as a sample of the obtained results. Similar graphs for Cases II and III may eventually be obtained from the performed computations. Fig. II-6 is very difficult to plot because of the large number of crests and troughs (56 crests and 55 troughs). A more accurate plot of Fig. II-6 could be obtained by increasing the number of entries in the performed computations. This would require about four times as many computations, i.e. σ would have to be incremented by 0.0025 in the interval from 0 to 4.

The values of η (r, t) for $t > 138.01$ have not been computed. However, the times of arrival of the crests and troughs may be computed using Eq. (II-19) for positive integers $m \geq 113$. While the times of arrival of crests and troughs are the same for all three cases, it should be noted that a crest in Case I may correspond to a trough in Case II, and vice-versa. For example, the time of arrival $t_{400} = 262.07$ minutes corresponds to a trough in Case I, a crest in Case II, and a crest in Case III. The question

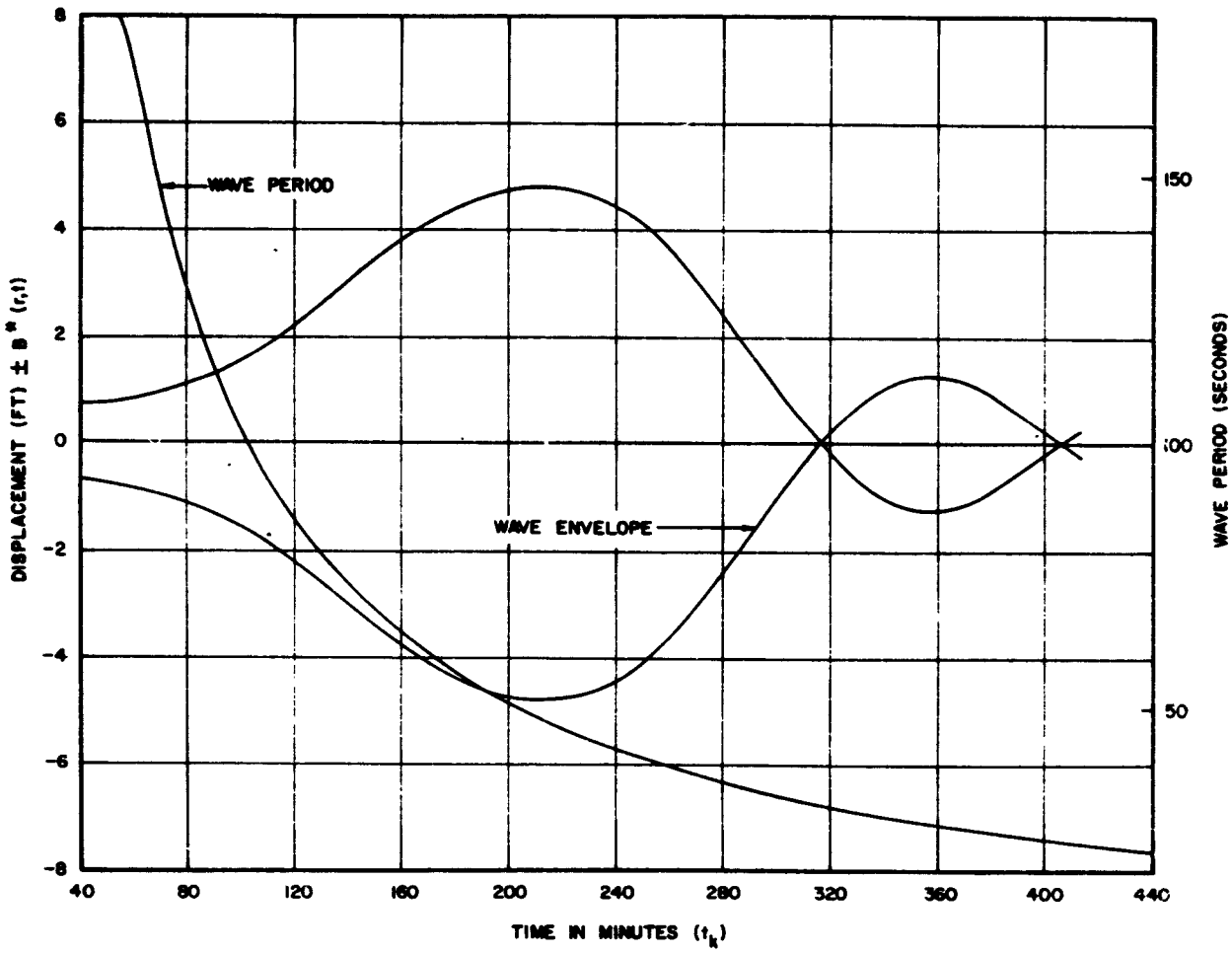

FIGURE II-3

WAVE ENVELOPE AND WAVE PERIOD VERSUS TIME FOR CASE I
(r = 300 NAUTICAL MILES)

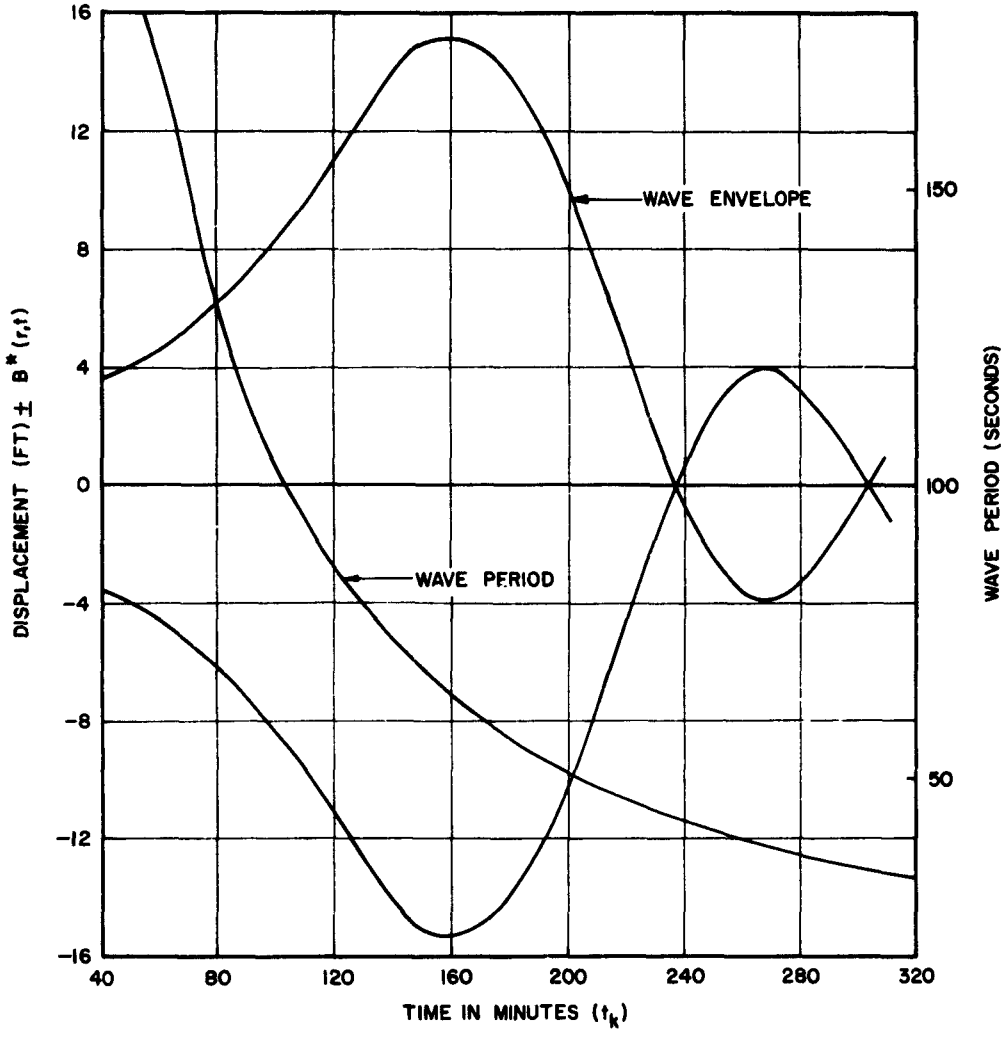

FIGURE II-4
WAVE ENVELOPE AND WAVE PERIOD VERSUS TIME
FOR CASE II (r = 300 NAUTICAL MILES)

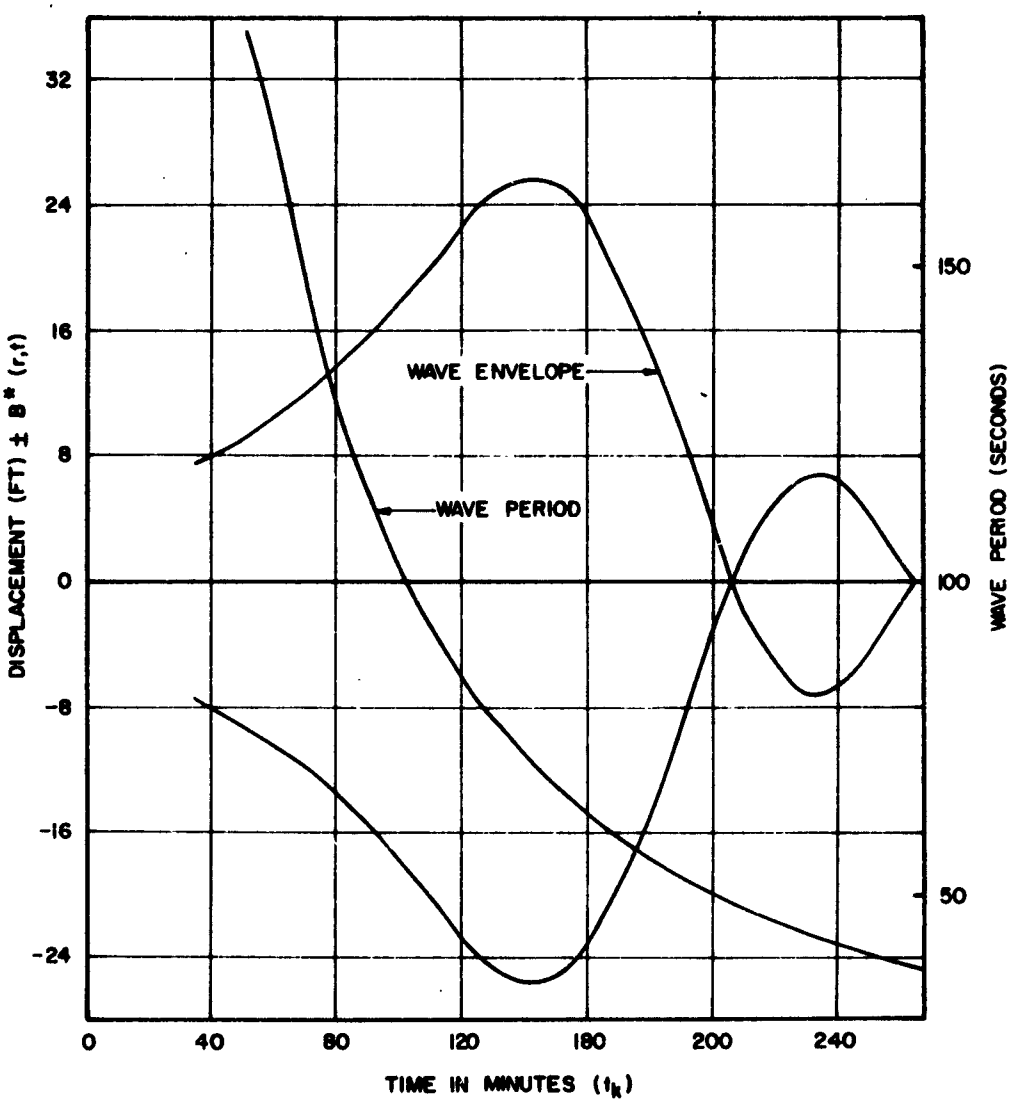

FIGURE II-5
WAVE ENVELOPE AND WAVE PERIOD VERSUS TIME FOR CASE III (r = 300 NAUTICAL MILES)

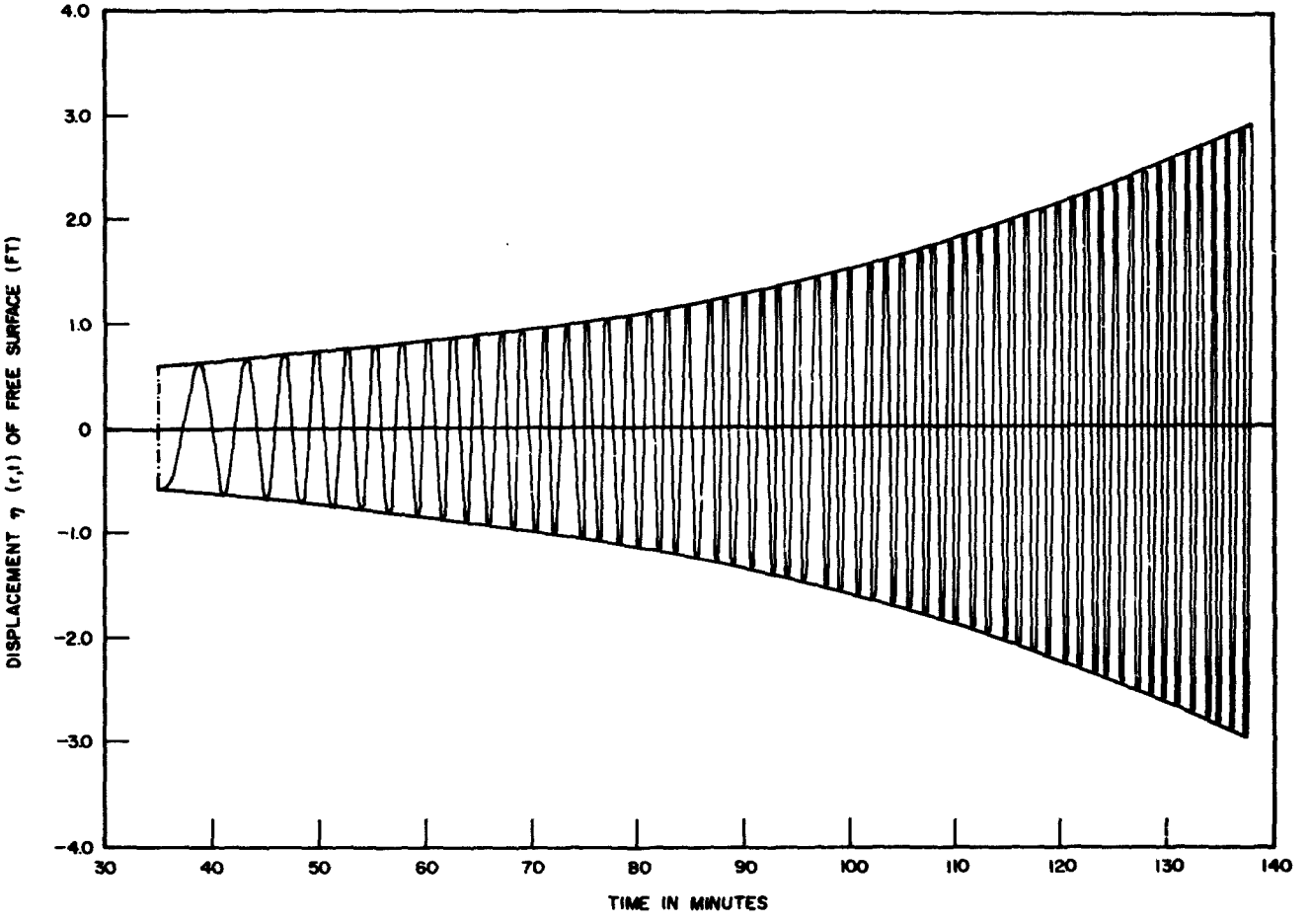

FIGURE II-6

DISPLACEMENT η (r, t) OF THE FREE SURFACE VERSUS TIME FOR CASE I (r = 300 NAUTICAL MILES)

of whether a given time of arrival t_n corresponds to a crest or a trough is settled by means of the following rule:

For positive integers n, the times of arrival t_n represent

1^o troughs for n even and $t_o \leq t_n \leq t_1^*$;

2^o crests for n odd and $t_o \leq t_n \leq t_1^*$;

3^o troughs for n even and $t_1^* \leq t_n \leq t_2^*$;

4^o crests for n even and $t_1^* \leq t_n \leq t_2^*$.

REFERENCES

Kaplan, Kenneth, Norman R. Wallace and Thomas C. Goodale, (1962), "Studies and Analyses of Explosion-Generated Surface Water Waves," United Research Services, Burlingame, California (Preliminary Draft).

Kranzer, Herbert C. and Joseph B. Keller (1955), "Water Waves Produced by Explosions," N. Y. U. Inst. of Math. Sci. AFSWP - 713.

LIST OF SYMBOLS
APPENDIX II

r		Distance from the center of disturbance
λ		Wave length
T		Wave period
h		Depth
η		Free surface elevation above still water level
R		Effective radius of disturbance
η_0		Depth of disturbance at $r = 0$
t		Time variable
σ	$=$	$\frac{2\pi h}{\lambda}$
$\overline{E}(s)$		Hankel transform of function $E(r)$
A	$=$	$\frac{\eta_0}{r^2}$
γ	$=$	$R\sqrt{2}$
θ^*	$=$	$2\pi\left(\frac{t}{T} - \frac{r}{\lambda}\right)$
$\xi(\sigma)$	$=$	$\left[-\sigma \frac{\phi(\sigma)}{\phi'(\sigma)}\right]^{\frac{1}{2}}$

APPENDIX III

SURFACE WAVES GENERATED BY DISTURBANCE ON SEA BED IN CONSTANT-DEPTH OPEN SEA

by

J. A. Hendrickson

1. INTRODUCTION

Even though the sea bed disturbance may, in actuality, be of a complex nature, it is reasonable to assume that the surface waves generated by the disturbance, at distances far removed from the source, will approximate those created by an equivalent source. We will assume equivalence on the basis of input energy and geometrical similitude. Since the actual source (nuclear explosion at sea bed) is three-dimensional in nature, we will assume an equivalent source in the form of a cylindrical upthrust of the sea bed. The time dependency of this upthrust will be assumed to be exponential in nature, with an extremely rapid time decay. This appears to approximate the energy dissipation of actual nuclear blasts. Finally, in order to complete the equivalence between our assumed model and the actual disturbance source, one can match the appropriate fraction of the nuclear blast energy to the energy input of our assumed source.

2. DESCRIPTION AND SOLUTION OF PROBLEM

Fig. III-1 shows the coordinate system and nomenclature appropriate to the assumed disturbance.

We assume the source is described as follows:

$$\eta^* = g(t)\ f(r) \tag{III-1}$$

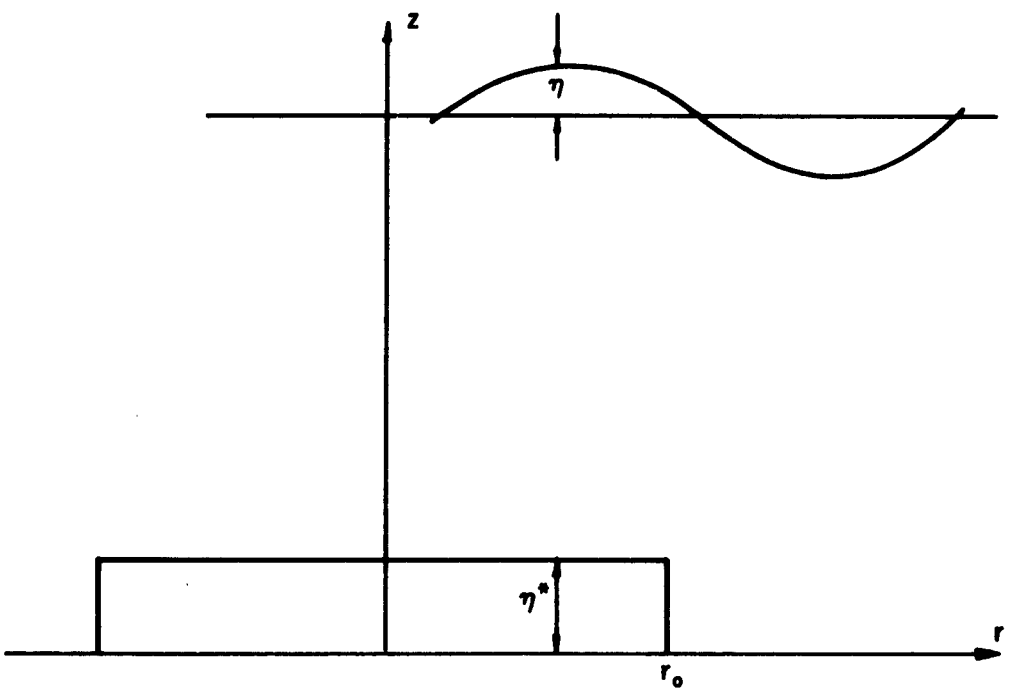

FIGURE III-1

NOTATION

where

$$g(t) = 1 - e^{-st}$$

$$f(r) = \left.\begin{matrix} B \\ 0 \end{matrix}\right\} \begin{matrix} r < r_o \\ r > r_o \end{matrix}$$

and

$$f(r) = \frac{B}{2}, \; r = r_o$$

The field equation of the potential function ϕ is assumed to be of the time independent form

$$\nabla^2 \phi = \frac{\partial^2 \phi}{\partial r^2} + \frac{1}{r}\frac{\partial \phi}{\partial r} + \frac{\partial^2 \phi}{\partial z^2} = 0 \qquad \text{(III-2)}$$

while the boundary conditions appropriate to our problem may be written as follows:

$$\eta_t^* = \phi_z \quad \text{at} \quad z = 0 \qquad \text{(III-3)}$$

and

$$\left.\begin{matrix} g\,\phi_z + \phi_{tt} = 0 \\ \phi_z = \eta_t \end{matrix}\right\} \quad \text{at} \quad z = d$$

Since we are dealing with a semi-infinite media, we must include all possible frequencies and wave lengths in the spectra of generated surface waves. Hence, it may be shown that the appropriate bounded solution to Eq. (III-2) may be written as

$$\phi = \int_o^\infty \int_o^\infty J_o(ur) \left[A(u,\sigma) \sinh uz + B(u,\sigma) \cosh uz \right] \cos \sigma t \; du \, d\sigma \qquad \text{(III-4)}$$

It is easily shown that the boundary condition at $z = d$ is satisfied provided

$$B(u,\sigma) = A(u,\sigma) \left\{ \frac{\sigma^2 \sinh ud - ug \cosh ud}{ug \sinh ud - \sigma^2 \cosh ud} \right\} \qquad \text{(III-5)}$$

From Eq. (III-1)

$$\eta_t^* = \left.\begin{array}{ll} Bse^{-st} & r < r_o \\ 0 & r > r_o \end{array}\right\}$$

It may be easily demonstrated from the Fourier-Bessel theory that η_t^* may equivalently be expressed as

$$\eta_t^* = \frac{2s^2 Br_o}{\pi} \int_o^\infty \frac{\cos \sigma t \, d\sigma}{\sigma^2 + s^2} \int_o^\infty J_1(ur_o)\, J_o(ur)\, du \qquad \text{(III-6)}$$

However, from Eq. (III-4), it is easily seen that

$$\phi_z \Big|_{z=0} = \int_o^\infty \cos \sigma t \, d\sigma \int_o^\infty u A(u,\sigma)\, J_o(ur)\, du \qquad \text{(III-7)}$$

Hence, using the first of Eqs. (III-3) and Eqs. (III-6) and (III-7), it is seen that the coefficient $A(u, \sigma)$ is given by the relation

$$A(u,\sigma) = \frac{2s^2 B r_o}{\pi u} \cdot \frac{J_1(u r_o)}{(\sigma^2 + s^2)} \qquad \text{(III-8)}$$

Thus, using the last of Eqs. (III-3) and Eqs. (III-4), (III-5) and (III-8), we obtain, after some simplification and rearranging

(III-9)

$$\eta_1 = -\frac{2s^2 B r_o}{\pi} \int_o^\infty \frac{J_1(ur_o)\, J_o(ur)}{\cosh ud}\, du \int_o^\infty \frac{\sigma^2 \cos \sigma t\, d\sigma}{(\sigma^2+s^2)\left[ug \tanh ud - \sigma^2\right]}$$

If we let $x = ud$, and integrate Eq. (III-9) with respect to time, we obtain

(III-10)

$$\eta = \frac{2s^2 B r_o}{\pi d} \int_o^\infty \frac{J_1(x\frac{r_o}{d})\, J_o(x\frac{r}{d})\, dx}{\cosh x} \int_o^\infty \frac{\sigma \sin \sigma t\, d\sigma}{(\sigma^2+s^2)\left[\sigma^2 - \frac{g}{d} x \tanh x\right]}$$

It may easily be shown that the second integral in Eq. (III-10) has the solution

(III-11)

$$\int_o^\infty \frac{\sigma \sin \sigma t\, d\sigma}{(\sigma^2+s^2)\left[\sigma^2 - \frac{g}{d} x \tanh x\right]} = \frac{\pi}{2}\left\{\frac{\cos\left[\frac{gt}{d}^2 x \tanh x\right]^{1/2} - \exp(-st)}{s^2 + \frac{g}{d} x \tanh x}\right\}$$

We are interested in the solution to Eq. (III-10) for the case $t > 0$, $s >> 1$. Since the integral of Eq. (III-10) is extremely convergent with x, we may substitute Eq. (III-11) into Eq. (III-10) and use the fact that $s >> 1$ with the approximate result

$$\eta \approx B\left(\frac{r_o}{d}\right) \int_0^\infty \frac{J_1\left(x\frac{r_o}{d}\right) J_o\left(x\frac{r}{d}\right) \cos\left[\frac{gt^2}{d} x \tanh x\right]^{1/2} dx}{\cosh x} \qquad \text{(III-12)}$$

If we write

$$W = \pi r_o^2 B \rho_w g d \qquad \text{(III-13)}$$

where ρ_w = density of fluid, we may rewrite Eq. (III-12) as follows:

$$\eta = 2K\left(\frac{r_o}{d}\right)^{-1} \int_0^\infty \frac{J_1\left(\frac{r_o}{d}x\right) J_o\left(\frac{r}{d}x\right) \cos\left(\frac{r}{d}\theta\sqrt{x \tanh x}\right) dx}{\cosh x} \qquad \text{(III-14)}$$

where $K = \dfrac{W}{2\pi \rho_w g d^3}$ and $\theta = \dfrac{t}{r}\sqrt{g d}$

Since we are ultimately interested in the asymptotic expansion of η for $\frac{r}{d} >> 1$, we note from Eq. (III-14) that the integrand vanishes as $x \to 0$. Hence the only contributions occur when $x > 0$. Thus we assume that $\frac{r}{d} x$ is large enough for the following asymptotic expansion to be valid:

$$J_o\left(\frac{r}{d}x\right) \approx \sqrt{\frac{2d}{\pi r x}} \cos\left(\frac{r}{d}x - \frac{\pi}{4}\right) \qquad \text{(III-15)}$$

Using the relation

$$\cos a \cos b = \frac{1}{2}\left[\cos(a+b) + \cos(a-b)\right]$$

we may write

$$\left[\cos\frac{r}{d}\left(x-\frac{\pi d}{4r}\right)\right]\left[\cos\left(\frac{r}{d}\theta\sqrt{x\tanh x}\right)\right]$$

$$=\frac{1}{2}\left\{\cos\frac{r}{d}\left(x+\theta\sqrt{x\tanh x}-\frac{\pi d}{4r}\right)\right. \qquad \text{(III-16)}$$

$$\left.+\cos\frac{r}{d}\left(x-\theta\sqrt{x\tanh x}-\frac{\pi d}{4r}\right)\right\}$$

Using Eqs. (III-15) and (III-16) with Eq. (III-17), we obtain the following approximate integral form for the surface profile valid for $\frac{r}{d} >> 1$:

(III-17)

$$\eta \approx 2K\left(\frac{r_o}{d}\right)^{-1}\sqrt{\frac{d}{2\pi r}}\int_0^\infty \frac{J_1\left(x\frac{r_o}{d}\right)\left\{\cos\frac{r}{d}\left(x+\theta\sqrt{x\tanh x}-\frac{\pi d}{4r}\right)+\cos\frac{r}{d}\left(x-\theta\sqrt{x\tanh x}-\frac{\pi d}{4r}\right)\right\}dx}{\sqrt{x}\quad\cosh x}$$

Since $\frac{r}{d} >> 1$, it is clear that the contribution of the term $\cos\frac{r}{d}\left(x+\theta\sqrt{x\tanh x}-\frac{\pi d}{4r}\right)$ in Eq. (III-17) may be ignored since a slight change in x causes the integrand to rapidly oscillate from positive to negative values in such a fashion that the net integral is approximately zero. The remaining term, however, possesses stationary points (dependent on θ) and will hence contribute a finite value to the total integral.

Hence we may write Eq. (III-17) as follows:

$$\eta \approx 2K\left(\frac{r_o}{d}\right)^{-1}\sqrt{\frac{d}{2\pi r}}\ R_e\int_0^\infty \psi(x)\exp\left(i\frac{r}{d}\right)\phi(x)\,dx \qquad \text{(III-18)}$$

where

$$\psi(x) = \frac{J_1\left(\frac{r_0}{d}x\right)\ \mathrm{sech}\ x}{\sqrt{x}}$$

and

$$\phi(x) = x - \theta\sqrt{x\ \tanh x} - \frac{\pi d}{4r}$$

Eq. (III-18) is of such a form that the method of "stationary phase" may be used to obtain a satisfactory solution. Although the method will not be described herein, the results will be used in solving Eq. (III-18) and the details of the method may be found in Stoker (1957).*

Given an integral of the form $I(K) = \int_a^b \psi(\xi, k)\, e^{ik\phi(\xi)}\, d\xi$ where $k >> 1$ while $\psi(\xi, k)$ is not a rapidly oscillating function of the variable ξ Then the value of $I(k)$ may be written as follows:

$$I(k) = \sum_r \psi(a_r, k)\left(\frac{2\pi}{k\left|\phi''(a_r)\right|}\right)^{1/2} \exp\left\{i\left(k\phi(a_r) \mp \frac{\pi}{4}\right)\right\} + O\left(\frac{1}{k}\right) \qquad \text{(III-19)}$$

where the sum is taken over the zeros a_r of $\phi'(\xi)$ in the region $a \leqslant \xi \leqslant b$ at which $\phi''(a_r) \neq 0$ The sign of the

---

* Stoker, J. J. (1957), "Water Waves," Pure and Applied Mathematics, Vol. IV, p. 181.

quantity $\pi/4$ in Eq. (III-19) is taken to be the same as the sign of $\phi''(\alpha_r)$. Hence, using Eq. (III-18) we desire the solution to the relation

$$\phi'(x) = 1 - \frac{\theta}{2} \frac{\left[\tanh x + x \operatorname{sech}^2 x\right]}{\sqrt{x \tanh x}} = 0 \qquad \text{(III-20)}$$

Let α_r be the r roots of Eq. (III-20). Hence

$$\theta = \frac{2\sqrt{\alpha_r \tanh \alpha_r}}{\tanh \alpha_r + \alpha_r \operatorname{sech}^2 \alpha_r} \qquad \text{(III-21)}$$

It may be shown that

(III-22)

$$\phi''(\alpha_r) = \frac{\theta}{2}\left\{\frac{\left[\tanh \alpha_r + \alpha_r \operatorname{sech}^2 \alpha_r\right]^2}{2(\alpha_r \tanh \alpha_r)^{3/2}} - \frac{2 \operatorname{sech}^2 \alpha_r}{(\alpha_r \tanh \alpha_r)^{1/2}}(1 - \alpha_r \tanh \alpha_r)\right\}$$

and it is to be noted that $\phi''(\alpha_r) \geq 0$, and that there is but one solution α_r to Eq. (III-21) for a given value of $\theta \geq 1$. Note that the value $\theta = 1$ corresponds to the arrival of a surface disturbance propagating with a phase velocity of value $\sqrt{gd}$.

Finally, using Eq. (III-14) we find, for $\frac{r}{d} >> 1$, the asymptotic behavior of η to be the following:

$$\eta = K \left(\frac{r}{d}\right)^{-1} \frac{J_1\left(a_r \frac{r_o}{d}\right)}{\left(\frac{r_o}{d}\right)} \; g(a_r) \cos\left(\frac{r}{d} f(a_r)\right) + O\left(\frac{r}{d}\right)^{-3/2} \qquad \text{(III-23)}$$

where

$$g(a_r) = \frac{2 \operatorname{sech} a_r}{\sqrt{a_r}\left[\phi''(a_r)\right]^{1/2}}$$

and

$$f(a_r) = \theta \sqrt{a_r \tanh a_r} - a_r$$

It may easily be shown that Eq. (III-23) has its maximum at $\theta = 1$ and that the peak amplitude (M. W. L. to crest elevation) is given by the expression

$$\eta_{\theta=1} = K \left(\frac{r}{d}\right)^{-1} \qquad \text{(III-24)}$$

The interesting thing to note from Eq. (III-24), remembering that $K = \frac{W}{d^3} \times \text{cst}$, is that the peak surface disturbance is only dependent on the source energy (W), the water depth (d), and the ratio of radial position to water depth $\left(\frac{r}{d}\right)$. Also the amplitude is inversely proportional to the radial position (in contrast to the inverse cube root of position for a two-dimensional source).

Because of the rapid convergence of the integral (see Eq. (III-15)) it is to be expected that the surface disturbance is relatively insensitive to the ratio $\frac{r_o}{d}$ (radius of surface disturbance to water depth) for values of $\frac{r_o}{d} < 1$. (This is so due to the relative independence on $\frac{r_o}{d}$ of the function $\frac{J_1\left(\frac{r_o}{d} x\right)}{\frac{r_o}{d}}$).

Fig. III-2 shows the relation $\frac{\eta}{k}$ vs θ as obtained from Eq. (III-23) for $\frac{r}{d} = 10$ and $\frac{r_o}{d} < 1$. Also shown in Fig. III-2 is the value of the integral of Eq. (III-14) vs. θ for $\frac{r}{d} = 10$ and $\frac{r_o}{d} = \frac{1}{2}$ obtained by numerical integration.

It may be seen that the agreement between the asymptotic approximate solution and the numerical solution is not too good for the first positive peak. However, the agreement on the first negative peak is quite good (10% error). Also, the agreement on the absolute maximum value of the integral is quite good.

It is felt that better agreement would be obtained for larger values of $\frac{r}{d}$ since such a case would improve the asymptotic approximations.

Finally, Figs. III-3 and III-4 show the results of the asymptotic integration for $\frac{r_o}{d} = \frac{1}{2}$ and $\frac{r}{d} = 100$ and 300 respectively.

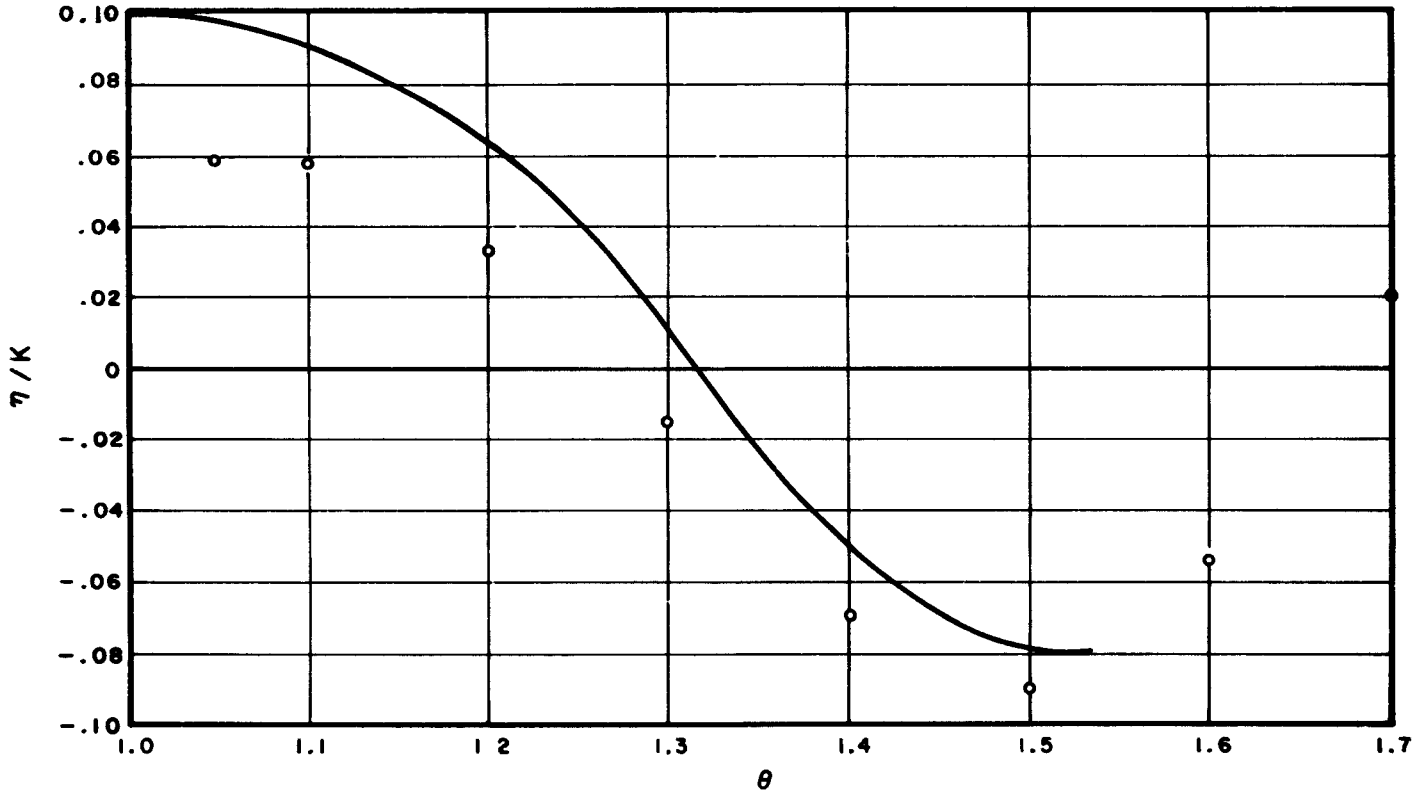

FIGURE III-2
SURFACE PROFILE DUE TO CIRCULAR SEA BED DISTURBANCES OF ENERGY W FOR $r_o/d = 1$, $r/d = 10$

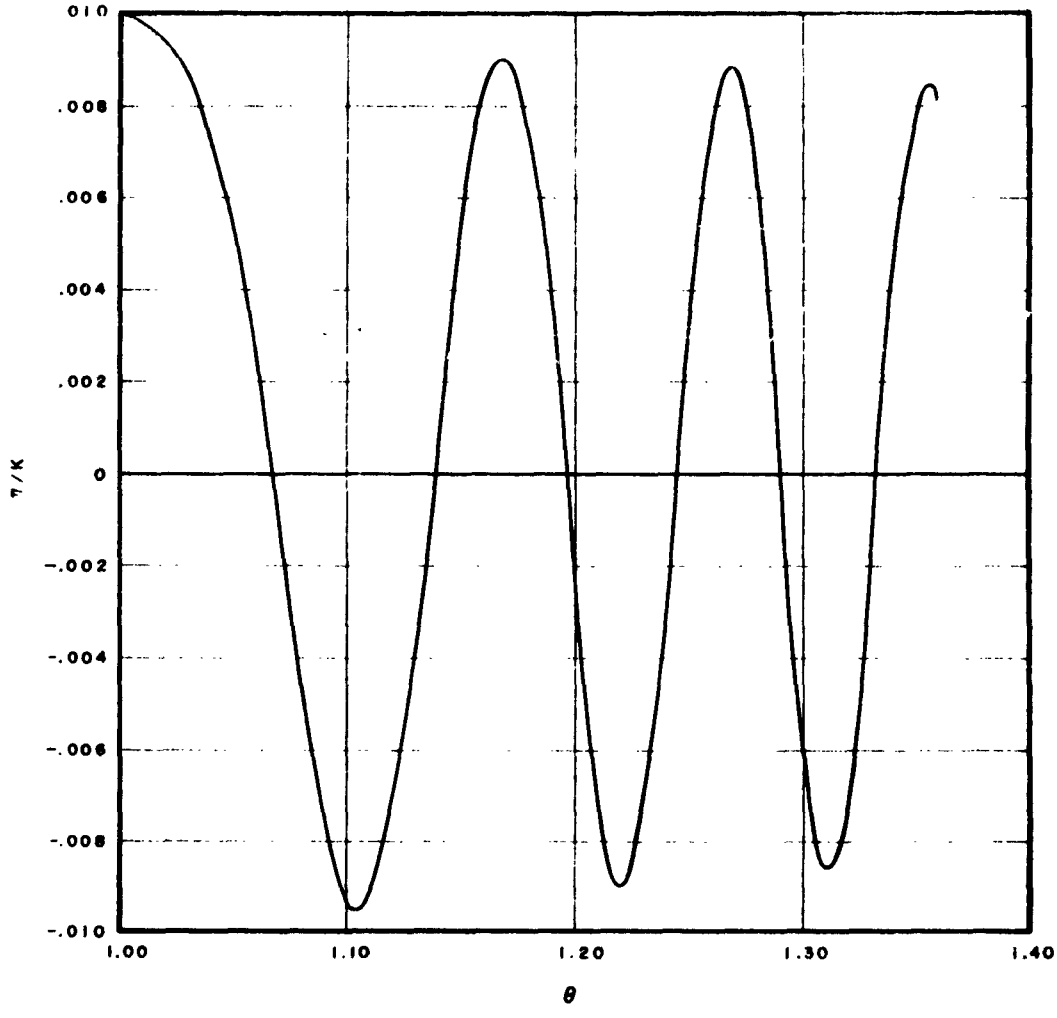

FIGURE III-3
SURFACE PROFILE $r_o/d = 1/2$, $r/d = 100$

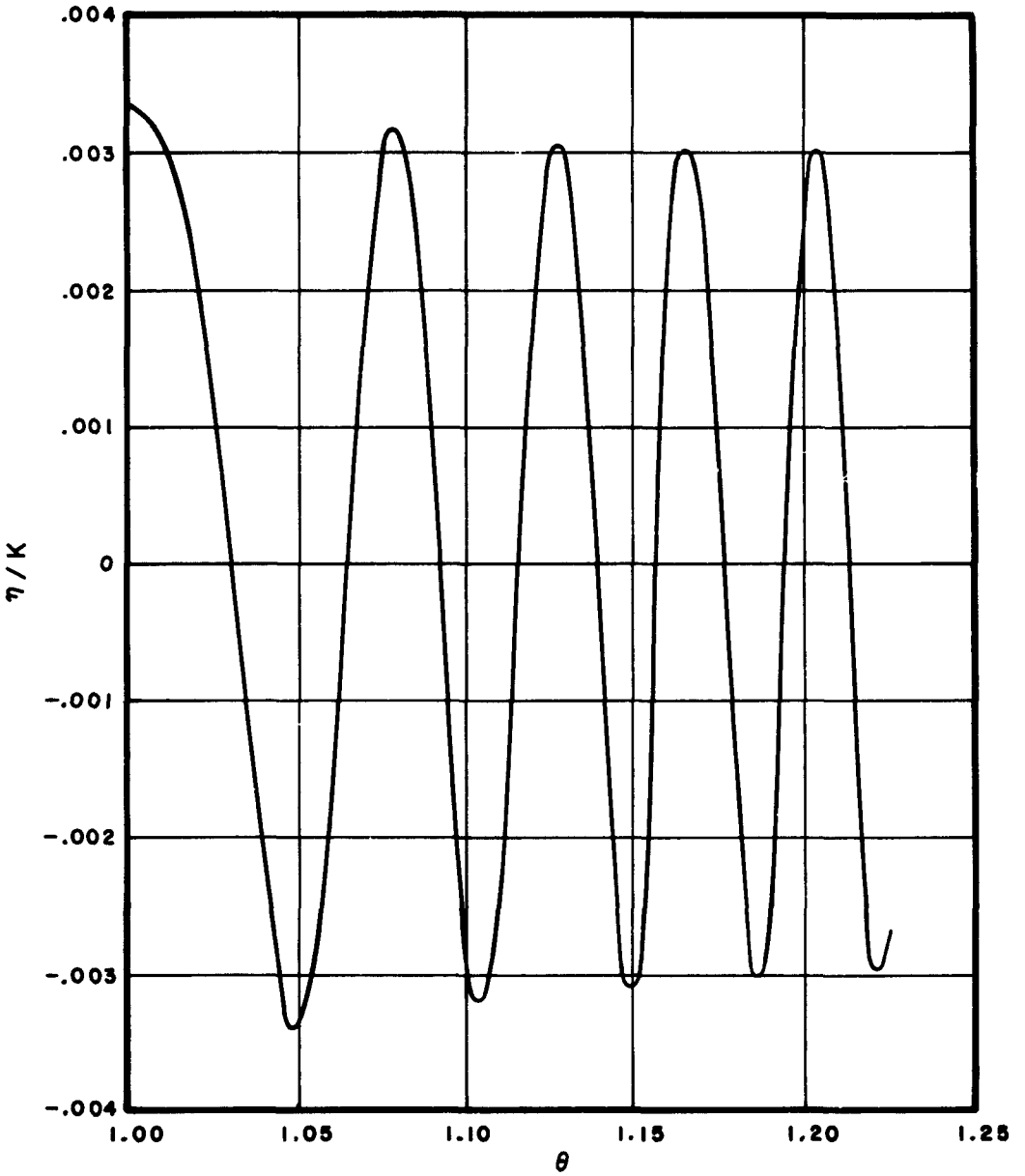

FIGURE III-4
SURFACE PROFILE $r_o/d = 1/2$, $r/d = 300$

LIST OF SYMBOLS
APPENDIX III

r	Horizontal distance from the origin
z	Vertical coordinates ($z = 0$ at the bottom)
η_1^*	Height of the bottom disturbance as function of time
t	Time
s	Coefficient of decay of the bottom disturbance with respect to time
r_o	Radius of the original disturbance
B	Final height of the bottom disturbance when time tends to infinity
ϕ	Velocity potential function
d	Depth (mid-water level: $z = d$)
u	Space frequency. Dimensionally equal to $\frac{2\pi}{L}$ where L is length
σ	Time frequency. Dimensionally equal to $\frac{2\pi}{T}$ where T is an interval of time
ρ_w	Density of fluid
g	Gravity acceleration
W	Energy of the original disturbance
K	Coefficient $= \frac{W}{2\pi \rho_w g d^3} = \frac{r_o^2 B}{2 d^2}$
θ	Dimensionless time $\frac{t}{r}\sqrt{gd}$

APPENDIX IV

THE PRINCIPLE OF SUPERPOSITION AND THE THEORY OF CAUCHY-POISSON

By

B. Le Méhauté

1. FOREWORD

The author has received some comments on the validity of the following calculations. Some consider this new approach as exact and powerful as the theories based on the principle of the stationary phase. At the opposite, some others consider this approach as invalid. Whatever its exactness, this work has been included in this report. The author already indicates some limits of validity of his calculations. It will be the subject of further investigation and up to other investigators to give the pros and cons of this new theory. It is pointed out that if this theory is found to be valid in some respects, it may become a powerful way of solving many related problems. It has been seen in Appendix I that the wave motion due to a disturbance of infinitesimal dimensions has been investigated by Cauchy-Poisson. In this appendix the principle of superposition is applied in order to calculate the wave motion due to a disturbance of finite dimension. It is demonstrated that:

a. The elevation becomes instantaneously infinite at the edge of the initial disturbance, whatever the intensity, the area and the shape of this disturbance. So, the splash phenomenon is demonstrated and explained.

b. Far from the impulse the wave pattern does not depend upon the area and shape of the impulse, but as a first approximation its amplitude is proportional to the total value of its intensity.

The wave motion caused by some particular simple shape of an initial disturbance of finite dimensions is calculated.

Then, a discussion gives the limits of validity and the physical meaning of the presented mathematical construction based on the principle of superposition and the theory of Cauchy-Poisson.

2. INTRODUCTION

The theory of waves produced by an impulse or an initial local disturbance on a free surface has been investigated, particularly by Cauchy-Poisson in the case of a three-dimensional motion, and by Lamb* in the case of a two-dimensional motion. (In the following, the notations of Lamb are used). In both cases, the solutions have been obtained by neglecting the convective inertia and friction forces, thus the theory is linear and valid for slow motion.

The calculations can be carried out by application of the Fourier double integral:

$$f(x) = \frac{1}{\pi}\int_0^\infty dk \int_{-\infty}^{\infty} f(d)\cos k(x-a)\,da$$

for a two-dimensional motion, or

$$f(\varpi) = \int_0^\infty J_0(k\varpi)\,k\,dk \int_0^\infty f(a)\,J_0(ka)\,a\,da$$

for a three-dimensional motion.

It has been assumed that the initial disturbance or initial impulse is confined to the immediate neighborhood of the origin so that $f(a)$ vanishes for all but infinitesimal values for a. (See Fig. IV-1) That is:

$$\int_{-\infty}^{\infty} f(a)da = \int_{-a_1}^{a_1} f(a)da = 1$$

* Lamb, H. (1932 Edn.) Hydrodynamics. Cambridge Univ. Press, Eng.

in the case of a two-dimensional motion, and

$$\int_0^{\infty} f(a)\, 2\pi a\, da = \int_0^{a_1} f(d)\, 2\pi a\, da = 1$$

in the case of a three-dimensional motion where a_1 is always an infinitesimal.

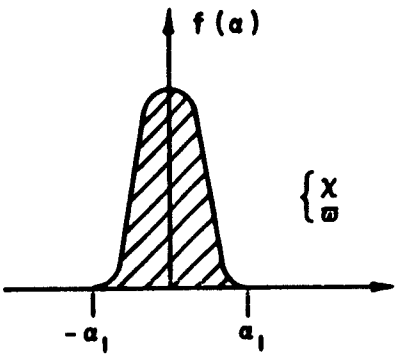

FIGURE IV-1
DEFINITION OF AN ELEMENTARY
FREE SURFACE DISTURBANCE

From this assumption, it has to be noted that since the integral has a finite value equal to unity and since a_1 is an infinitesimal, $f(a)$ must be infinity. This assumption is in complete contradiction with the assumption of linear theory which requires the motion to be very slow and even infinitesimal in order to be exact.

Later on, other studies were made to investigate the wave motion due to a disturbance of finite dimensions. These were also based on the assumption of linear theory and on the use of the Fourier integral. In this case the initial disturbance was not assumed to be confined to the immediate neighborhood of the origin, but instead, it was assumed to be distributed on a given range.

Hence, the later theories were more realistic and more in accordance with physical phenomena. Unfortunately, the difficulty in the evaluation of the Fourier integral limited the initial disturbance $f(\alpha)$ to relatively simple form.

In this appendix an attempt has been made to find a more general method for application to more complicated forms of initial disturbance including those varying with time. It is the results of these investigations which are presented here.

This method is based on the principle of superposition and the theory of Cauchy-Poisson. Indeed, since this theory is linear, the principle of superposition is theoretically valid and the wave motion caused at a given time and at a given location by a definite disturbance varying with time should be the sum of wave motions due to infinitesimally small disturbances occurring at various initial times t_o.

Here a quotation of Lamb is worth recalling:

> "In any practical case, however, the initial elevation is distributed over a band of finite breadth; we will denote this breadth by 1. The disturbance at any point P is made up of parts due to the various elements, $d\alpha$, say, of the breadth 1; these are to be calculated by the preceding formulae, and integrated over the breadth of the band. In the result,the mathematical infinity and other perplexing peculiarities, which we meet with in the case of a concentrated line-source, disappear. It would be easy to write down the requisite formulae, but, as they are not very tractable, and contain nothing not implied in the preceding statement, they may be passed over."

3. GENERAL PROCESS OF CALCULATION

It is recalled that the solutions for the elevation as a function of time t and distance from the origin(χ or ϖ) are, in the case of a two-dimensional motion

$$\eta = \frac{1}{\pi\chi}\left[\frac{gt^2}{2\chi} - \frac{1}{3.5}\left(\frac{gt^2}{2\chi}\right)^3 + \frac{1}{3.5.7.9}\left(\frac{gt^2}{2\chi}\right)^5 - \cdots\right] \cdots \qquad \text{(IV-1)}$$

and in the case of a three-dimensional motion

$$\zeta = \frac{1}{2\pi\varpi^2}\left[\frac{1^2}{2!}\frac{gt^2}{\varpi} - \frac{1^2.3^2}{6!}\left(\frac{gt^2}{\varpi}\right)^3 + \cdots\right] \cdots \qquad \text{(IV-2)}$$

From the assumption that the motion is linear, it is evident that if the integral of initial elevation (or impulse) has a value A instead of unity:

$$\int_{-\infty}^{\infty} f(a)\, da = A$$

or

$$\int_{-\infty}^{\infty} f(a)\, 2\pi a\, da = A$$

η and ζ are given by the above formulas (IV-1) and (IV-2) respectively multiplied by A.

These two expressions may be written as

$$\eta = \frac{A}{\pi\chi}\sum_{n=0}^{\infty}\frac{(-1)^n}{1.3.5.7\ldots(4n+1)}\left(\frac{gt^2}{2\chi}\right)^{2n+1} \cdots \qquad \text{(IV-3)}$$

and

$$\zeta = \frac{A}{2\pi\varpi^2} \sum_{n=0}^{\infty} \frac{(-1)^n \left[1.3.5\ldots(2n+1)\right]^2}{(4n+2)!} \left(\frac{gt^2}{\varpi}\right)^{2n+1} \qquad \text{(IV-4)}$$

Now, consider the cases where the initial disturbance is located at a point $x = X$, in the case of a two-dimensional motion (See Fig. IV-2), and at a point $Z = \rho_0 e^{i\theta}$ in the case of a three-dimensional motion (See Fig. IV-3). Z is a complex number.

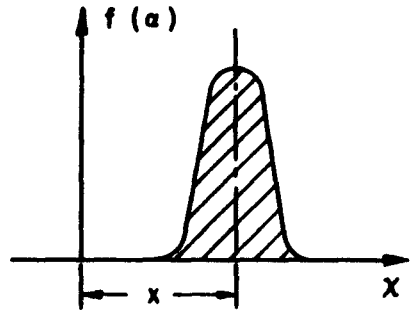

FIGURE IV-2
NOTATION FOR TWO-DIMENSIONAL DISTURBANCE

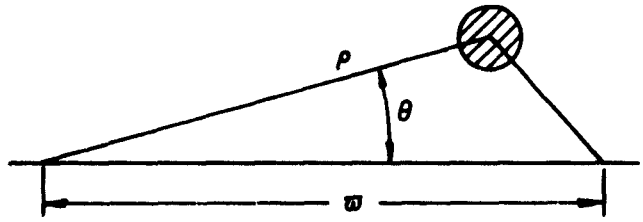

FIGURE IV-3
NOTATION FOR THREE-DIMENSIONAL DISTURBANCE

The above formulas (IV-1) and (IV-2) are valid provided x and w are replaced by $X - X$, $w - \rho e^{i\theta}$ respectively. The argument for w is taken to be zero by reason of symmetry.

A similar change of origin of time may also be inserted by replacing t by $(t - t_1)$ involving an initial perturbance at time t_1. Inserting these values and assuming that A depends upon the location X, or (ρ, θ) and time t_1, one obtains:

$$\eta = \frac{A(X,t_1)}{\pi(X-X)} \sum_{n=0}^{\infty} \frac{(-1)^n}{1.3.5...(4n+1)} \cdot \left[\frac{g(t-t_1)^2}{2(X-X)}\right]^{2n+1}$$

and

$$\zeta = \frac{A(\rho,\theta,t_1)}{\pi(w-\rho e^{i\theta})^2} \sum_{n=0}^{\infty} \frac{(-1)^n\left[1.3..(2n+1)\right]^2}{(4n+2)!} \left[\frac{g(t-t_1)^2}{w-\rho e^{i\theta}}\right]^{2n+1}$$

From the assumption that the theory is linear, the principle of superposition may be applied, and it is deduced that the free surface is obtained by a superposition of all the perturbances created at different places and at different times. In the following t_1 will be taken equal to zero.

In particular, one can imagine that there is a perturbance

$A(X)$ at any place $-R \leq X \leq R$

$A(\rho,\theta)$ at any place $\begin{cases} 0 < \rho \leq R \\ 0 \leq \theta \leq 2\pi \end{cases}$

such that

$$A(X) = \int_{X-a_1}^{X+a_1} f(X)\, dX$$

$$A(\rho,\theta) = \int_{\rho-a_1}^{\rho+a_1} f(\rho,\theta)\, d\theta\, d\rho$$

In that case $f(X)$ and $f(\rho,\theta)$ do not need to be infinite to produce finite wave and consequently A may be infinitesimally small, since it is now the product of a finite value and an infinitesimally small area. However, the total values

$$\int_{-R}^{R} f(X)\, dX \qquad \text{and} \qquad \int_0^R \int_0^{2\pi} f(\rho,\theta)\, d\theta\, d\rho$$

in which R has a finite value, have a finite value and involve a finite amount of energy, which is the total energy of the initial perturbance.

Now at a given time t and at a given place x or $(\varpi,0)$ the wave motion will be according to the principle of superposition, the sum of all the elementary wave motions caused by the various places X or (ρ,θ).

Hence, η and ζ are given by the following integrals where x and t are considered as constant and X or (ρ,θ) as variable:

$$\eta = \int_{-R}^{R} \frac{f(X)}{\pi(x-X)} \sum_{n=0}^{\infty} \frac{(-1)^n}{1.3\ldots(4n+1)} \left[\frac{gt^2}{2(x-X)}\right]^{2n+1} dX$$

$$\zeta = \int_0^R \int_0^{2\pi} \frac{f(\rho,\theta)}{2\,(\varpi-\rho e^{i\theta})^2} \sum_{n=0}^{\infty} \frac{(-1)^n \left[1.3\ldots(2n+1)\right]^2}{(4n+2)!} \left[\frac{gt^2}{\varpi-\rho e^{i\theta}}\right]^{2n+1} d\theta\, d\rho$$

or rearranging:

$$\eta = \frac{1}{\pi}\sum_{n=0}^{\infty}\frac{(-1)^n}{1.3.\ldots.(4n+1)}\left(\frac{gt^2}{2}\right)^{2n+1}\int_{-R}^{R}\frac{f(X)\,dX}{(x-X)^{2n+2}}$$

$$\zeta = \frac{1}{2\pi}\sum_{n=0}^{\infty}\frac{(-1)^n\left[1.3\ldots(2n+1)\right]^2}{(4n+2)!}\left(\frac{gt^2}{2}\right)^{2n+1}\int_{0}^{R}\int_{0}^{2\pi}\frac{f(\rho\,\theta)\,d\theta\,d\rho}{(\omega-\rho e^{i\theta})^{2n+3}}$$

Without any more calculation, it may be seen that when x or ω is large with respect to the maximum values for X or ρ that is R, such that X and ρ may be neglected in the expressions $(x - X)$ and $(\omega - \rho e^{i\theta})$, the obtained formulas for η and ζ are the same as formulas (IV-1) and (IV-2) above provided the second term is multiplied by

$$\int_{-R}^{R} f(X)\,dX \qquad \text{and} \qquad \int_{0}^{R}\int_{0}^{2\pi} f(\rho,\theta)\,d\theta\,d\rho$$

respectively; that is, by the total value of the initial disturbance. This means that far from the initial disturbance the wave pattern does not depend upon the shape and stretch of the disturbance, and the elevation is linearly correlated with the total impulse or disturbance. This result is consistent with the above remark on the multiplication factor A. But in that case, this multiplication factor is the sum of all the infinitesimal local values $A(X)$ or $A(\rho,\theta)$.

Moreover, it may be noticed that when x and ϖ approach R, then η and ζ tend to infinity (except when t = 0), since the numerator has a finite value, whatever the shape for f(x) and $f(\rho,\theta)$. This is in accordance with the well known fact that when a circular plate falls into water, the free surface suddenly rises very high in the shape of a duke's crown at the edge of the plate.

Later, the validity of such a theory will be discussed. Now some specific simple cases are calculated.

4. THE ANALYSIS OF SOME SPECIFIC CASES

First the case of a two-dimensional motion caused by a uniform disturbance is analyzed. In this case f(X) is a constant: say f(X) = b (See Fig. IV-4).

$$\int_{-\infty}^{\infty} f(X)\,dX = \int_{-R}^{R} f(X)\,dX = 2Rb$$

Then:

$$\eta = \frac{b}{\pi}\sum_{n=0}^{\infty} \frac{(-1)^n}{1.3.\ldots(4n+1)}\left(\frac{gt^2}{2}\right)^{2n+1}\int_{-R}^{R}\frac{dX}{(X-X)^{2n+2}}$$

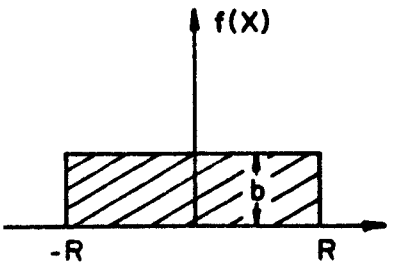

FIGURE IV-4
MATHEMATICAL MODEL DISTURBANCE

The following general integral I_n permits the direct establishment of the complete series:

$$I_n = \int_{-R}^{R} \frac{dX}{(x-X)^{2n+2}} = \frac{1}{2n+1}\left[\frac{1}{(x-R)^{2n+1}} - \frac{1}{(x+R)^{2n+1}}\right]$$

Finally:

$$\eta = \frac{b}{\pi}\sum_{n=0}^{\infty} \frac{(-1)^n}{1.3..(4n+1)}\left(\frac{gt^2}{2}\right)^{2n+1} \cdot \frac{1}{2n+1}\left[\frac{1}{(x-R)^{2n+1}} - \frac{1}{(x+R)^{2n+1}}\right]$$

or developing

$$\eta = \frac{b}{\pi}\left[\frac{gt^2}{2}\left(\frac{1}{x-R} - \frac{1}{x+R}\right) - \frac{1}{3.5}\left(\frac{gt^2}{2}\right)^3 \frac{1}{3}\left(\frac{1}{(x-R)^3} - \frac{1}{(x+R)^3}\right) + \cdots\right]$$

It is verified that when $x \to \mp R$. $\eta \longrightarrow \infty$ except when $t = 0$. On the other hand, when x^2 tends to be large with respect to R^2, it is found after a number of simplifications:

$$\eta = \frac{2Rb}{\pi x}\sum_{n=0}^{\infty} \frac{(-1)^n}{1.3...(4n+1)}\left(\frac{gt^2}{2\pi}\right)^{2n+1}$$

which is formula (IV-3) in which $2Rb$ has taken the place of A; only the elevation depends upon the value of the disturbance, but the wave pattern is identical.

Now considering the base of an impulse in the form of parabola;

$$f(X) = b - aX^2$$

Then

$$\eta = \frac{1}{\pi} \sum_{n=0}^{\infty} \frac{(-1)^n}{1.3\ldots(4n+1)} \left(\frac{gt^2}{2} \right)^{2n+1} \int_{-R}^{R} \frac{(b - aX^2)\, dX}{(x - X)^{2n+2}}$$

The general integral value I_n is found to be

$$I_n = \int_{-R}^{R} \frac{(b - aX)\, dX^2}{(x - X)^{2n+2}} = \left\{ \frac{1}{(2n+1)(x-X)^{2n+1}} \right\}_{-R}^{R}$$

$$\times \left\{ b - a \left[x^2 + (2n+1) \left(\frac{(x-X)}{2n-1} - \frac{2\,(x-X)}{2n} \right) \right] \right\}_{-R}^{R}$$

It may also be seen that when $x \rightarrow \mp R$, I_n and η tend to infinity. Similarly, after a number of computations (neglecting R^2 before x^2), it is found that when $x^2 \gg R^2$

$$I_n = \frac{2\left(bR - \frac{aR^3}{3}\right)}{(2n+1)\, x^{2n+1}}$$

Inserting this value I_n , the Eq. (IV-3) for η is recognized provided A is replaced by $2\left(bR - \frac{aR^3}{3}\right)$.

It may be verified that this is the total value of the initial disturbance given by the integral:

$$\int_{-R}^{R} f(X)\, dX = \int_{-R}^{R} (b - aX^2)\, dR = 2\left(bR - \frac{aR^3}{3}\right)$$

The case of an initial disturbance in the form of a cylinder may also be easily analyzed by calculating the integral

$$I = \int_0^R \int_0^{2\pi} \frac{d\theta \, d\rho}{(\varpi - \rho e^{i\theta})^{2n+3}}$$

The result is obtained in the form of a recurrence formula, the number of terms increasing with the value for η .

The length of the obtained formulas does not justify writing them down in this appendix since they contain nothing not already implied in the previous formulas.

5. DISCUSSION OF THE VALIDITY OF THIS PROCESS OF CALCULATION

Now it is time to question the validity of such a theory as it has been developed for the Cauchy-Poisson theory. Does this mathematical model have a physical significance?

First of all, it is recalled that the Cauchy-Poisson wave motion involves an infinite amount of energy. As previously mentioned, this paradox is explained by saying that the initial disturbance, being infinitesimally small in width, must have an infinite amplitude for its total area to be finite. It has been noted previously that this statement is in complete disagreement with the fact that the theory is based on the assumption that the motion is infinitesimal everywhere, including the origin. Moreover, as also previously mentioned, the fact that the initial disturbance is exerted instantaneously involves an infinite power

during an infinitesimal time interval. This power causes an infinite velocity at origin which is again incompatible with the assumption of linear theory.

The case of an initial disturbance of finite dimension, as it has been analyzed in this paper, also contains a paradox: as it has been explained, the value for f(X) does not need to be infinite to create a wave pattern of finite dimensions. Even this statement permits the principle of superposition to be theoretically valid as a first approximation. It would not be valid if f(X) was infinite. However, it is found that the amount of wave energy produced by an initial disturbance of finite energy is infinite, and in particular that the elevation at the edge of the disturbance tends to infinity.

In the case where the initial disturbance is distributed over a finite breadth, we again quote Lambs "the mathematical infinity (for f(α)) and other perplexing peculiarities, which we meet with in the case of a concentrated line-source, disappear." Indeed they should disappear; however, they do not disappear. Hence these considerations have led the author to maintain that the Cauchy-Poisson theory is a pure mathematical construction which can represent only a limited amount of physical facts. It must be recalled here that frictional effects are neglected. The infinite amplitude of the initial disturbance and its infinite power are not compatible with the assumption that an infinitesimal motion is linear, thus, problem presents a singularity at the origin. This limits the validity of the theory and does not permit strict application of the principle of superposition.

However, a number of results do have a physical significance. These are: (1) far from the origin the wave motion does not depend upon the width and shape of the initial disturbance. Its amplitude, under the assumption that the wave motion is small, is proportional to the total value of the impulse; (2) the value for the elevation at the edge of the initial impulse, which is zero at time zero, tends at once to infinity at time $t = \epsilon$, despite the fact that the initial impulse has a limited energy. Indeed, it is necessary to keep in mind the fact that this limited energy is theoretically exerted instantaneously, that it involves an infinite power. But since the amount of available energy is finite, this instantaneous rise of water must last a very short time. In fact, this is observed when a body is thrown into water. Water rises very high at the edge of the body, then falls down and is followed by small oscillations about the still-water level. It is evident that the friction forces also have a definite influence in causing this damping.

6. CONCLUSION

To conclude this discussion, the present theory based on the principle of superposition permits an explanation of the splash of water caused by a disturbance of finite dimensions.

Incompatibility between the linearization and the infinite power at the origin, and friction forces, limit its validity for describing the true physical situation. Moreover, it has always been assumed that the initial disturbance acts instantaneously. In the case of a disturbance of finite dimension, the inertia of the involved mass also has an effect.

It has been seen in Appendix I that other theories exist which seem to give fairly good agreement with physical facts but their validity is limited to the large values for x and ϖ respectively. These do not explain the splash phenomenon as has been attempted in this paper.

These other theories, based on the use of the Fourier integral in which $f(\alpha)$ is not confined to the neighborhood of the origin, could probably be generalized as indicated in this paper for a disturbance of any shape which could also be a function of space and time. Their investigation may also be of particular interest for calculating the long waves due to a traveling atmospheric perturbance varying with time.

LIST OF SYMBOLS

APPENDIX IV

x	Horizontal coordinate in a two-dimensional motion
ϖ	Horizontal coordinates in a three-dimensional motion (complex number)
α	Horizontal spread of an original disturbance
$f(\alpha)$	Function characterizing the original disturbance
η	Free surface elevation in a two-dimensional motion
ζ	Free surface elevation in a three-dimensional motion
A	Value for the initial total impulse
t	Time
n	Integer index
X	Coordinate for an elementary initial elevation into a two-dimensional motion
(ρ,θ)	Cylindrical coordinates for an elementary initial elevation into a three-dimensional motion (ρ : modulus, θ : argument)
Z	$\rho e^{i\theta}$ (complex number)
R	Horizontal spread for the original disturbance
b	Height of the original disturbance

APPENDIX V

THE SHOALING, DAMPING, BREAKING AND RUN-UP OF LONG WAVES OVER THE CONTINENTAL SHELF

ON SATURATED AND NONSATURATED BREAKERS

by

B. Le Méhauté

1. INTRODUCTION

In this appendix the problems associated with a wave traveling over the continental shelf are analyzed.

First a choice must be made from among all existing theories of waves traveling over gentle slopes in order to select the most convenient theory for application to this problem. It is shown that in most cases the waves appear as a succession of solitary waves and from existing experimental data it is demonstrated that no reliable theory exists.

Wave damping due to bottom friction is analyzed and a formula is proposed which takes into account bottom friction and shoaling effects.

The very important distinction between saturated and nonsaturated breakers is introduced. This study is of major importance in this report because the demonstration of the natural protection afforded by the continental shelf relies on this theory.

Finally a brief literature survey of previous work done on the wave run-up due to long waves is given.

2. THE CHOICE OF THEORIES

It is most important to be aware of the most convenient existing theories for treating the problem of wave motion on the continental shelf. These wave motions of interest are characterized by:

a. Their period T ranges from 50 to 200 seconds.

b. Their wave height H ranges from 0 to 150 feet.

c. The depth d is smaller than 600, and most often smaller than 100 feet.

A first indication of the essential wave characteristics is obtained from the graph presented in Fig. I-4 of Appendix I. It is seen that the most significant factors are $\frac{d}{\lambda_0}$ and $\frac{H}{\lambda_0}$ where λ_0 is the wave length in deep water, or alternatively, simply $\eta_0 \lambda^2 d^{-3}$ i.e. $\eta_0 T^2 g d^{-2}$ with $\lambda = T\sqrt{gd}$ where η_0 is the elevation of the wave crest above the still water level. Knowing H, η_0 can be calculated from Fig. I-3 of Appendix I. Then it is easily seen that the value to be considered for η_0 is almost the same as the value for H. When $\frac{d}{T^2}$ is very small, the smallest value which occurs in this study for $\eta_0 T^2 g d^{-2}$ is 17H over the continental shelf. Hence it is seen that the waves over the continental shelf can be considered as a succession of solitary waves and the solitary wave theory should be a sound basis for preliminary analysis of the phenomena involved. Later it will be seen that this statement may require some reservations and that many refinements will be necessary. The cnoidal wave theory has been shown to often be a better representation for the wave motion in very shallow water. (See Wiegel (1960).)

3. ON THE SHOALING EFFECT

a. Hydrodynamic Solutions

A number of theoretical studies have been carried out in recent years on the problems of water waves on a slope. In particular, significant contributions have been made by Miche (1944), Stoker (1947), Biesel (1952), Peters (1952), Roseau (1952), Keller (1958), Carrier and Greenspan (1958) and Williams (1959).

Solutions have been obtained by direct integration of the momentum equation and continuity relationships for various boundary conditions, including that of an inclined sea bottom. Some of these theories are solutions of linear equations valid for short waves. Hence they cannot be applied to the present problem because of the relative importance of nonlinear terms (convective inertia). An interesting nonlinear solution for long waves has been developed by Carrier and Greenspan. But the vertical acceleration, which is important for near-breaking waves (see Appendix VI), and the damping due to bottom friction have been neglected. Also, the solutions would not hold true for breaking inception.

A theoretical solution for the present problem has also been obtained by Kishi (1962). The most important results of this study are reproduced in this report. Kishi starts from the basic long wave equations in the usual symbols:

Momentum: $$\frac{\delta u}{\delta t} + u \frac{\delta u}{\delta x} = - g \frac{\delta \eta}{\delta x}$$

Continuity: $$\frac{\delta \eta}{\delta t} + \frac{\delta \left[u (d + \eta)\right]}{\delta x} = 0$$

with $c = \left[g (d + \eta)\right]^{1/2}$ and, assuming that

$$u = 2 \sqrt{gd} \left[\sqrt{1 + \frac{\eta}{d}} - 1\right], \qquad \text{(V-1)}$$

it is found that for two locations along the wave path (1 and 2) and with $\eta_o \cong H$:

$$\frac{d_2}{d_1} = \left[\frac{\left[1 + \frac{H_1}{d_1}\right]^{\frac{1}{2}} - 1}{\left[1 + \frac{H_2}{d_2}\right]^{\frac{1}{2}} - 1}\right]^{\frac{4}{5}} \left[\frac{6\left[1 + \frac{H_1}{d_1}\right]^{\frac{1}{2}} - 1}{6\left[1 + \frac{H_2}{d_2}\right]^{\frac{1}{2}} - 1}\right]^{\frac{6}{5}} \qquad \text{(V-2)}$$

which permits the calculation of H_2 as a function of d_2 from the knowledge of H_1 and d_1. It is interesting to note that when H/d is small, the classical Green's law is found: $\frac{H_2}{H_1} = \left(\frac{d_1}{d_2}\right)^{1/4}$.

Although this theory may be quite useful, it must be pointed out that the derivation of Eq. (V-2) is based on the assumption (V-1). Some doubts can be expressed as to the validity of (V-1). Also, in practice the use of (V-2) would involve trial and error computation of H_2 in terms of H_1, d_1 and d_2. Because of these two objections, Eq. (V-2) is not further used but has been mentioned as a possible approach for further investigation.

Also, it will be seen in the following appendix that the vertical acceleration, neglected by Kishi, takes on great importance over a gentle slope such as encountered on the continental shelf. In fact, it is the key for explaining the paradox of long waves indicated by many authors. This paradox -- the Earnshaw paradox (1845) -- is that the long wave theory gives rise to a bore, whatever the wave height even over a horizontal bottom. In fact, it is known that some tsunami waves over a steep slope, as on the Pacific coast, never break. The sea level varies gently with time only.

b. The Energy Method

The second method consists of assuming that the wave motion on a sloping bottom is the same as on a horizontal bottom. Then when the wave motion has been so determined, it is assumed that the rate of transmitted energy is constant.

The great advantage of this method is its simplicity, permitting an estimation of the damping due to friction.

This method works particularly well on a nearly-horizontal plane as is encountered, for example, on the continental shelf of the Atlantic coast where the slope is between 2/10,000 and 5/10,000. Near the shoreline the slope becomes steeper, ending with a 1/15 slope on the beach. In this area the wave motion can no longer be considered as similar to the motion on a horizontal plane. The wave profile loses its symmetrical shape. Also a part of the wave energy is reflected in such a way that the assumption on the transmission of wave energy is not fully satisfied. It is then necessary to apply an analytical or numerical method. Despite these limitations, the energy method is a reasonable preliminary guide for studying wave motion over the continental shelf.

When applied to the solitary wave theory, the principle of conservation of rate of transmitted energy gives

$$E\ V\ b = \frac{8}{3\sqrt{3}}\ H^{3/2}\ d^{3/2}\ V\ b = \text{constant}$$

where H is the wave height

V is the wave celerity = $\sqrt{g\,(d + H)}$

b is the distance between orthogonals, proportional to the radial distance R in the case of circular waves over concentric bottom contours.

Then between two points (1) and (2) at radial distances R_1 and R_2

$$\frac{H_2}{H_1} = \left(\frac{d_1+H_1}{d_2+H_2}\right)^{\frac{1}{3}} \left(\frac{d_1}{d_2}\right) \left(\frac{R_1}{R_2}\right)^{\frac{2}{3}} \cong \left(\frac{d_1}{d_2}\right)^{\frac{4}{3}} \left(\frac{R_2}{R_1}\right)^{\frac{2}{3}} \qquad \text{(V-3)}$$

c. **Experimental Facts**

Experiment shows that due to partial reflection over a slope, the exponent 4/3 in (V-3) is generally too high (Ippen and Kulin (1954)). It can only be considered as a limit when the slope tends to zero. The following graphs, based on experimental results, give the value for n as a function of the slope (Fig. V-1). It is then seen that over the continental shelf, the following law, where n = 1, is more realistic:

$$\frac{H_2}{H_1} = \left(\frac{d_1}{d_2}\right) \left(\frac{R_1}{R_2}\right)^{\frac{2}{3}} \qquad \text{(V-4)}$$

It must be noted that such a law will also be in accordance with the assumption that the transmitted energy is a constant: E b = constant. This assumption is far more reasonable that E V b = constant because this latter law implies that the energy of the wave increases when the celerity decreases, which is not physically reasonable.

Also, according to some experimental results presented in Fig. V-2, it seems that the law of variation of wave height with the depth follows the solitary wave theory as presented in Eq. (V-3) only in a narrow range near the breaking depth d_b (Munk (1949)). According to these experiments, when $\frac{d}{d_b}$ is larger than 1.4, the Airy law applies despite the fact that $\eta_o \lambda^2 d^{-3}$ is much larger than the required value presented in Appendix I, i.e. 0.01. The Airy law is based on the assumption that the rate of transmitted energy of a periodic gravity wave, given by the linear theory, is a constant, i.e. H^2 V b = constant, where V is the group velocity.

Applied to long waves ($V = \sqrt{gd}$), the well-known Green's law is obtained:

$$\frac{H_2}{H_1} = \left(\frac{d_1}{d_2}\right)^{\frac{1}{4}} \left(\frac{b_1}{b_2}\right)^{\frac{1}{2}}$$

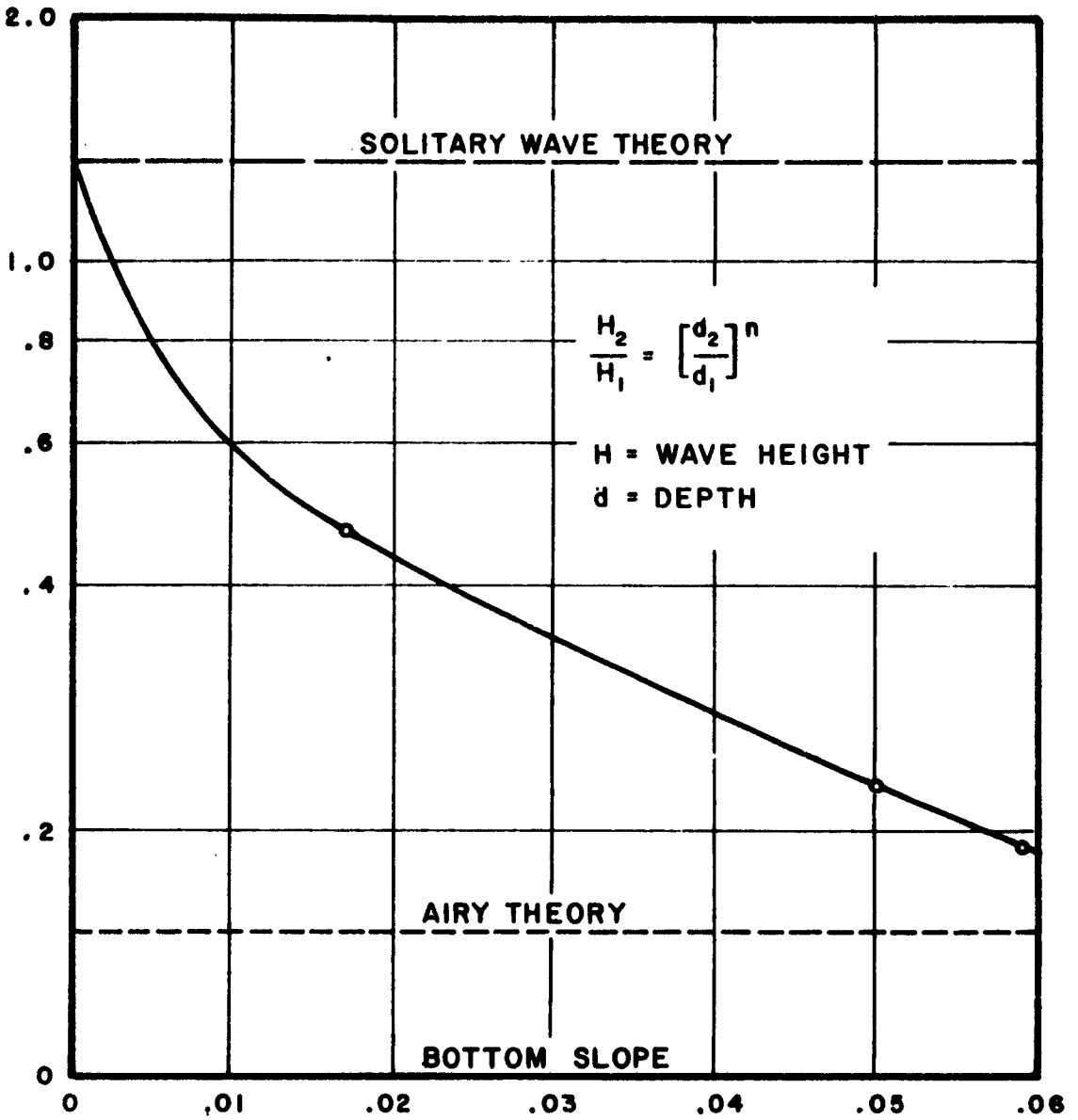

FIGURE V-1
WAVE HEIGHT VARIATIONS VERSUS BOTTOM SLOPE

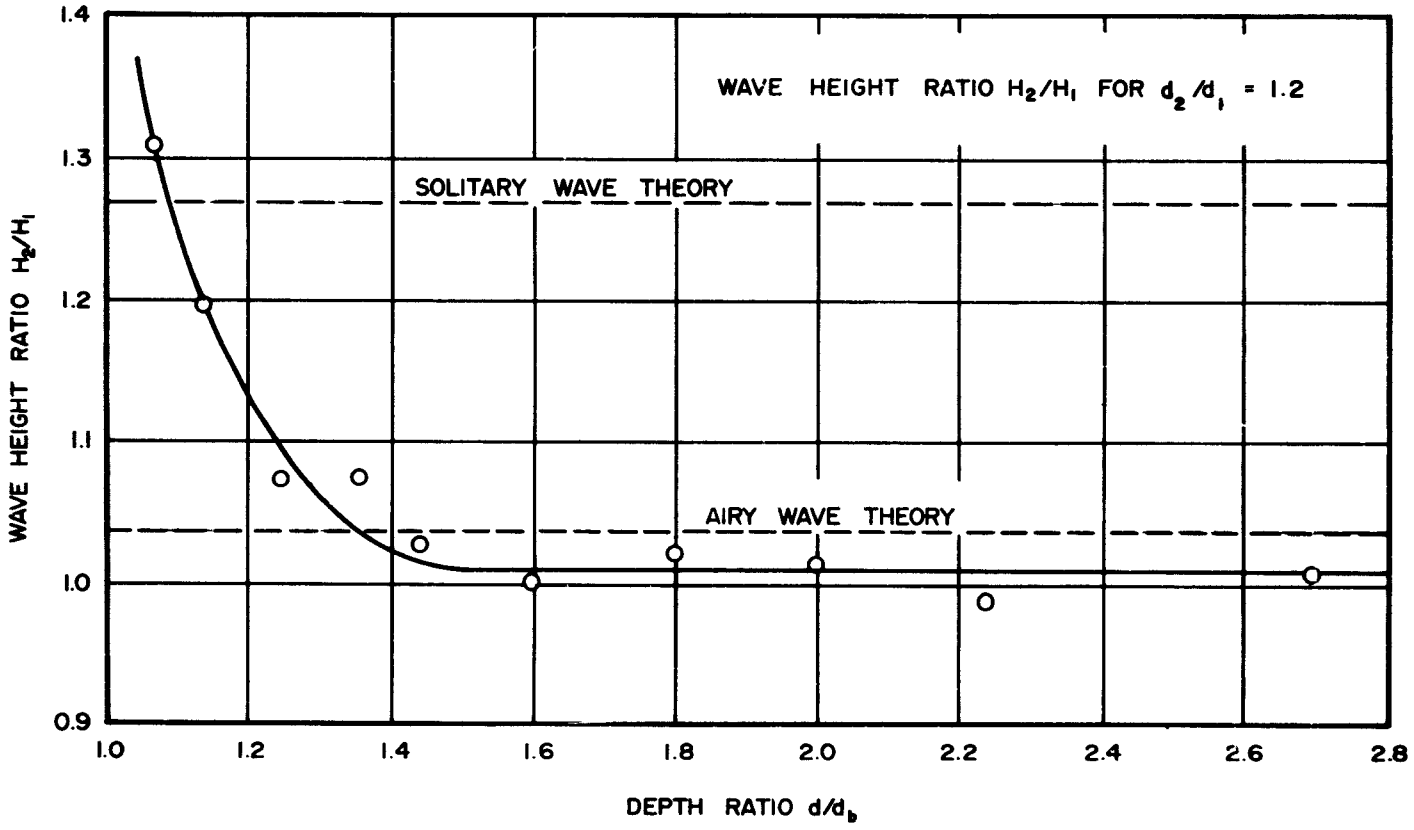

FIGURE V-2
INCREASE IN WAVE HEIGHT FOR A % DECREASE IN DEPTH

A modification of Green's law is suggested to take account of the nonlinear effect as follows:

$$\frac{H_2}{H_1} = \left(\frac{d_1 + H_1}{d_2 + H_2}\right)^{\frac{1}{4}} \left(\frac{b_1}{b_2}\right)^{\frac{1}{2}} \qquad \text{(V-5)}$$

As a general conclusion, despite the fact that the wave motion over the continental shelf is represented fairly well by a solitary wave, experiments show that the shoaling effect given from the solitary wave theory cannot be applied blindly. The shoaling effect is certainly very dependent upon the slope and the Airy theory seems to be much more in accordance with fact when $\frac{d}{d_b} > 1.4$.

It must be noted that it is the essential characteristic of a solitary wave to travel without deformation on a horizontal bottom. Hence these discrepancies are not surprising. The real law can only be given by a general application of the method of characteristics with very small intervals with the use of a digital computer. This problem will be considered in another appendix.

4. THE DAMPING EFFECT DUE TO BOTTOM FRICTION

Most of the theoretical studies on wave damping have been carried out for periodic waves: Boussinesq (1877), Hough (1877), Basset (1888), Lamb (1932), Keulegan (1948), Biesel (1949), Putnam and Johnson (1949), Miche (1954), Reid and Bretschneider (1954), among others.

As in the case of the analysis of a wave on a sloped bottom, two methods exist to attack the problem. The first method -- the analytical method -- consists of solving directly the basic differential equations -- momentum, continuity -- taking a friction term into account. Theoretically,

this method presents the advantage of giving not only the damping, but also the deformation of wave motion due to friction forces (and convective inertia). This is important for very long waves in shallow water such as tidal waves in an estuary. This method is essential for studying the transformation of the wave into a tidal bore.

For the problem under study the second method, the energy method, is simpler and will be as accurate for the wave over the continental shelf before breaking. It consists also of the determination of the wave motion independently of the friction forces over a horizontal bottom. As a consequence, the wave profile is symmetrical. This approximation is valid because the decay of wave amplitude over a wave length is small and the slope is very gentle.

The damping effect is then simply defined as a decay in wave height calculated from energy considerations: the loss of energy over a given wave length is equal to the variation of wave energy. This could be expressed in two ways: the first is particularly convenient for periodic waves:

$$\frac{d(P\,b)}{dx} = -\,b\,D_f \qquad \text{(V-6)}$$

where P is the power per unit width or energy propagated per unit time through a vertical area of depth d and unit width:

$$P = \frac{1}{2}\,\rho\,g\left(\frac{H}{2}\right)^2 \frac{V}{2}\left[1 + \frac{\frac{4\pi d}{L}}{\sinh\frac{4\pi d}{L}}\right]$$

where H is the wave height, V the wave celerity ($\sqrt{gd}$), d the depth, L the wave length (T $\sqrt{gd}$), x is the distance measured along the wave ray in the direction of propagation of the wave, b is the distance between wave orthogonals of two wave rays. Hence, for long waves:

$$P = \frac{1}{2} \rho g \left(\frac{H}{2}\right)^2 (gd)^{\frac{1}{2}} \qquad \text{(V-7)}$$

In the present case b is proportional to R, i.e. the distance from the original disturbance; hence b can be replaced by R in Eq. (V-5). D_f is the average amount of energy dissipated per unit area at the bottom per unit time. It can be calculated theoretically when the flow is laminar, but it has been shown that the flow is turbulent when (Collins (1961))

$$\frac{H}{\sqrt{T}} > 1.08 \sinh \frac{2\pi d}{L}$$

or $H > 1.2 \sqrt{\frac{d}{T}}$ in ft.-sec. units for long waves. This condition is always verified in the present case. Hence D_f will instead be:

$$D_f = \frac{4}{L} \int_0^{\frac{L}{4}} \frac{4}{T} \int_0^{\frac{T}{4}} \tau u_B \, dt \, dx \qquad \text{(V-8)}$$

where u_B is the bottom velocity and τ the shearing stress. Here for a coefficient of friction f,

$$\tau = \rho f u_B |u_B| \qquad \text{(V-9)}$$

and according to the Airy theory applied to long waves:

$$u_B = u(x,t) = \frac{H}{2} \sqrt{\frac{g}{d}} \cos(kt - mx) \qquad \text{(V-10)}$$

where $k = \frac{2\pi}{T}$ and $m = \frac{2\pi}{L} = \frac{2\pi}{T\sqrt{gd}}$

Then, introducing these values it is found that

$$D_f = \frac{1}{8} \frac{4}{3\pi} \rho f H^3 \left(\frac{g}{d}\right)^{\frac{3}{2}} \qquad \text{(V-11)}$$

and inserting (V-7) and (V-11) into (V-6):

$$\frac{d}{dx}(H^2 R \sqrt{d}) = -\frac{4}{3\pi} f H^3 R d^{-\frac{3}{2}} \qquad \text{(V-12)}$$

Dividing by $H^2 R \sqrt{d}$, integrating over a small interval $x_2 - x_1 = \Delta x = \Delta R$ and replacing e^{-ax} by $1 - ax$, it is found:

$$H_2 = H_1 \left(\frac{R_1}{R_2}\right)^{\frac{1}{2}} \left(\frac{d_1}{d_2}\right)^{\frac{1}{4}} \left[1 - \frac{2}{3\pi} f \frac{H_1 \Delta R}{d_1^2}\right] \qquad \text{(V-13)}$$

which permits step-by-step calculation of H. When $f = 0$, the classical Green law is easily recognized.

This formula will have to be inverted if one wants to evaluate the deep water wave height as a function of the shallow water wave heights. In particular the negative sign in the expression between brackets becomes positive.

For the solitary wave theory it is more exact to apply the same type of calculation to the transmitted energy rather than to the power. Then,

$$\frac{d(E V b)}{dx} = -b \frac{dE}{dt} \qquad \text{(V-14)}$$

The energy of a solitary wave is

$$E = \frac{8}{3\sqrt{3}} \rho g H^{\frac{3}{2}} d^{\frac{3}{2}} \qquad \text{(V-15)}$$

and $V = \sqrt{g\ (d + H)}$, where H is the maximum height above the still water level of the solitary wave, and d the depth. (In this case $\eta_0 = H$)

The rate of loss of energy due to bottom friction is:

$$\frac{dE}{dt} = \int_{-\infty}^{\infty} \tau u_B \, dx \qquad \text{(V-16)}$$

By inserting the classical relationships $u_B \cong u = V \frac{\eta}{d}$ and $\eta = \frac{H}{\cosh^2 \alpha}$ where $\alpha = \sqrt{\frac{3}{4}} \left(\frac{H}{d}\right)^{1/2} \frac{x - Vt}{d}$ and η is the free surface elevation above the still water level, it is found that

$$\frac{dE}{dt} = \frac{2}{\sqrt{3}} \rho f V^3 \left(\frac{H}{d}\right)^{\frac{3}{2}} H \int_{-\infty}^{\infty} \frac{d\alpha}{\cosh^6 \alpha} \qquad \text{(V-17)}$$

By use of the Gudermannian of α it is found that the integral has a value 16/15. Hence, finally

$$\frac{dE}{dt} = \frac{32}{15\sqrt{3}} \rho f \frac{H^{\frac{5}{2}} V^3}{d^{\frac{3}{2}}} \qquad \text{(V-18)}$$

After insertion of these values and since b is proportional to R, after integration it is found that

$$H_2 = H_1 \left(\frac{d_1 + H_1}{d_2 + H_2}\right)^{\frac{1}{3}} \left(\frac{d_1}{d_2}\right) \left(\frac{R_1}{R_2}\right)^{\frac{2}{3}} \left[1 - \frac{8}{15} \frac{f H_1 \Delta R}{d_1^2}\right] \qquad \text{(V-19)}$$

This formula also permits step-by-step calculation of H.

It is seen that the loss of energy in a solitary wave height H is more important than in a periodic wave of the same wave height.

When f = 0 and the motion is two-dimensional, the classical law

$$\frac{H_2}{H_1} = \left(\frac{d_1}{d_2}\right) \left(\frac{d_1 + H_1}{d_2 + H_2}\right)^{\frac{1}{3}} \cong \left(\frac{d_1}{d_2}\right)^{\frac{4}{3}} \qquad \text{(V-20)}$$

is easily recognized. Now the problem is how to determine the friction factor f in Eq. (V-13) and (V-20).

In the case of viscous flow, the periodic motion in the boundary layer on a smooth plane is relatively well known. The thickness of the boundary layer δ is proportional to $\sqrt{\nu T}$, that is, it increases with the period.

In the case of turbulent flow, it is known that δ also increases with T. The exact increase of δ is unknown. In the case of long

waves over a shallow bottom it is reasonable to admit that all velocity distribution along a vertical at a given time is very similar to that of a steady flow. In a word, unsteady motion appears as a succession of steady flows insofar as the friction effect is concerned. Then f can be expressed as a function of the Chezy coefficient C_h , which can be expressed as a function of the Manning coefficient n:

$$f = \frac{g}{C_h^2} = g \frac{n^2}{(1.486)^2 d^{\frac{1}{3}}} = 14.6 \frac{n^2}{d^{\frac{1}{3}}} \quad \text{(ft-sec. units)} \qquad \text{(V-21)}$$

The choice of n is delicate; however it can tentatively be considered as equal to 0.02, which is usually given for a bottom composed of gravel. But, it may be expected to range between 0.015 and 0.025 due to the dual uncertainty of the bottom roughness and the application of the Manning formula to unsteady motion. In relatively deep water the depth d in formula (V-21) should rather be replaced by the thickness of the turbulent boundary layer δ . Unfortunately, it has been seen that δ also is unknown.

However, it must be mentioned that the tidal problem in an estuary has been studied satisfactorily by use of the Chezy (or Manning) coefficient. All other factors being equal, only a slightly different value for C_h has been found for a decelerated flow than for an accelerated flow.

5. ON THE BREAKING INCEPTION AND NONSATURATED BREAKERS

It is commonly admitted that breakers on a beach can be separated into spilling breakers on a very flat slope and plunging breakers on a steeper slope. Plunging breakers are sometimes called surging breakers

on a very steep slope. The separation of breakers into categories is based on visual observations rather than on any hydrodynamical criterion. However, the essential hydrodynamical characteristics of these breakers will be reviewed; then a theory for nonsaturated breakers developed (Le Mehaute (1962)).

The profile of a spilling breaker remains, for the most part, almost symmetrical and the wave breaks by curling over slightly at the crest (Fig. V-3). As long as the foam of the breaker is small by comparison with the "bulk" water, which happens on a very gentle slope, the wave presents roughly the main characteristics of a solitary wave, even after breaking inception. But, due to the spilling breaker, a given amount of energy is dissipated in such a way that the wave crest follows the breaking index curve defined by $H = 0.78\ d$. Then the spilling breaker is transformed into a bore when the slope becomes steeper. When the slope is steep before breaking inception, the wave profile first loses its symmetrical shape, then a plunging breaking wave generates a bore directly.

In the following an attempt is made to investigate analytically these described phenomena. As before, two methods exist. The first method, the energy method, is only approximate but gives a great amount of information from relatively simple calculations. The second method, the analytical method, is more accurate but requires tedious computations for each particular case.

It will be seen that the second method is an application of the method of characteristics and requires some refinements for analyzing the surf zone and calculating the wave run-up. This will be presented in Appendix VI.

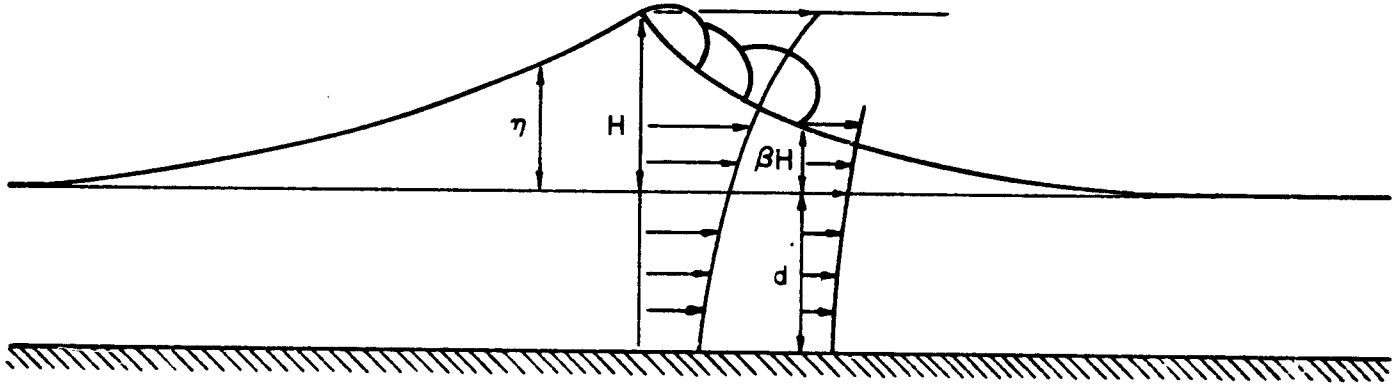

SPILLING BREAKER

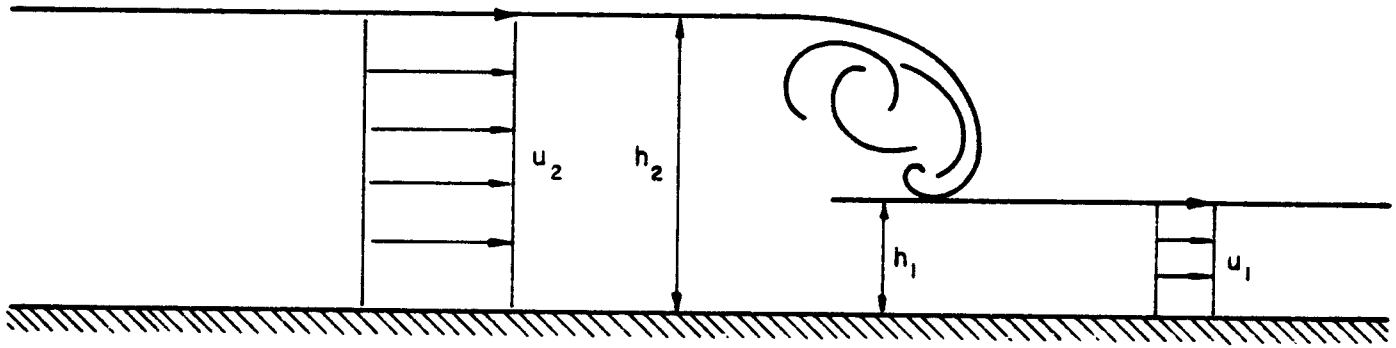

FULLY DEVELOPED BORE

FIGURE V-3
SPILLING BREAKER AND FULLY DEVELOPED BORE

In the energy method the rate at which the energy is lost due to bottom friction is $\frac{dE}{dt}\Big|_b$ and to spilling breakers is $\frac{dE}{dt}\Big|_s$. Hence:

$$\frac{d(EC)}{dx} = -\left[\frac{dE}{dt}\Big|_b + \frac{dE}{dt}\Big|_s\right] \qquad \text{(V-22)}$$

$\frac{dE}{dt}\Big|_b$ is given by Eq. (V-18) as

$$\frac{dE}{dt}\Big|_b = \frac{32}{15\sqrt{3}}\,\rho\, f\,\frac{H^{\frac{5}{2}}\,V^3}{d^{\frac{3}{2}}} \qquad \text{(V-18A)}$$

The rate of loss of energy due to a spilling breaker is very similar to that of a tidal bore (which is a shock wave). In the case of a shock wave it is known that (See Fig. V-3) (Stoker (1957)):

$$\frac{dE}{dt} = \rho\, g\, Q\,\frac{(h_2 - h_1)^3}{4 h_1\, h_2} \qquad \text{(V-23)}$$

where h_1 and h_2 are the depths before and after the front of the bore, respectively, and Q is the discharge due to the moving bore. It must be remembered that the above formula is based on the assumption that the vertical distribution of the horizontal velocity u is uniform.

In the case under study the spilling breaker is due to the fact that the horizontal velocity at the crest becomes greater than the wave celerity V. By analogy (see Fig. V-3) $h_2 = d + H$ and $h_1 = d + \beta H$ where β is always smaller than unity and can be zero at the limit. The vertical velocity distribution, and consequently the discharge, is directly related to the average horizontal velocity. Hence the discharge could be written:

$$Q = (d+H)\,u_2 - (d+\beta H)\,u_1 = V\,\frac{H}{d}\left[d + H - \beta\,(d+\beta H)\right]$$

Inserting these values into Eq. (V-23) and defining B as follows:

$$\left.\frac{dE}{dt}\right|_s = \rho g V \frac{H}{d}\left[d + H - \beta(d+\beta H)\right]\frac{H^3(1-\beta)^3}{4(d+H)(d+\beta H)} = \rho g B \frac{VH^4}{4d^2} \qquad \text{(V-24)}$$

B will be called the "breaking coefficient." The breaking coefficient B is the ratio of the rate of energy dissipated by the spilling breaker to the rate of energy which could be dissipated by a bore of front height equal to the height of the solitary wave which generated it. B = 0 corresponds to no breaking (β = 1). A small value for B corresponds to a little spilling breaking near the crest (β close to unity); i.e. a partial breaking or a nonsaturated breaker. It is difficult to ascertain the maximum value for B by the energy method. However, it is certain that B cannot be larger than unity (β = 0). Then total breaking occurs and the breaker becomes a saturated breaker or fully developed bore. Further consideration will be given to the physical meaning of B later.

Now, by introducing equalities (V-15), (V-18A) and (V-24) into Eq. (V-22), it is found that

$$\frac{d}{dx}\left[H^{\frac{3}{2}} d^{\frac{3}{2}} V\right] = -\left[\frac{4}{5}\frac{f}{g}\frac{H^{\frac{5}{2}}}{d^{\frac{3}{2}}} + \frac{3\sqrt{2}}{32}\frac{BVH^4}{d^2}\right] \qquad \text{(V-25)}$$

which gives after division by $H^{3/2}d^{3/2}V$, integration over a small interval $\Delta x = x_2 - x_1$, and since $e^{-ax} \cong 1 - ax$:

$$H_2 = H_1\left(\frac{d_1}{d_2}\right)\left(\frac{V_1}{V_2}\right)^{\frac{2}{3}}\left[1 - \frac{8}{15}\frac{f H_1 V_1^2 \Delta x}{g d_{1-2}^3} - \frac{\sqrt{2}}{16}\frac{B H_1^{\frac{5}{2}} \Delta x}{d_{1-2}^{\frac{7}{2}}}\right] \qquad \text{(V-26)}$$

When all friction effects are neglected (f = 0) and there is no breaking (B = 0), the classical law

$$\frac{H_2}{H_1} = \frac{d_1}{d_2}\left[\frac{d_1 + H_1}{d_2 + H_2}\right]^{\frac{1}{3}} \cong \left(\frac{d_1}{d_2}\right)^{\frac{4}{3}} \qquad (V\text{-}27)$$

is easily recognized. It has already been pointed out that such a law is not too well verified experimentally (see Fig. V-1 and V-2).

Despite these limitations the physical interpretation of this study will be based on Eqs. (V-25) and (V-26) because the spilling breaker effect tends to replace the variation of wave height by a simple law expressed as $H = 0.78\ d$, even though Eq. (V-27) is not verified experimentally. When $H < 0.78\ d$, there is no breaking and the breaking coefficient $B = 0$. Then $V = \left[g\ (d + H)\right]^{1/2}$. Moreover, assuming H is small by comparison with d,

$$H_2 = H_1 \left(\frac{d_1}{d_2}\right)^{\frac{4}{3}} \left[1 - \frac{8}{15} \frac{f H_1 \Delta x}{d_{1\text{-}2}^2}\right] \qquad (V\text{-}28)$$

This equation has already been found (c.f. V-19).

When $H_b = 0.78\ d_b$, there is inception of breaking and the breaking coefficient B becomes greater than zero. In the case of a small spilling breaker, V retains its value $V = \left[g\ (d + H)\right]^{1/2}$. Then, replacing these values for H and V in Eq. (V-25),

$$\frac{d}{dx}\ (d^{7/2}) = 1.1\ \frac{f}{g}\ d^{5/2} + 0.07\ B\ d^{5/2}$$

i.e. the slope $S = \frac{d}{dx}\ (d) = 0.01\ f + 0.02\ B$ or within the known limits:

$$0 \leq B = 50S - 0.5f < 1 \qquad (V\text{-}29)$$

It is seen that the breaking coefficient B increases with the slope: the steeper the slope, the greater the rate at which the energy is dissipated by the spilling breaker.

It may occur that due to bottom friction B always retains a zero value despite the shoaling when $S < 0.01 f$ as is easily seen from Eq. (V-29). This result can also be found directly from Eq. (V-25) by replacing H by 0.78d and equating B to zero.

Inserting the value (V-21) for f , a criterion for damping without breaking is proposed:

$$S < \frac{14.6n^2}{100 d^{\frac{1}{3}}}$$

i.e. with the Manning coefficient n = 0.02: (d in feet)

$$S < \frac{6.10^{-5}}{d^{\frac{1}{3}}} \qquad \text{(V-30)}$$

On the other hand, it has been seen that B cannot exceed unity. This happens when $S = 0.02 + 0.01 f \cong 0.02$. When S = 0.02, then the breaker is "saturated." Fig. V-4 illustrates these considerations.

Now a complete physical interpretation can be drawn from the previous considerations. If the slope is always smaller than $6.10^{-5} / d^{1/3}$, then the wave height is completely damped by bottom friction. There is no breaking and no run-up. This occurrence is very rare.

On a steeper slope there is a maximum amount of wave energy that a solitary wave can transmit towards the shoreline over a given depth. This maximum energy is reached when H = 0.78 d. If the amount of energy passing through a given plane tends to be larger than this maximum value, a spilling breaker will dissipate the difference. This occurs on a relatively gentle slope and such a condition represents a nonsaturated breaker, in which case the wave height is directly related only to the depth. The run-up is negligible.

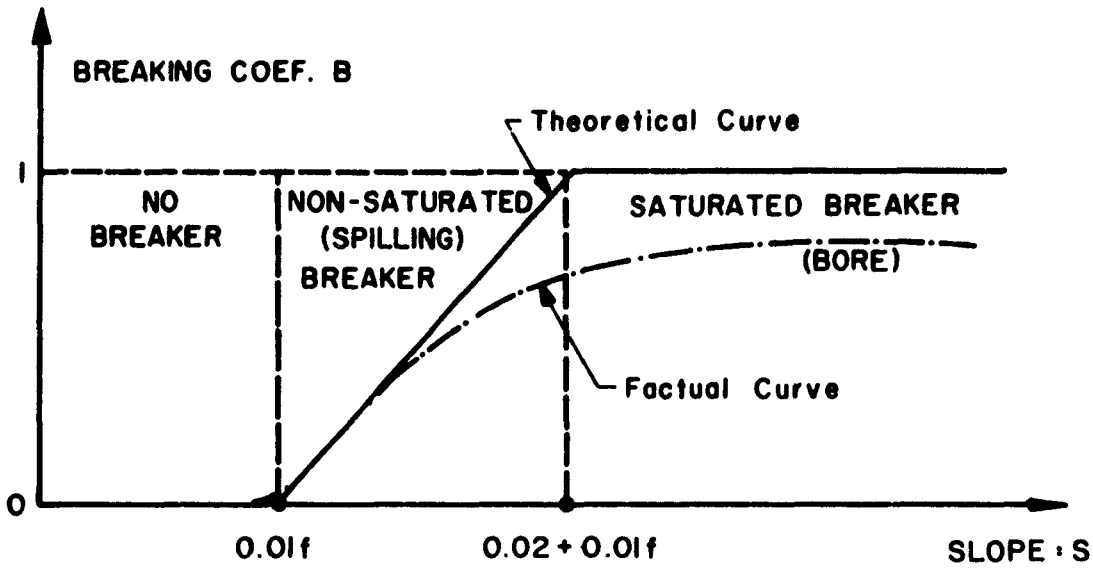

FIGURE V-4
BREAKING COEFFICIENT VERSUS SLOPE

It is seen, also, that there is a limiting amount of energy which could be dissipated by a breaker over a given length. Hence, when the slope becomes steeper and steeper, the regulating effect of the spilling breaker reaches its limit when $B = 1$. Then the breaking index curve is surpassed by the height of the bore front. There is run-up. The words "saturated" and "nonsaturated" breakers are now defined, explained and justified.

A very important conclusion is also drawn: on a beach having its curvature upwards, the maximum possible wave run-up is given by the wave which breaks at a depth where the slope is equal to 0.02. It is known that if d_b is the depth over that slope, the corresponding wave height is $H_b = 0.78\, d_b$. Any wave having a greater height breaks sooner, dissipating its energy following the breaking index curve up to the plane where the slope becomes larger than 0.02.

In fact the theoretical value 0.02 for the critical slope (corresponding to $B = 1$) may be replaced by a more factual and conservative value 0.01 . The exact determination of this value requires further investigation by the method of characteristics as given in Appendix VII.

The results of this section are summarized in Fig. V-5 by three typical cases. It must be noted that the run-up in cases I and II is the same despite the different deep water wave heights.

A very important conclusion can be drawn from this study. Since the continental shelf has a very gentle slope averaging 4/10,000, it acts as a natural protection. The breaking coefficient B keeps a very small value most of the time. The breaker is far from being saturated. The

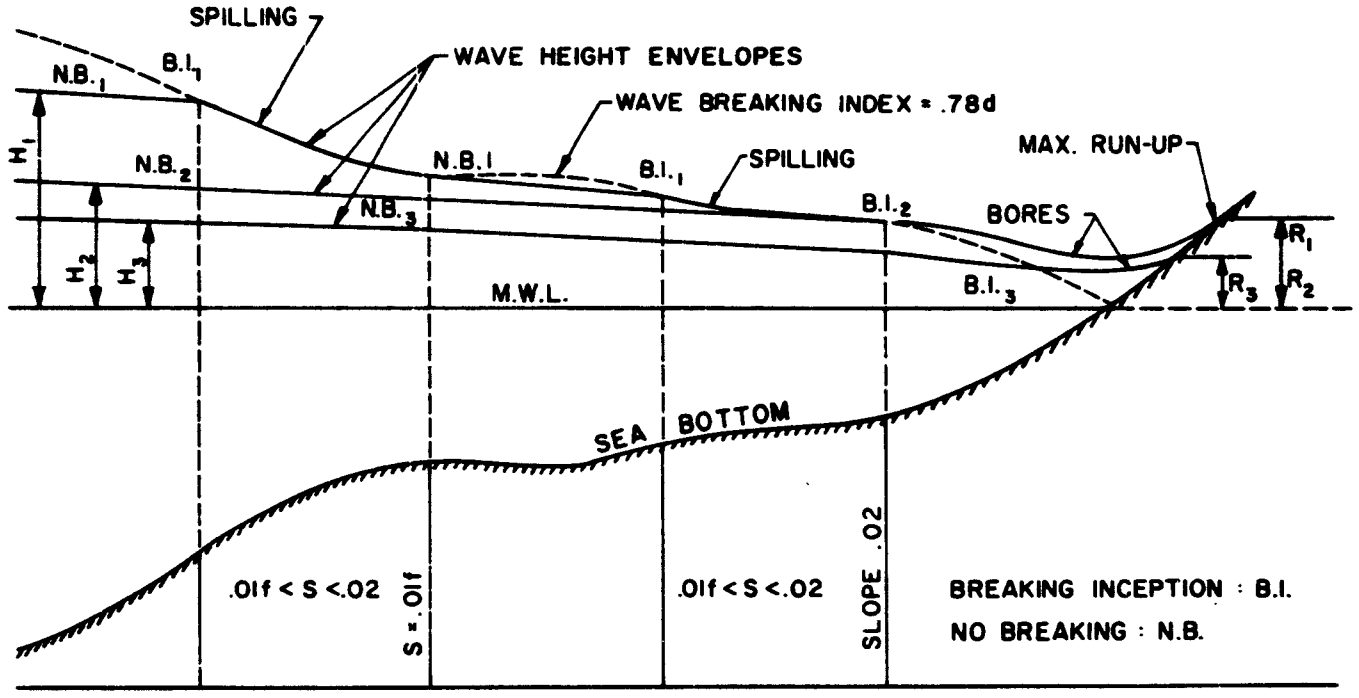

FIGURE V-5
ILLUSTRATION OF SATURATED (BORE) AND NONSATURATED (SPILLING) BREAKERS

maximum wave destruction depends upon the depth where the slope is near 0.01 and the depth at this slope is less than 30 feet. Hence the maximum possible destruction is due to a wave height based on $H = 0.78\ d$ or $0.78 \times 30 = 23$ feet. Also, the maximum possible wave entering the Chesapeake Bay is also directly given by the very simple rule $H = 0.78\ d$. This wave is a gentle spilling breaker in the shape of a limit solitary wave.

6. A LITERATURE SURVEY ON THE WAVE RUN-UP OF LONG WAVES

No theories exist for calculating the wave run-up on a slope prior to this study. Appendix VI of this report establishes a theory for this purpose. Some experimental information on this phenomenon does exist. Unfortunately, these experiments were carried out on slopes which were too steep for application of the results to the problem under study. However, the results do give some information on the general trend. This information will be applied to the problem under consideration. It must be noted, however, that this application requires some extrapolation and is, therefore, subject to possible error.

It was found by Kaplan (1955) that on a slope of 1/30

$$\frac{R}{H} = 0.381 \left(\frac{H}{L}\right)^{-.316} \qquad \text{(V-31)}$$

where R is the vertical run-up above the still water level, and H and L are the wave height and wave length at the toe of the slope. (See Fig. V-6)

On a slope of 1/60, he found that

$$\frac{R}{H} = 0.206 \left(\frac{H}{L}\right)^{-.315} \qquad \text{(V-32)}$$

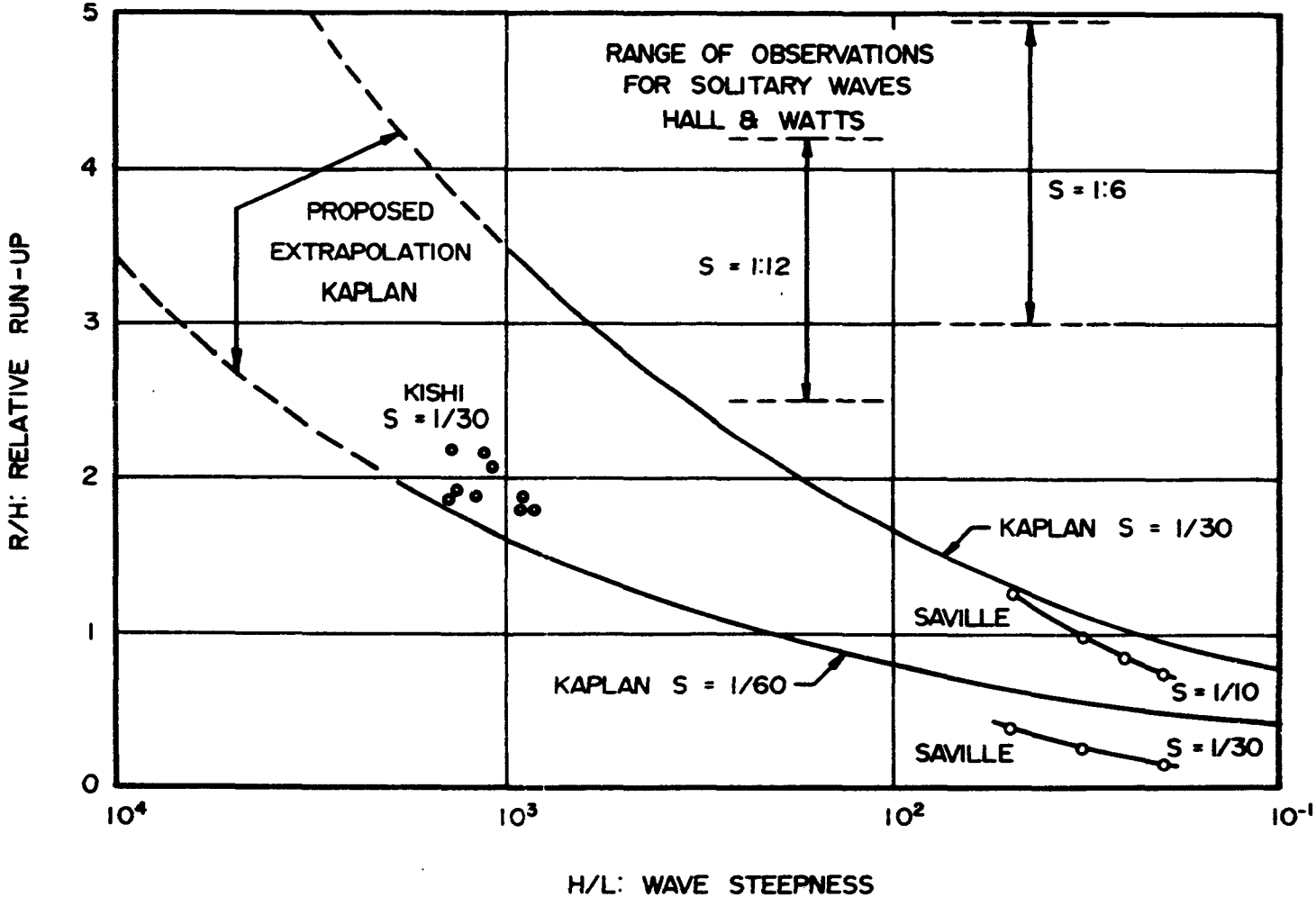

FIGURE V-6

EXPERIMENTAL OBSERVATIONS ON WAVE RUN-UP

The interesting fact emerging from these tests is that the value of $\frac{R}{H}$ does not depend upon the depth at the toe of the slope. These laws were verified for values of $\frac{H}{L}$ ranging from 8×10^{-2} to 2×10^{-3}. They were also proposed for extrapolation for smaller values of $\frac{H}{L}$.

Some recent experiments on a slope of 1/30 by Kishi (1962) for $7 \times 10^{-3} < \frac{H}{L} < 2 \times 10^{-3}$ gave smaller values for $\frac{R}{H}$, namely $\frac{R}{H} \cong 2$. But this could be due to the fact that Kishi worked to a very small scale for which scale effects may not be negligible.

Some experiments have also been carried out by J. V. Hall and G. M. Watts (1953) on the run-up of a solitary wave. They give:

$$\frac{R}{d} = 11(S)^{0.67} \left(\frac{H}{d}\right)^{1.9(S)^{0.35}} \qquad \text{(V-33)}$$

for any slope between 5^{o} and 12^{o}. However, on reworking the data provided by Hall and Watts, it is found that $\frac{R}{H}$ is close to 3 on a slope 5^{o} and 10^{o}.

From this scattered information, combined with the previous theory on nonsaturated breakers and the results obtained in the following appendix, it can be tentatively concluded that for an average slope as usually encountered,

$$\frac{R}{H_b} \cong 2.5$$

H_b being the wave height (0.78 d) at a depth d where the slope is 0.02.

REFERENCES

Basset (1888). Hydrodynamique

Biesel, F. (1949). "Notule Hydraulique." La Houille Blanche, Sep-Oct

Biesel, F. (1952). "Study of Wave Propagation in Water of Gradually Varying Depth." Gravity Waves, U.S. National Bureau of Standards Circular 521

Boussinesq (1877). Essais sur la theorie de eaux courantes

Bretschneider, C. L. and R. O. Reid (1954). "Changes in Wave Height due to Bottom Friction, Percolation and Refraction." Tech. Memo No. 45, Beach Erosion Board, Dept. of the Army Corps of Engineers, 36pp.

Carrier, G. F. and H. P. Greenspan (1958). "Water Waves of Finite Amplitude on a Sloping Beach." Journal of Fluid Mechanics, Vol. 4, Part 1, p. 97, May

Collins, J. I. (1961). "Effect on Mass Transport of the Onset of Turbulence at the Bed Under Periodic Gravity Waves." ASME-EIC Hydraulics Conference, Montreal, Paper number 61, EIC-8

Earnshaw, S. (1845). Transactions, Cambridge Philosophical Society, Vol. VIII

Hall, J. V. and G. M. Watts (1953). "Laboratory Investigation of the Vertical Rise of Solitary Waves on Impermeable Slope." Tech Memo No. 33, Beach Erosion Board, U.S. Army Corps of Engineers.

Hough (1877). Proceedings, London Math. Soc., Vol. XXVIII, p. 264

Ippen, A. T. and G. Kulin (1954). "The Shoaling and Breaking of the Solitary Wave." Proceedings, Vth Conference on Coastal Engineering, Grenoble, France, September, p. 27

Kaplan, K. (1955). "Generalized Laboratory Study of Tsunami Run-up." Tech. Memo No. 60, Beach Erosion Board, Dept. of the Army Corps of Engineers

Keller, J. B. (1958). "Surface Waves on Water of Nonuniform Depth." Journal of Fluid Mechanics, V. 4, Pt. 6, Nov.

Keulegan, G. H. (1948). "Gradual Damping of Solitary Waves." Jour. Res., Nat. Bur. of Standards, Vol. 40, pp. 487-498

Kishi, Tsutomu (1962). "Transformation, Breaking and Run-up of Long Waves of Finite Height." Presented at VIIIth Conference on Coastal Engineering, Mexico City, November, 1962.

Lamb, H. (1932). Hydrodynamics. Dover Publications, Sixth Edition, p. 625

Le Méhauté, B. (1962). "On Nonsaturated Breakers and the Wave Run-up." VIIIth Conference on Coastal Engineering, Mexico City, Nov. 1962.

Miche, A. (1944). "Mouvements ondulatiores de la mer en profondeur constante on decroissante." Ann. des ponts et chaussees, pp. 131-164, 270-292, 369-406

Miche, R. (1954). "Train d'ondes oceaniques." COEC, Ministere defense nationale, No. 135

Munk, W. H. (1949). "The Solitary Wave Theory and Its Application to Surf Problems." Annals, New York Academy of Sciences, Vol. 51, Art. 3, p. 392

Peters, A. S. (1952). "Water Waves over a Sloping Beach." Communications on Pure and Applied Mathematics, Vol. 5, pp. 87-108

Putnam, J. A. and J. W. Johnson (1949). "The Dissipation of Wave Energy by Bottom Friction." Transactions, Amer. Geophysical Union, Vol. 30, No. 1, pp. 67-74

Roseau, M. (1952). "Contribution a la theorie des ondes liquides de gravite en profondeur variables." Publications Scientifiques et Techniques du Ministere de l'Air, No. 275, Paris

Stoker, J. J. (1947). "Surface Water in Water of Variable Depth." Quarterly of Applied Mathematics, Vol. 5, pp. 1-54

Stoker, J. J. (1957). Water Waves, Interscience Publishers, N. Y. p. 319

Wiegel, R. L. (1960). "A Presentation of Cnoidal Wave for Practical Applications." Journal of Fluid Mechanics, pp. 273-286

LIST OF SYMBOLS

APPENDIX V

d	Water depth
λ_o	Wave length in deep water
λ or L	Wave length in shallow water
T	Wave period
η	Elevation of wave surface above still water level
η_o	Maximum value of η at the wave crest
H	Wave height
u	Horizontal velocity
x	Horizontal coordinates
E	Wave Energy
V	Wave celerity for a long wave in shallow water
b	Distance between two orthogonals
R	Radial distance from the original disturbance Also Vertical wave run-up
Sub $_b$	Related to breaking characteristics
n	Exponent for variation of wave height with depth vs. bottom slope
S	Bottom slope
P	Wave power per unit width
D_f	Amount of energy dissipated by bottom friction per unit area
τ	Shearing stress per unit area
u_B	Bottom velocity

$$a = \sqrt{\frac{3}{4}} \left(\frac{H}{d}\right)^{1/2} \frac{x - V t}{d}$$

h_2 Depth on the high side of the bore

h_1 Depth on the low side of the bore

Q Discharge due to the moving bore

f Friction coefficient = $\frac{g}{C_h^2}$

g Gravity acceleration

C_h Chezy coefficient

n Manning coefficient

β Coefficient characterizing the height of the front of a spilling breaker

B Breaking coefficient: ratio of the energy dissipated by a spilling breaker and the energy which can be dissipated by a bore of same height

APPENDIX VI

THE WAVE RUN-UP
BY THE METHOD OF CHARACTERISTICS

By
B. Le Méhauté

1. INTRODUCTION

This appendix presents the results of theoretical investigations on the wave run-up which have been carried out by the method of characteristics.

This powerful method has been of great use in many scientific fields. It has been in common use in hydraulics for studying flood routing and tidal waves in estuaries. It is also used for studying water hammer in pipe lines, and has been introduced in meteorology by Freeman (1951).

It seems that Stoker (1957) was the first to propose the application of the method of characteristics to the problem of a wave breaking on a beach. However, he did not study the problem of the run-up on a dry bed. Hence this particular problem has been solved in this report.

The various topics of investigation are:

a. Establishment of the basic equations of the motion prior to wave breaking. It is shown that the vertical acceleration, usually neglected, has an important effect. The corresponding correction term is given.

b. The basic principle of the method of characteristics is recalled. Dimensionless parameters are introduced.

c. The input and limit of the waves are defined by a limit solitary wave where the slope becomes steeper than a given value such as 0.02. It is assumed that such a wave on a more gentle slope follows the breaking index curve as demonstrated in the previous appendix.

d. The problem of nonsaturated breaker inception is discussed.

e. The method for studying nonsaturated breaker propagation, and bore propagation, is given.

f. The particular problem of the bore reaching the shoreline is theoretically analyzed when the bottom friction is neglected.

g. The run-up on a dry bed with bottom friction is also theoretically analyzed in various cases corresponding to various simplifying assumptions. Then the links between the motion over a dry bed and the bore reaching the shoreline with bottom friction are established.

h. Finally, an application of the method is carried out and suggestions for further investigations are given.

2. THE BASIC EQUATIONS AND ASSUMPTIONS

The classical equation for long waves in shallow water neglects the vertical component of velocity, vertical acceleration and the bottom friction forces. They are: (see Fig. VI-1 for notation)

Momentum: $$\frac{\partial u}{\partial t} + u \frac{\partial u}{\partial x} = - g \frac{\partial \eta}{\partial x} \qquad \text{(VI-1)}$$

Continuity: $$\frac{\partial \eta}{\partial t} + \frac{\partial u(d + \eta)}{\partial x} = 0 \qquad \text{(VI-2)}$$

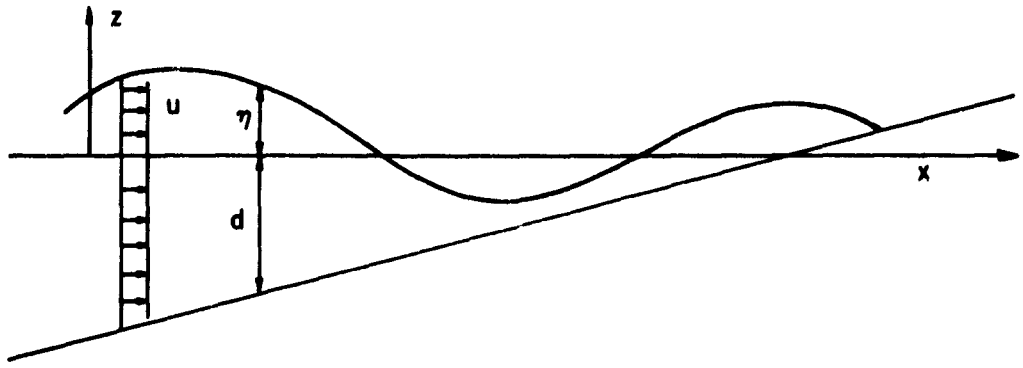

FIGURE VI-1
NOTATION

It is recalled that these equations are based on the assumption that the distribution of horizontal velocity u is uniform. Hence u is the average velocity in a cross section.

It has already been pointed out by Stoker and others that the method of characteristics, as previously applied, gives a wave profile much more unsymmetrical than usually observed at sea or in a wave flume. This limitation on the validity of the theory is of small importance on a comparatively steep slope, but becomes very important on a gentle slope such as is usually encountered over the Atlantic continental shelf.

The theory of nonsaturated breakers (LeMéhauté 1962) presented in the previous appendix, which is based on the assumption that the wave

profile is symmetrical, certainly gives a better approximation on a very gentle slope. For example, at the limit, if the study of the propagation of a solitary wave over a horizontal bottom is treated by the method of characteristics, the wave profile becomes rapidly unsymmetrical (Fig. VI-2). A bore appears even if the starting wave is not a limit solitary wave. ($H/d < 0.78$). However, it is well known by direct integration and experiments that a solitary wave over a horizontal bottom travels without deformation, the wave profile always being symmetrical (see McCowan (1891) and Munk (1949)). This fact proves some deficiencies in the method of characteristics as previously used. Ursell and Birkhoff (1949) present this as a paradox, the Earnshaw paradox (1845), also encountered in gas dynamics. Birkhoff even states that nobody knows the explanation. Stoker (1957), Laitone (1961) and others also discuss the problems of steady state in long waves. Stoker states that the steady state can be reached provided the theories are carried out at a high order of approximation (p. 342). Briefly, the explanation of this paradox and this deficiency of the method of characteristics applied to long waves are due to the fact that the vertical acceleration and path curvature effects (particularly important at the crest of a near-breaking wave) are neglected and consequently the pressure distribution is assumed to be hydrostatic. The solitary wave theory takes account of this path curvature effect by assuming that the vertical velocity is linearly distributed from the bottom to the free surface:

$$w = \frac{d + z}{d + \eta} \frac{d\eta}{dt} \cong \frac{d + z}{d + \eta} \frac{\partial \eta}{\partial t}$$

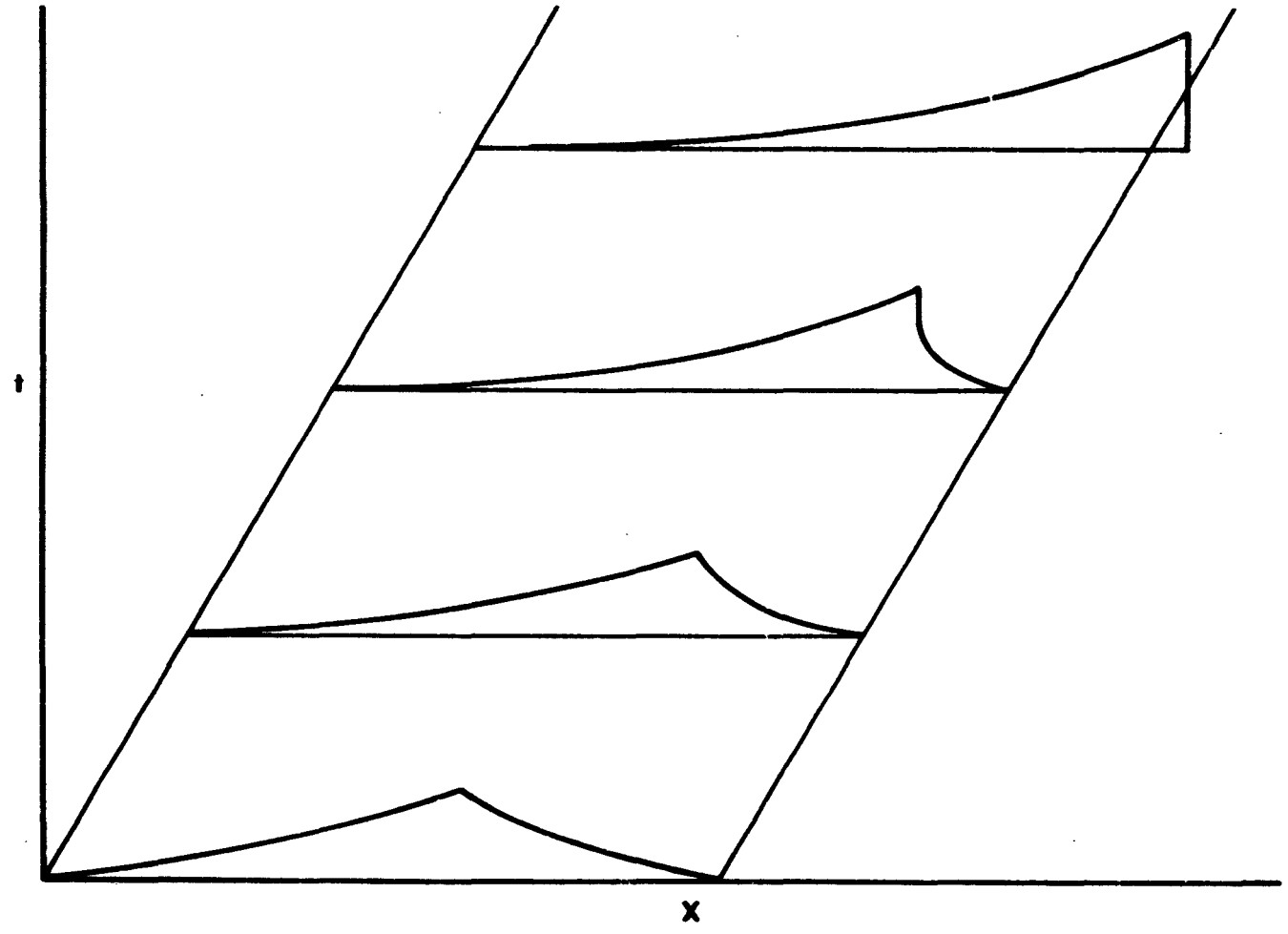

FIGURE VI-2
DEFORMATION OF A SOLITARY WAVE OVER A HORIZONTAL BOTTOM BY THE METHOD OF CHARACTERISTICS

Then it is found that the correcting term to be inserted on the right side of the momentum Eq. (VI-1) is:

$$-\frac{d+\eta}{3}\quad\frac{\partial^3\eta}{\partial t^2\,\partial x} \qquad \text{(VI-3)}$$

A similar term can also be added to take into account the influence of the slope of the sea bottom on the path curvatures. The length of the equation which is thus obtained is such that its insertion for practical computation is not justified. Moreover, the corresponding error is very small for two reasons:

1. On a steep slope, the slope has an effect on the path curvature, but it will be seen that the total path curvature effect is small by comparison with the term $-gS$ which appears in the momentum equation (S is the slope).

2. On a gentle slope the total path curvature effect is of great importance, but the correction to the path curvature effect caused by the bottom slope becomes negligible as long as the slope of the free surface is large by comparison with the bottom slope. This is always the case for a near-breaking wave close to the crest and at some distance from the crest, the path curvature is unimportant.

To conclude this discussion, the proposed correction term Eq. (VI-3) can be considered as a sufficient approximation -- but also as a necessary correction -- for a wave traveling on a very gentle slope. It is pointed out that when the bottom slope tends to zero, the solitary wave theory is more exact. Consequently, the theory previously presented in Appendix V can be considered as the limit case, obtained by a direct integration where the path curvature effect is taken into account.

It has been pointed out that the bottom friction forces have been neglected in the previous momentum Eq. (VI-1). If, as already assumed in Appendix V, the shearing stress at the bottom is quadratic and the wave motion appears as a succession of steady flows then the Chezy formula gives for the friction term F:

$$F = - \frac{g}{C_h^2} \quad \frac{u|u|}{(d + \eta)}$$

$(d + \eta)$ being the hydraulic radius in this case.

It can be seen that by taking "reasonable" values for C_h the bottom friction effect is also relatively negligible when the slope is larger than 1/10, but becomes very important on a very gentle slope, as does the path curvature effect. However, it will be seen that the friction term is particularly important when the bore reaches the shoreline and for the run-up computations on a dry bed, whatever the slope.

These two necessary correction terms show the importance of the notion of nonsaturated breakers introduced in Appendix V for calculating the maximum possible wave run-up. Since nonsaturated breakers follow the breaking index curve, it is sufficient to start the computations by the method of characteristics from a limiting solitary wave on a slope where the breaker tends to be saturated: $S = 0.02$ or $S = 0.01$ for safety. This consideration should permit elimination of a tremendous amount of calculation in studying the wave traveling over the continental shelf because it would require taking account of the path curvature term and bottom friction terms.

It will be seen that the method of characteristics accumulates errors. Hence the necessary simplifying hypothesis which has been assumed to perform the calculation in the energy method in Appendix V does not give a greater error than does the more theoretically exact method of characteristics when the calculations have to be performed over a long distance.

Finally, it is pointed out that the basic momentum and continuity Eq. (VI-1) and (VI-2) assumed that the vertical velocity distribution was uniform. Actually the velocity distribution of a near-breaking wave does not satisfy this assumption. As already pointed out, for a spilling breaker the velocity near the crest becomes larger than the wave celerity. Because of this phenomenon, a loss of energy is not taken into account by the method of characteristics. The solution may consist of imposing, for example, a maximum value to the wave height: $H = 0.78\,d$. This correction may have some importance if the method of characteristics is begun on a very gentle slope. But since we already know that the breaking index curve is followed, this correction is unnecessary when we start the method of characteristics on a slope steeper than the critical slope 0.02. Then the spilling breaker generates a bore very quickly and the correction due to non-uniform velocity distribution is negligible.

The basic starting equations will finally become:

$$\frac{\delta u}{\delta t} + u\,\frac{\delta u}{\delta x} = -g\,\frac{\delta \eta}{\delta x} - g\,\frac{u|u|}{C_h^{\,2}(d+\eta)} - \frac{d+\eta}{3}\,\frac{\delta^3 \eta}{\delta t^2\,\delta x} \qquad \text{(VI-4)}$$

$$\frac{\delta \eta}{\delta t} + \frac{\delta u(d+\eta)}{\delta x} = 0 \qquad \text{(VI-5)}$$

3. THE BASIC PRINCIPLE OF CALCULATION OF THE METHOD OF CHARACTERISTICS

Now some elementary transformations must be performed. Dimensionless terms are also introduced.

First it is seen that the wave motion is completely defined as a function of time and space by the elevation η (x, t) and horizontal velocity u(x, t). It will be more convenient to define the wave motion by two terms u (x, t) and c (x, t), which are both dimensionally equivalent to velocities, the definition of c being:

$$c = \left[g(d + \eta) \right]^{\frac{1}{2}} \qquad \text{(VI-6)}$$

The definition for c is arbitrary and can be modified in an attempt to eliminate the path curvature term in the calculations. For example, c can be taken to be

$$c = \left[g(d + \eta) \left(1 + \frac{\delta^2 (d + \eta)}{3g \, \delta t^2} \right) \right]^{\frac{1}{2}}$$

But such a definition for c also requires the neglect of a few terms. In the present phase of this study the value $c = \left[g (d + \eta) \right]^{1/2}$ will be used. However, it is interesting to note this possibility in view of further investigations. Another way of defining c will also be obtained by assuming that a solitary wave must travel without deformation over a horizontal bottom.

From Eq. (VI-6) it is deduced that

$$2c \frac{\delta c}{\delta *} = g \frac{\delta \eta}{\delta *} + g \frac{\delta d}{\delta *} \qquad \text{(VI-7)}$$

Hence

$$g \frac{\partial \eta}{\partial x} = 2c \frac{\partial c}{\partial x} - g \frac{\partial d}{\partial x} = 2c \frac{\partial c}{\partial x} + gS$$

Also

$$\frac{g\, u\,|u|}{C_h^2 (d+\eta)} = \frac{g^2}{C_h^2} \left(\frac{u}{c}\right)^2$$

and from the continuity equation:

$$\frac{\partial u(d+\eta)}{\partial x} + \frac{\partial (d+\eta)}{\partial t} = 0$$

(VI-8)

$$\frac{d+\eta}{3} \frac{\partial^3 (d+\eta)}{\partial t^2 \partial x} = -\frac{d+\eta}{3} \frac{\partial^3 [u(d+\eta)]}{\partial x^2 \partial t} = \frac{c^2}{3g^2} \frac{\partial^3 (uc^2)}{\partial x^2 \partial t}$$

Inserting these relationships into the momentun Eq. (VI-4) gives:

$$\frac{\partial u}{\partial t} + u \frac{\partial u}{\partial x} + c \frac{\partial 2c}{\partial x} = G_* = -gS - \frac{g^2}{C_h^2} \left(\frac{u}{c}\right)^2 + \frac{c^2}{3g^2} \frac{\partial^3 (uc^2)}{\partial x^2 \partial t} \quad \text{(VI-9)}$$

In the following the right-hand side of Eq. (VI-9) will called G_* even if friction and path curvature terms are neglected. The continuity Eq. (VI-8), in terms of u and c, also becomes:

$$\frac{\partial (uc^2)}{\partial x} + \frac{\partial c^2}{\partial t} = 0$$

i.e.

$$\frac{\partial 2c}{\partial t} + u \frac{\partial 2c}{\partial x} + c \frac{\partial u}{\partial x} = 0 \qquad \text{(VI-10)}$$

Adding and subtracting successively Eq. (VI-9) and (VI-10) gives

$$\frac{\partial}{\partial t}(u + 2c) + (u + c) \frac{\partial}{\partial x}(u + 2c) = G_* \qquad \text{(VI-11)}$$

$$\frac{\partial}{\partial t}(u - 2c) + (u - c) \frac{\partial}{\partial x}(u - 2c) = G_* \qquad \text{(VI-12)}$$

It is seen that these expressions are the total differential with respect to time of $(u + 2c)$ and $(u - 2c)$ provided $\frac{dx}{dt} = u + c$ and $\frac{dx}{dt} = u - c$ respectively. Hence,

$$\frac{d}{dt}(u + 2c) = G_* \quad \text{along a line} \quad \frac{dx}{dt} = u + c$$

$$\frac{d}{dt}(u + 2c) = G_* \quad \text{along a line} \quad \frac{dx}{dt} = u - c$$

Before explaining the mathematical process based on this equation, it is particularly convenient when performing the calculations -- and also in order to give more generality to the obtained results -- to use dimensionless terms. For this purpose, let $C_* = \sqrt{g d_1}$ where d_1 is an arbitrary length. It is most convenient to let d_1 equal the depth at the point where the calculation of the method of characteristics will begin. This depth could be chosen as the depth where the slope is 0.01, i.e. where the breaker tends to become saturated and where the input can be taken to be a limit solitary wave. Then inserting the relationships:

$$x = X d_1 \qquad X = \frac{x}{d_1}$$

$$t = \frac{d_1 T}{C_*} \qquad T = \frac{C_* t}{d_1}$$

$$u = C_* U \qquad U = \frac{u}{C_*}$$

$$c = C_* C \qquad C = \frac{c}{C_*}$$

the above Eq. (VI-11) and (VI-12) (where G_* is expressed as given in Eq. VI-9)) become, after some elementary calculations:

$$\frac{d}{dT}(U \mp 2C) \doteq G = -S - \frac{g}{C_h^2}\left(\frac{U}{C}\right)^2 \begin{cases} - \frac{C^2}{3} \frac{\delta^3(C^2)}{\delta T^2 \delta X} & \text{or} \\ + \frac{C^2}{3} \frac{\delta^3(UC^2)}{\delta X^2 \delta T} \end{cases} \qquad \text{(VI-13)}$$

along $\frac{dX}{dT} = U \mp C$. Now the principle of calculation based on this set of equations can be explained.

It is seen that $G_* = g G$. Knowing U, C, and G at two points (1) and (2) in a T-X diagram (see Fig. VI-3), namely U_1, C_1, G_1, U_2, C_2, G_2, U and C can be calculated at a third point (3), U_3 and C_3 by the following processes. A line of slope $\frac{1}{U_1 + C_1}$ is drawn from point (1) and a line of slope $\frac{1}{U_2 - C_2}$ from point (2). Point (3) is defined by the intersection of these two lines. Then from Eq. (VI-13) we know that:

$$\Delta (U + 2C) = G_1 \Delta T_{1-3} \quad \text{along the line} \quad \frac{1}{U_1 + C_1} = \frac{dT}{dX}$$

$$\Delta (U - 2C) = G_2 \Delta T_{2-3} \quad \text{along the line} \quad \frac{1}{U_2 - C_2} = \frac{dT}{dX}$$

Hence,

$$\begin{cases} U_3 + 2C_3 = U_1 + 2C_1 + G_1 \ \Delta T_{1-2} \\ U_3 - 2C_3 = U_2 - 2C_2 + G_2 \ \Delta T_{2-3} \end{cases}$$

and

$$\begin{aligned} U_3 &= \frac{U_1 + U_2}{2} + C_1 - C_2 + G_1 \ T_{1-2} + G_2 \ \Delta T_{2-3} \\ C_3 &= \frac{U_1 - U_2}{4} + \frac{C_1 + C_2}{2} + G_1 \ T_{1-2} - G_2 \ \Delta T_{2-3} \end{aligned} \qquad \text{(VI-14)}$$

which permits calculation of U_3 and C_3. Repeating this process of calculation for each point of the T - X diagram permits calculation of the complete wave evolution as a function of space and time.

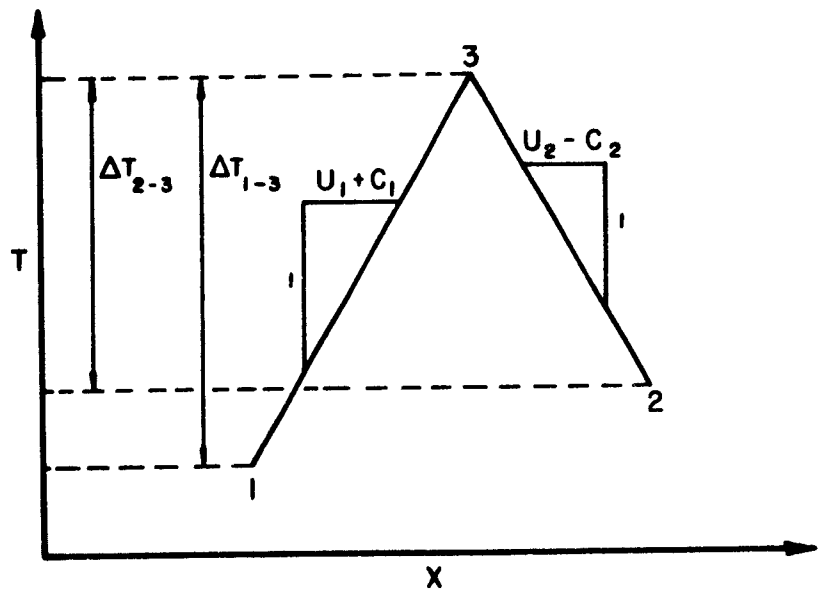

FIGURE VI-3
BASIC PRINCIPLE OF THE METHOD OF CHARACTERISTICS

The calculation of G is tedious but not difficult. The friction term $\frac{g}{C_h^2}\left(\frac{U}{C}\right)^2$ is often small and can usually be neglected near breaking inception. But, it becomes important when the wave reaches the shoreline and is essential for the run-up on a dry bed. On the other hand, the curvature term, while being important near breaking inception, becomes negligible for the run-up on a dry bed. Both of these terms must be compared quantitatively with (-S).

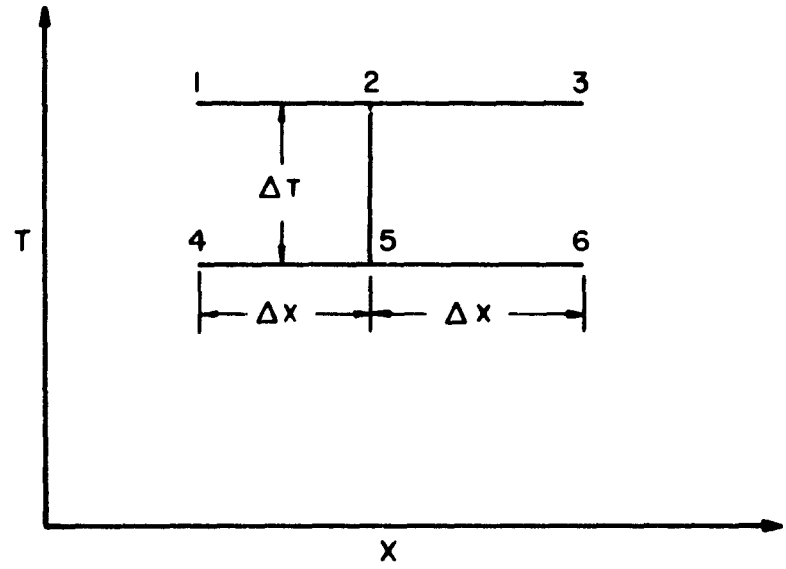

FIGURE VI-4
CALCULATION OF CURVATURE TERM

The calculation of the curvature term is complex. Moreover, it is effectively negligible when the slope is greater than 1/10. It can be evaluated from the knowledge of U and C at six points on the T-X

diagram (see Fig. VI-3A) by the formula:

$$\frac{\partial^3(UC^2)}{\partial X^2 \partial T} \cong \frac{1}{\Delta X^2 \Delta T} \left[U_1 C_1^2 - 2U_2 C_2^2 + U_3 C_3^2 - U_4 C_4^2 \right.$$

$$\left. + 2 U_5 C_5^2 - U_6 C_6^2 \right]$$

The evaluation of these points generally requires a great amount of interpolation; hence, despite the fact that it is theoretically possible and despite its importance, it may be theoretically unrealistic to take this term into account even on a gentle slope, unless the calculations are done by a computer.

These considerations again demonstrate the importance of the study presented in the previous appendix on saturated and nonsaturated breakers. Since we know from these computations that a nonsaturated breaker remains roughly symmetrical in shape and follows the breaking index curve, a great number of computations are saved by taking the input on a slope of 0.01 as has already been pointed out.

4. THE INPUT DEFINITION AND WAVE "LIMITS"

As already pointed out, the maximum possible wave run-up can be determined when the input is defined by a limit solitary wave where the slope tends to become steeper. According to the classical solitary wave theory (see Munk (1949)) C and U can be obtained respectively from the following equations

$$\eta = \frac{H}{\cosh^2 \alpha} \qquad \text{where} \qquad \alpha = \sqrt{\frac{3}{4}} \left(\frac{H}{d}\right)^{\frac{1}{2}} \frac{x - Vt}{d} \tag{VI-15}$$

$$u = V \frac{\eta}{d} \qquad \text{and} \qquad V = \left[g(d + H) \right]^{\frac{1}{2}}$$

from which U and C at time T = 0 can easily be determined. However, it is recalled that u as given by this expression is an approximate velocity. It is more exact to define an input by the average velocity $\bar{u}(x) = \frac{1}{d + \eta} \int_{-d}^{\eta} u(x, z)\, dz$ where

$$u(x,z) = N \frac{1 + \cos M \frac{z}{d} \cosh M \frac{x}{d}}{\left(\cos M \frac{z}{d} + \cosh M \frac{x}{d}\right)^2}$$ and N and M are given by

$$N = \frac{2}{3} \sin^2 \left[M \left(1 + \frac{2}{3} \frac{H}{d}\right)\right] \text{ and } \frac{H}{d} = \frac{N}{M} \tan^{\frac{1}{2}} \left[M \left(1 + \frac{H}{d}\right)\right]$$

Possible input definitions expressed as a function of X at T = 0 are represented in Fig. VI-5. They are limit solitary waves over a horizontal bottom. They are supposed to represent spilling breakers over a very gentle slope, reaching a steeper slope. They must be expressed by dimensionless parameters U and C as functions of X and T.

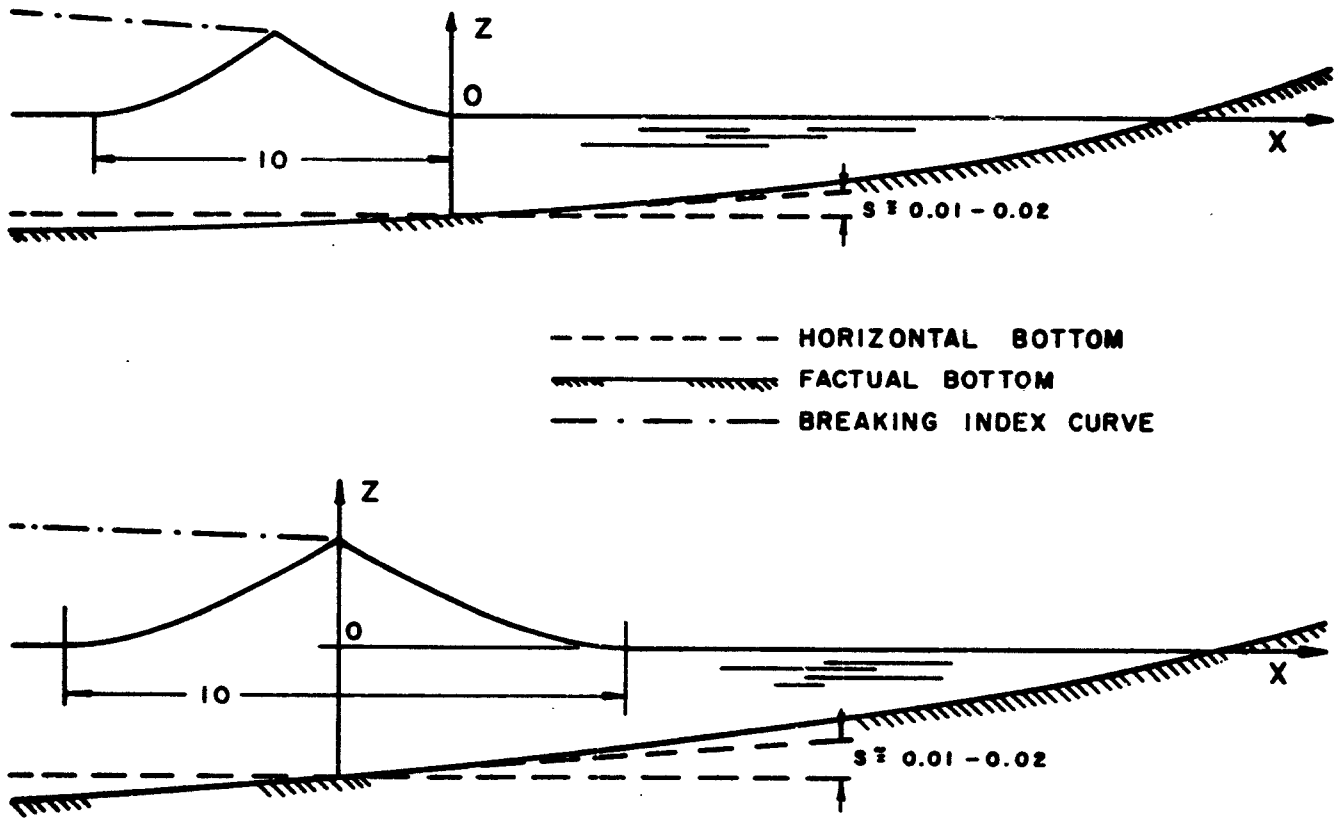

FIGURE VI-5
INPUT DEFINITIONS

It is known that the solitary wave has no theoretical horizontal limits. However, in practice $U \cong 0$ and C is very close to unity over a length of $X = 10$. The friction and curvature terms also tend to zero. Hence this can be considered as defining the limit of the wave. The location of the complete limits of the wave in the T-X diagram and the corresponding value for C can be calculated by exact integration in the case where S is a constant.

At the limit $\frac{dT}{dT} = \frac{1}{U + C} = \frac{1}{C}$ because $U = 0$.

Hence, $\frac{dT}{dX} = \frac{C_*}{c} = \left(\frac{d_1}{d}\right)^{1/2}$ because: $c = \sqrt{gd}$

$\eta = 0$

i.e.

$$\frac{dT}{dX} = \left(\frac{d_1}{d_1 - SX}\right)^{1/2} = \frac{1}{[1 - SX]^{1/2}}$$

For example, in the first case presented in Fig. VI-4, the shoreward limit is defined by the equation:

$$T = \int \frac{dX}{(1-SX)^{1/2}} = \frac{2}{S}\left[1 - (1-SX)^{1/2}\right] \qquad \text{(VI-17)}$$

since $X = 0$ for $T = 0$. The seaward limit is defined by the following two functions: (1) on the horizontal bed ($X < 0$)

$$\frac{dT}{dX} = \frac{1}{C} = \left(\frac{d_1}{d_1}\right)^{1/2} = 1, \quad T = L + X \qquad \text{(VI-18)}$$

L being the "wave length" (L = 10)

(2) on the slope, it is easily seen that

$$T = L + \frac{2}{S}\left[1 - (1 - SX)^{1/2}\right] \qquad \text{(VI-19)}$$

Along these limits, $U = 0$ and $C = \left(\frac{d}{d_1}\right)^{1/2} = (1 - SX)^{1/2}$ (VI-20)

A number of calculations can be eliminated by considering that the slope does not have any influence on the wave motion as long as the characteristic U - C (of slope $\frac{1}{U - C} = \frac{1}{-C} = -1$) coming from the point X = 0, T = 0 does not cross a characteristic U + C. Hence, the input can be taken along this characteristic (U - C) (line AB on Fig. VI-5)) by a simple projection of the values of U and C from AD to AB. Even projecting them to AE will introduce only a very small error because the effect of the slope on the wave motion remains small as long as the wave elements do not encroach on the slope.

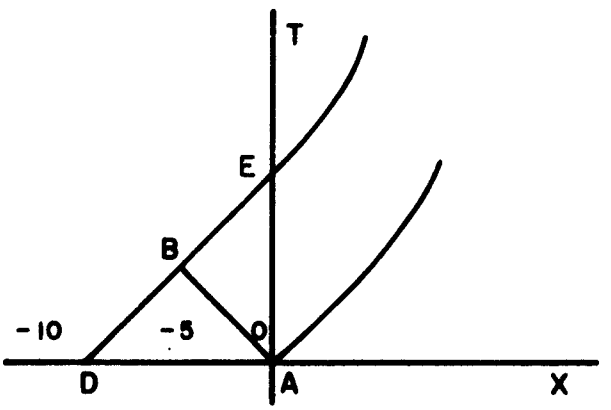

FIGURE VI-6
WAVE LIMITS AND INPUT DEFINITION

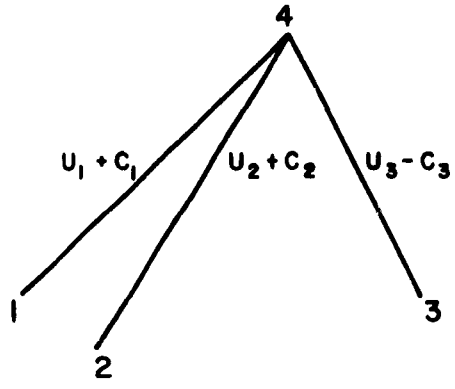

FIGURE VI-7
BORE INCEPTION

5. BORE INCEPTION AND CALCULATIONS

Now the very important phenomenon of the bore inception is analyzed.

When the two characteristics (U + C) cross each other (point 4 on Fig. VI-7)), then two sets of values for U and C are obtained at point 4, namely U_{u_4}, C_{u_4}, U_{d_4} and C_{d_4} from the equations:

$$\begin{cases} U_u + 2C_u = U_1 + 2C_1 + G\,\Delta\, T_{1-4} \\ U_u - 2C_u = U_3 - 2C_3 + G\,\Delta\, T_{3-4} \end{cases} \qquad \text{(VI-21)}$$

and

$$\begin{cases} U_d + 2C_d = U_2 + 2C_2 + G\,\Delta\, T_{2-4} \\ U_d - 2C_d = U_3 - 2C_3 + G\,\Delta\, T_{3-4} \end{cases} \qquad \text{(VI-22)}$$

Physically this means that the wave profile is vertical at that point. There is bore inception U_d and C_d characterising the value of U and C just in front of the bore and U_u and C_u just at the top of the front of the bore.

Then there is a discontinuity in the T-X diagram. The classical method no longer applies along a line which crosses the line $W = \frac{dX}{dT}$ ($W = w / \sqrt{g d_1}$, w being the speed of the bore).

Before studying the bore equations, some further considerations on the bore inception must be given.

It can easily be seen that all the (U + C) characteristics on the front side of the wave converge, while all characteristics on the back side of the wave diverge. Hence the bore inception on the T-X diagram depends upon the chosen interval ΔX for the input definition. The smaller the interval, the sooner the bore appears. In fact, since input is a limit solitary wave, it is normal that the bore begins as soon as the effect of the slope is felt, i.e. at the intersection of the characteristics (U - C) coming from $T = 0$, $X = 0$. But the loss of energy due to a small spilling breaker near the crest is negligible as long as the initial interval ΔX for two characteristics (U + C) is small.

Along a line crossing the W line, the momentum and continuity equations are those of a shock wave, i.e. from elementary hydraulics. (See Fig. VI-8).

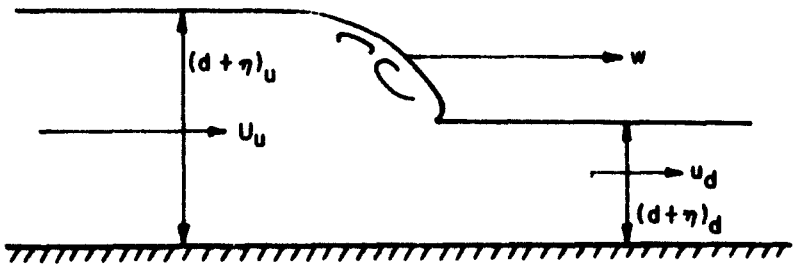

FIGURE VI-8
BORE NOTATION

$$\rho g \frac{(d+\eta)_u^2}{2} - \rho g \frac{(d+\eta)_d^2}{2} = \rho (d+\eta)_d (u_d - u_u)(w - u_d)$$

$$u_u (d+\eta)_u = w \left[(d+\eta)_u - (d+\eta)_d \right] + u_d (d+\eta)_d \quad \text{(VI-24)}$$

i.e. after inserting the dimensionless notation U_u, U_d, C_u, C_d, W

$$C_u^4 - C_d^4 = 2 C_d^2 (W - U_d)(U_u - U_d) \quad \text{(VI-25)}$$

$$U_u C_u^2 - U_d C_d^2 = W (C_u^2 - C_d^2) \quad \text{(VI-26)}$$

from which it is found that the dimensionless velocity of the bore W is:

$$W = U_d + \frac{C_u}{C_d}\left[\frac{C_u^2 + C_d^2}{2}\right]^{1/2} \qquad \text{(VI-27)}$$

Then a W line from the bore inception must be drawn in the T-X diagram with a slope such as $\frac{dX}{dT} = W$. It must be noted that this line is between the line of slope $U_u + C_u$ and $U_d + C_d$ (see Fig. VI-9). But W also varies as a function of X . Hence it must be computed step by step

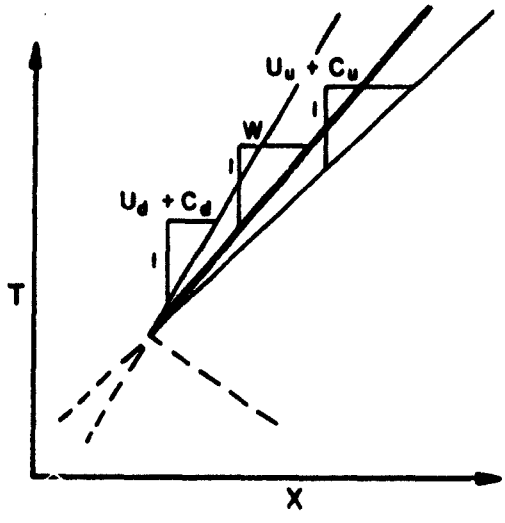

FIGURE VI-9
BORE CHARACTERISTICS
AFTER INCEPTION

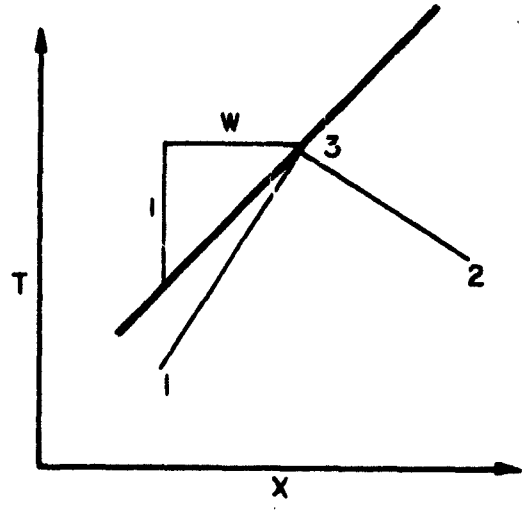

FIGURE VI-10
ON THE LOW SIDE OF THE BORE

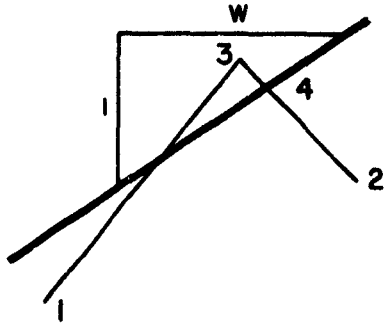

FIGURE VI-11
INTERPOLATION

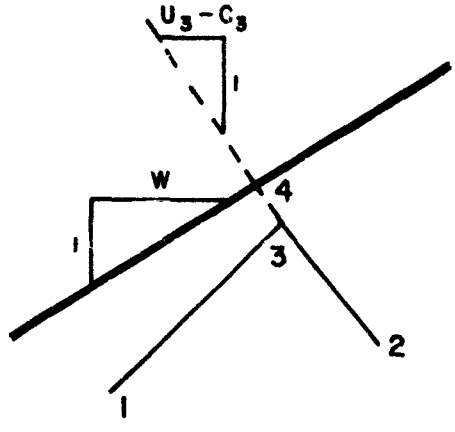

FIGURE VI-12
EXTRAPOLATION

First it must be noted that U and C can always be calculated by the classical process on the low side of the bore, i.e. in front of the bore because W is always greater than (U + C) on that side (see Fig. VI-10). But point (3) of Fig. VI-10, calculated from points (1) and (2), does not necessarily coincide with any point of the W line. Hence U_d and C_d just in front of the bore must be determined either by interpolation between (2) and (3) along the line $(U_2 - C_2)$ (see Fig. VI-11) or by extrapolation from (2) to (3) along a line $(U_3 - C_3)$ (see Fig. VI-12).

This work is greatly simplified when the W line crosses the "limit" of the wave (defined by Eq. (VI-17) because then the bore travels on still water with

$$U_d = 0$$

$$C_d = \left(\frac{d}{d_1}\right)^{1/2} = (1 - SX)^{1/2} \qquad \text{(VI-28)}$$

Now three other unknowns remain: namely U_u, C_u, and the W values for the following step. Hence three equations are necessary. These three equations are given by the continuity and momentum for the bore and have been already expressed in (VI-25) and (VI-26). Another equation is given from the classical relationship

$$d\ (U + 2C) = G\ dT$$

applied along the $(U_0 + C_0)$ line on the high side of the bore and which crosses the W line at the point to be determined. (See Fig. VI-13).

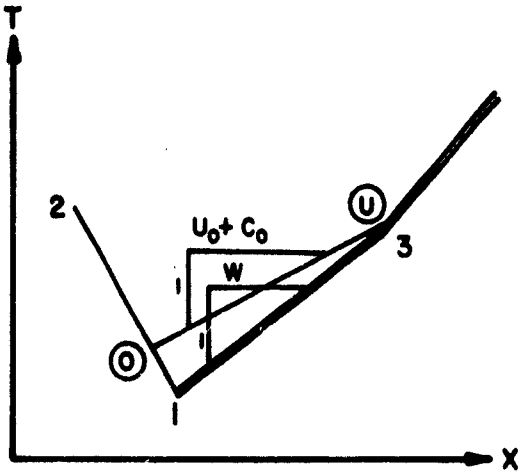

FIGURE VI-13
ON THE HIGH SIDE OF THE BORE

For this purpose the determination of the values U_0 and C_0 of point (0) can be done theoretically on the $(U_1 - C_1)$ line by interpolating the U and C values between (1) and (2). Then

$$\left(U_u + 2C_u\right)_3 = U_0 + 2C_0 + G\,\Delta\,T_{0-u} \qquad \text{(VI-29)}$$

In practice points (0) and (1) are so close to each other that the values for U_0 and C_0 can sometimes be taken as U_{u_1} and C_{u_1}.
Then Eq. (VI-29) is replaced by:

$$\left(U_u + 2C_u\right)_3 = \left(U_u + 2C_u\right)_1 + G_1\,\Delta\,T_{1-3} \qquad \text{(VI-30)}$$

Now U_u , C_u and W can be determined from Eqs. (VI-25), (VI-26), and (VI-29) or (VI-30).

The solution of this system is given by the following set of equations:

$$\frac{Y^4 - 1}{2Y\left[1 + Y^2\right]^{1/2}} + 2Y = K \qquad \text{(VI-31)}$$

where

$$Y = \frac{C_u}{C_d}$$

$$K = \frac{\left(U_0 + 2C_0\right) - U_d + G\,\Delta\, T_{0-u}}{C_d} \qquad \text{(VI-32)}$$

$$U_0 + 2C_0 \cong \left(U_u + 2C_u\right) \quad \text{step before} \qquad \text{(VI-33)}$$

The function K = f(Y) has been drawn for a range of possible values for Y. Then Y is determined graphically from the enclosed curve Fig. VI-14. If Eq. (VI-31) is mathematically solved, then six values for Y can be found, but only one has a physical significance. This value can easily be known since $Y = \frac{C_u}{C_d}$ always varies slowly along the W line.

When C_u is calculated, then U_u is easily obtained from Eq. (VI-30). Then W can be calculated for the following interval by formula (VI-27).

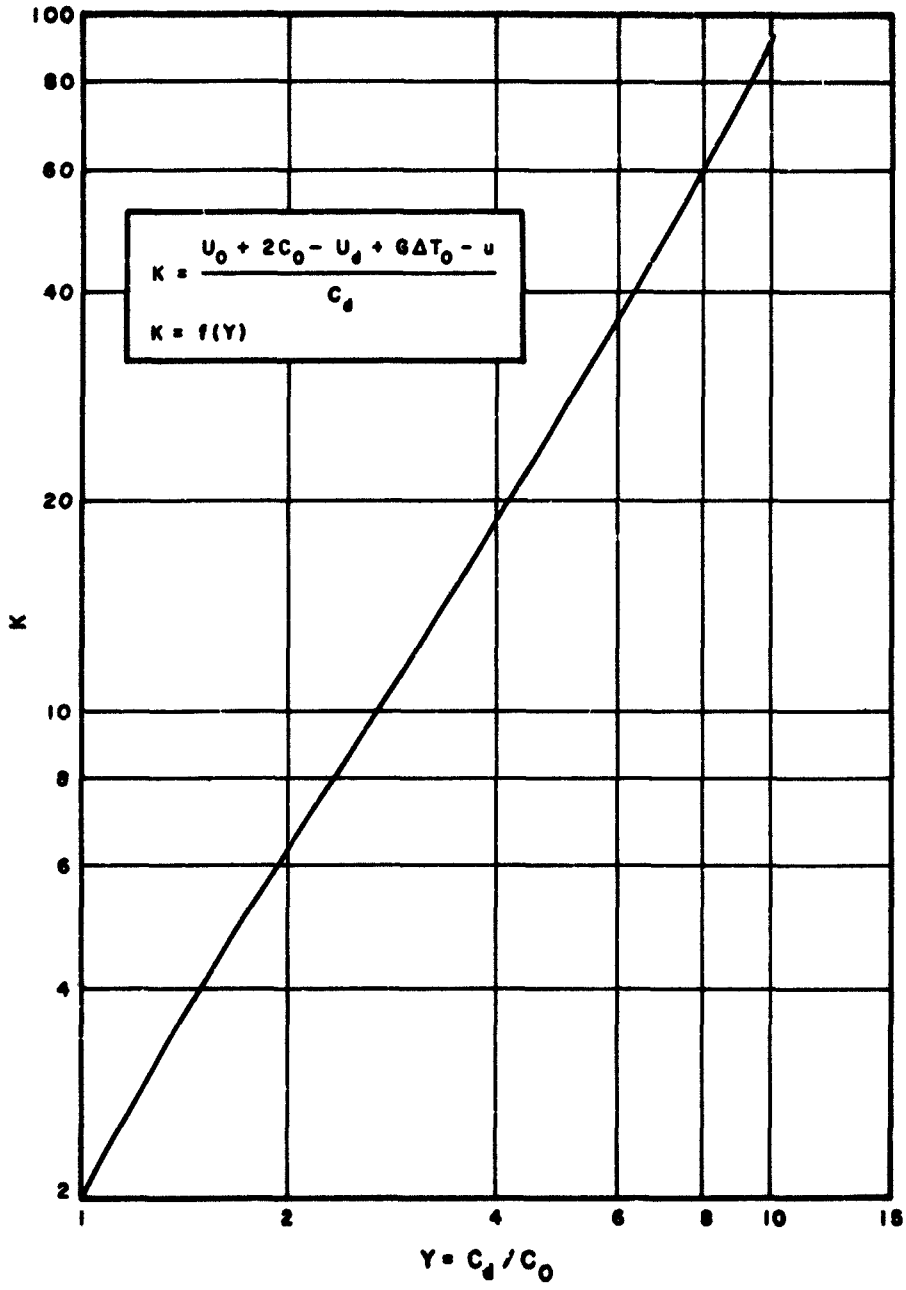

FIGURE VI-14

GRAPHICAL REPRESENTATION OF THE FUNCTION

$\frac{C_u}{C_d} = f(K)$ FOR BORE CALCULATIONS

6. A BORE REACHING A ZERO DEPTH WITHOUT BOTTOM FRICTION

Now the particular problem of the bore reaching the shoreline is analysed. This problem has already given rise to a number of interesting studies of a mathematical nature: Whitham (1958), Keller, et. al. (1960), Ho and Meyer (1962). The following calculations are developed from a different approach but give similar results. A careful comparison of these various studies has not been considered as being within the scope of this study because of the rather academic nature of the research. It will be seen in the following section that for practical purposes the bottom friction forces completely change the results presented in this section.

Consider the bore formula:

$$W = \frac{C_u}{C_d} \left[\frac{C_u^2 + C_d^2}{2} \right]^{1/2} \qquad \text{(VI-34)}$$

It is seen that $C_d \rightarrow 0$ near the shoreline, and at the same time

$$\frac{d(C_d)}{dX} = \frac{d\left[\sqrt{1 - SX}\right]}{dX} \rightarrow -\infty$$

Hence the variations of W_1 and also U_u and C_u must be expected to be very large near the shoreline. The step-by-step process of calculation based on the assumption of slow variations is no longer valid as the shoreline is approached.

From formula (VI-34), it is seen that when $C_d \rightarrow 0$, W can have any value depending upon the value for C_u. In fact, it has been

found by Freeman that W can never exceed $U_u + C_u$. Indeed the wave elements which yield up their energy to the bore arrive at a speed $U + C$. The dissipation of energy due to the bore causes C_u to decrease in such a way that the speed of the bore W also decreases to a value $U_u + C_u$ after which more energy is provided from behind the bore. Hence the Freeman limit $W < U_u + C_u$ shows that W is finite if U_u and C_u are finite. It can easily be seen from characteristic equation along any characteristic

$$\left(U_u + 2C_u\right) = \left(U + 2C\right) + G\Delta T = Cst \qquad \text{(VI-35)}$$

that U_u and C_u can never be infinity. (They are both positive).

Moreover, consider the relationship (VI-34) in which W is finite and $C_d \to 0$. It is seen that this can be achieved only if both $C_u \to 0$ and $\frac{C_u}{C_d} \to \infty$. Hence C_d must be an infinitesimal of higher order than C_u. The Eq. (VI-35) becomes, at the shoreline:

$$U_u = U_S = U + 2C + G\Delta T \qquad \text{(VI-36)}$$

This means that the bore (or shock wave) disappears at the shoreline and that the potential energy (function of C_u) is suddenly completely transformed into kinetic energy (function of U_u). Moreover, by continuity it must be expected that

$$W \to U_u \qquad \text{(VI-37)}$$

which is in agreement with the Freeman limit. It is seen also that the Freeman limit is reached only at the shoreline where

$$W \rightarrow U_u + C_1 \rightarrow U_u = U_s$$

Hence at the shoreline the characteristic equation can be written:

$$d\left(U_u + 2C_u\right) = -S\,dT = -\frac{S\,dX}{U_u} \qquad \text{(VI-38)}$$

or

$$U_u\,d\left(U_u + 2C_u\right) + d\left(C_d^{\,2}\right) = 0 \qquad \text{(VI-39)}$$

Letting $\alpha = \frac{U_u}{C_d}$ and $\beta = \frac{C_u}{C_d}$ Eqs. (VI-34) and (VI-37) give:

$$\frac{W}{C_d} = \alpha = \beta\left[\frac{1+\beta^2}{2}\right]^{1/2} \qquad \text{(VI-40)}$$

Dividing (VI-38) by $C_d^{\,2}$, inserting α and β, and the value for α given by (VI-40), then expressing α as a function of β and C_d as a function of S and X, it is found that:

$$\frac{\beta\left[\frac{1+\beta^2}{2}\right]^{1/2} d\left[\beta\left(\frac{1+\beta^2}{2}\right)^{1/2} + \beta\right]}{\beta\left[\frac{1+\beta^2}{2}\right]^{1/2}\left[\left(\frac{1+\beta^2}{2}\right)^{1/2} + 1\right]^{-2}} = \frac{S\,dX}{1-SX} \rightarrow +\infty \qquad \text{(VI-41)}$$

β is always larger than unity (and even tends to infinity) hence, the denominator of the left hand term is positive. Hence Eq. (VI-41) implies that $\frac{d\beta}{\beta} \rightarrow \infty$, since $\beta = \left(\frac{C_u}{C_d}\right)$ already tends to infinity for W to be finite, $d\beta$ must also tend to infinity but at a higher rate. Consequently, since $\frac{d(C_d)}{dX} \rightarrow -\infty$, then $\frac{d(C_u)}{dX}$ also $\rightarrow -\infty$ but at a much greater rate.

Moreover, from the characteristic Eq. (VI-38), it is seen that since $\frac{d(C_u)}{dX} \rightarrow -\infty$, $\frac{d(U_u)}{dX} \rightarrow +\infty$. Accordingly $\frac{dW}{dX} \rightarrow +\infty$.

To sum up these results, near the shoreline if the bottom friction forces are neglected:

$U_d = 0$	$\frac{d(U_d)}{dX} = 0$
$C_d \to 0$	$\frac{d(C_d)}{dX} \to -\infty$
$C_u \to 0$	$\frac{d(C_u)}{dX} \to -\infty$
$\frac{C_u}{C_d} \to \infty$	$\frac{d\left(\frac{C_u}{C_d}\right)}{dX} \to \infty$
$W \to U_u$: finite	$\frac{dW}{dX} \to \frac{d(U_u)}{dX} \to \infty$

The bore disappears at the shoreline and is replaced by a "rarefaction wave" which appears as an edge of water climbing over a dry bed.

U_u at the shoreline (called U_s in the following) can then be approximated very simply. Since it is known that C_u at the shoreline tends to zero and that $\frac{dX}{dT} = W \to U_u + C_u$, U_s can be given by:

$$U_s = (U_u + 2C_u) + G \Delta T \qquad \text{(VI-42)}$$

In practice the values U_u and C_u can be taken from the step prior to the quick variations of W, U_u and C_u. For example, the point could be chosen where $\frac{dW}{dX} = 0$. In practice, also, the rate of variation which follows is so quick that if $G \Delta T$ is taken to be $-S \Delta T$, it is found to be negligible in Eq. (VI-42) and this equation may be taken quite simply as $U_s = U_u + 2C_u$. This equation

explains the sudden increase of water velocity near the shoreline when the shock wave or bore disappears.

7. THE WAVE RUN-UP CALCULATION ON A DRY BED

At the extreme edge of water $C = 0$, because $\eta = -d$. Hence, the characteristic equations is simply:

$$dU = G\,dT \text{ along } \frac{dX}{dT} = U \qquad \text{(VI-43)}$$

Hence $d\left(\frac{U^2}{2}\right) = -S\,dX$ and neglecting the friction forces:

$$\frac{U^2}{2} = \frac{U_s^2}{2} - S(X - X_s) \qquad \text{(VI-44)}$$

where X_s is the shoreline coordinate.

The vertical run-up can be calculated directly in the case where it is the first wave element which has the most energy

$$\frac{R}{d_1} = \left(X_{max} - X_s\right) S = \frac{U_s^2}{2} = \frac{u_s^2}{2gd_1} \qquad \text{(VI-45)}$$

However, the following wave elements usually overtake the first one, so increasing the run-up and generating a "roll-wave." The exact calculation of the run-up is then difficult because at the front of the wave: $U + C = U - C$. This difficulty is automatically solved if the friction forces are taken into account as follows.

It is seen that if at the front of the wave $C \to 0$, the friction term $f\left(\frac{U}{C}\right)^2$ tends to infinity. Hence the edge of water is cut short and the leading front appears as an almost vertical wall of water which has the physical appearance of a bore. Then, the basic equation for the leading wave element is:

$$d(U+2C) = -\left[S + f\left(\frac{U}{C}\right)^2\right] \frac{dX}{U+C} \qquad \text{(VI-46)}$$

For reason of similitude, there exists between U and C a linear relationship: $U = A\,C$. The value of A depends upon the friction coefficient. This value can be determined by anology with a boundary layer problem. If, more simply, one assumes that at the front of the wave all particles have the same velocity u , the convective inertia is zero. Also, the local inertia $\rho \frac{\delta u}{\delta t}$ is negligible by comparison with the pressure gradient and friction term. Hence by equating pressure, gravity, to bottom friction forces, it gives Fig. VI-15.

$$(d+\eta)\left[\frac{d(d+\eta)}{dx} - S\right] - \frac{f}{g}\,u^2 = 0 \qquad \text{(VI-47)}$$

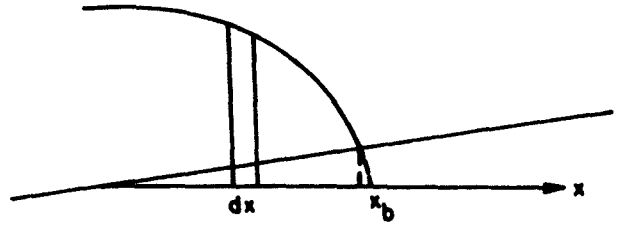

FIGURE VI-15
WAVE FRONT ON A DRY BED

Also, the slope S is small. Hence, by integrating Eq. (VI-47)

$$(d+\eta)^2 = \frac{2f}{g}\left(x_b - x\right) \quad u^2$$

x_b being the coordinate at the extreme front of water. It is seen that the front of water is in the form of a parabola.

Also, for reason of similitude, the length of the front of water ($x_b - x_1$), is proportional to u^2 such as ($x_b - x_1$) = Bu^2. Hence $C^4 = 2\,f\,B\,U^4$ and $A = (2\,f\,B)^{1/4}$

An adaptation from a work of Keulegan (1949) gives A = 1/2. Whatever the value for A , Eq. (VI-45) can be written

$$(1 + A)(1 + 2A) \quad \frac{d}{dX}\left(\frac{U^2}{2}\right) + \left(\frac{f}{A^2} + S\right) = 0 \qquad \text{(VI-48)}$$

which gives for U:

$$\frac{U^2}{2} = \frac{U_n^{\,2}}{2} - \left[S + \frac{f}{A^2} \right] \frac{X - X_n}{(1 + A)(1 + 2A)} \qquad \text{(VI-49)}$$

The leading front characteristic is determined graphically step by step, by the intersection of the curve $\frac{dX}{dT} = U$ where U is given by the Eq. (VI-49) and the (U + C) characteristics catching up the leading front. The value of U at the intersection is determined along this characteristic (U + C) from the equation:

$$\left(U_o + 2C_o\right) = (1 + 2A)\,U + G\Delta T \qquad \text{(VI-50)}$$

The wave front becomes increasingly insensitive to the following wave elements. The maximum run-up is found when $\frac{dX}{dT} \rightarrow 0$, for all characteristics (U + C).

Now the problem of the bore near the shoreline with bottom friction can be solved. It has been seen that when $C_d \rightarrow 0$, $C_u \rightarrow 0$, $W \rightarrow U_u$, and $\frac{dC_u}{dX} \rightarrow -\infty$. In fact such limits are unrealistic because they are obtained by neglecting the bottom friction, which is never negligible near the shoreline. Hence, in practice the theoretical curves shown in Fig. VI-16 should be replaced by more factual curves. These factual curves are obtained by considering the relationship which exists between U and C at the front of the run-up on a dry bed. This relationship has been previously established and depends upon the friction coefficient f. Hence, as soon as the relationship $U_u = AC_u$ is verified, the motion must be considered as a motion on a dry bed. The bore theory is no longer valid.

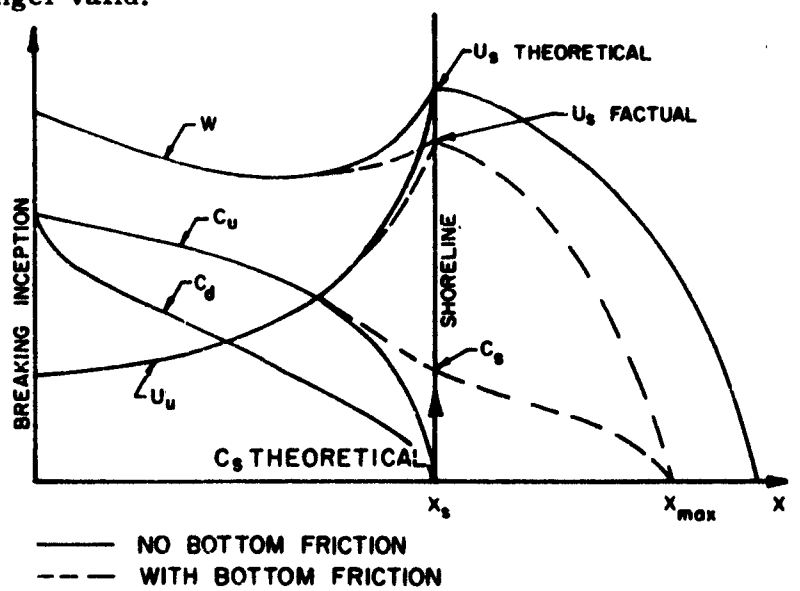

FIGURE VI-16
BORE CHARACTERISTICS

8. APPLICATION

The method described in the previous section has been partly applied by R. S. Grewal over a beach of constant 1/10 slope, corresponding to one of the highest beach slopes. Since it was the purpose of this study to find a method of computation for the run-up, such a steep slope was chosen because it permitted investigation of all the various theoretical aspects of the problem with less calculation than a more gentle slope. Also, since the path curvature is very tedious to calculate and does not present any theoretical difficulties, it can justifiably be neglected for a slope of 1/10. The bottom friction term is also negligible except near the shoreline.

For sufficient accuracy, at least four characteristic numbers are necessary to perform the calculations because errors accumulate rapidly.

The input definition has been calculated as indicated in section 4. The results are presented in Table VI-1 for $0 > X > 5$. They are symmetrical around $X = -5$ for $-5 > X > -10$.

TABLE VI-1

INPUT DEFINITIONS

X	0	-0.5	-1.0	-1.5	-2.0	-2.5
U	0.0133	0.0227	0.0360	0.0633	0.0864	0.1191
C	1.000	1.000	1.000	1.005	1.015	1.029
X	-3.0	-3.5	-4.0	-4.5	-5.0	
U	0.1801	0.2598		0.3535	0.4771	0.6032
C	1.063	1.118	1.204	1.300	1.334	

The corresponding results are presented in Fig. VI-17. Fig. VI-18 is an enlarged portion of Fig. VI-17 near the shoreline. Fig. VI-19 represents the successive wave profiles obtained from Fig. VI-17 and VI-18.

Because such results have a definite value, the values of W, U and C for all the points are given in Tables VI-2 and VI-3 and Figures VI-20 and VI-21 give the values of U_d, C_d, U_u, C_u, W and η as functions of X and T respectively.

Now the run-up can be calculated from the following set of equations. Since $G \Delta T$ is small, U_s and C_s at the shoreline are obtained from

$$U_s + 2 C_s = U_u + 2 C_u$$

Taking the last obtained values for U_u and C_u at $X = 9.52$ (the shoreline is at $X = 10$), one obtains:

$$U_s + 2 C_s = 1.223 + 2 (.635) = 2.493$$

And from the relationship $U_s = A C_s$ where A is arbitrarily chosen as 0.34 for example, it is found that $U_s = 1.568$, and $C_s = 0.466$.

The application of the method presented in section 7 has not been performed quantitatively because it was beyond the scope of the present project. The Fig. VI-22 gives a qualitative aspect of the characteristic method over a dry bed. Some quick calculations seem to show that $\frac{R}{H} = 2.82$. In fact the final result depends upon the value for A.

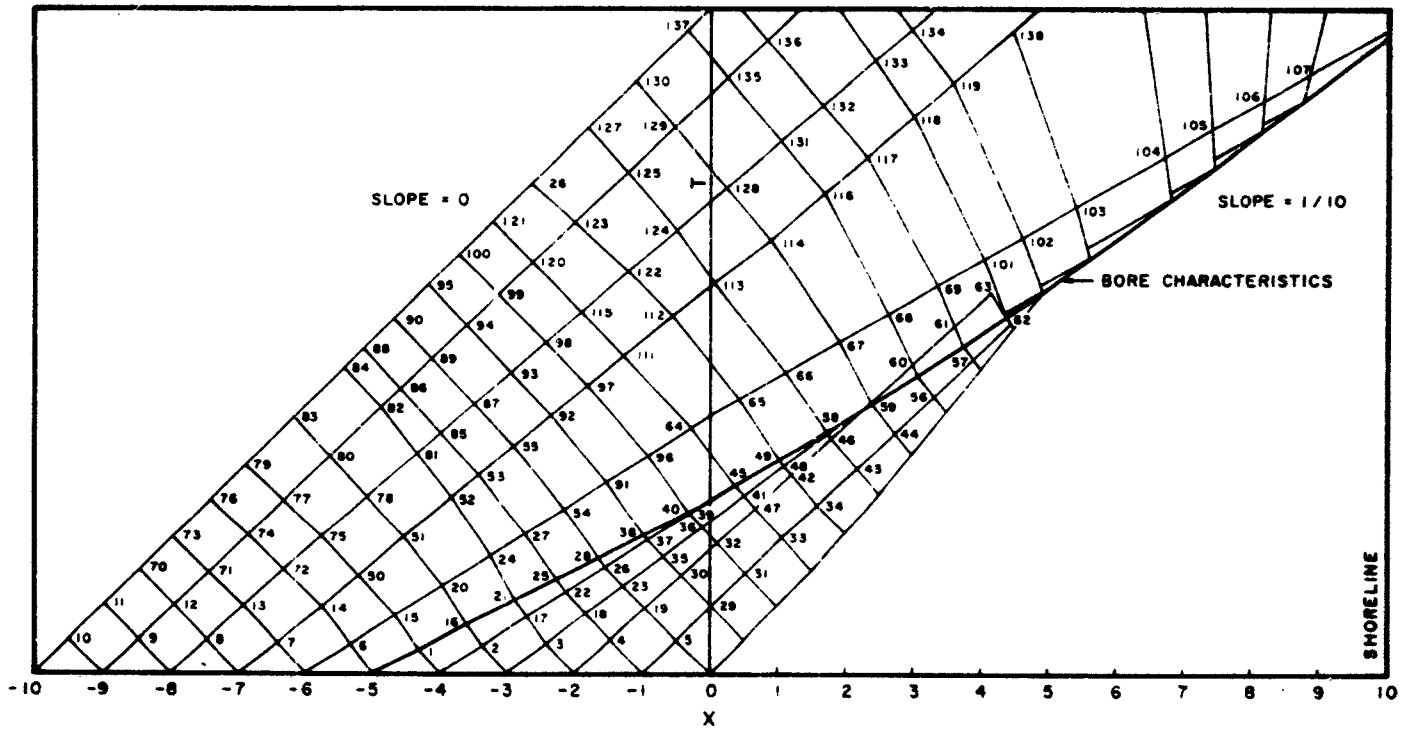

FIGURE VI-17
APPLICATION OF THE METHOD OF CHARACTERISTICS OVER A 1/10 BOTTOM SLOPE

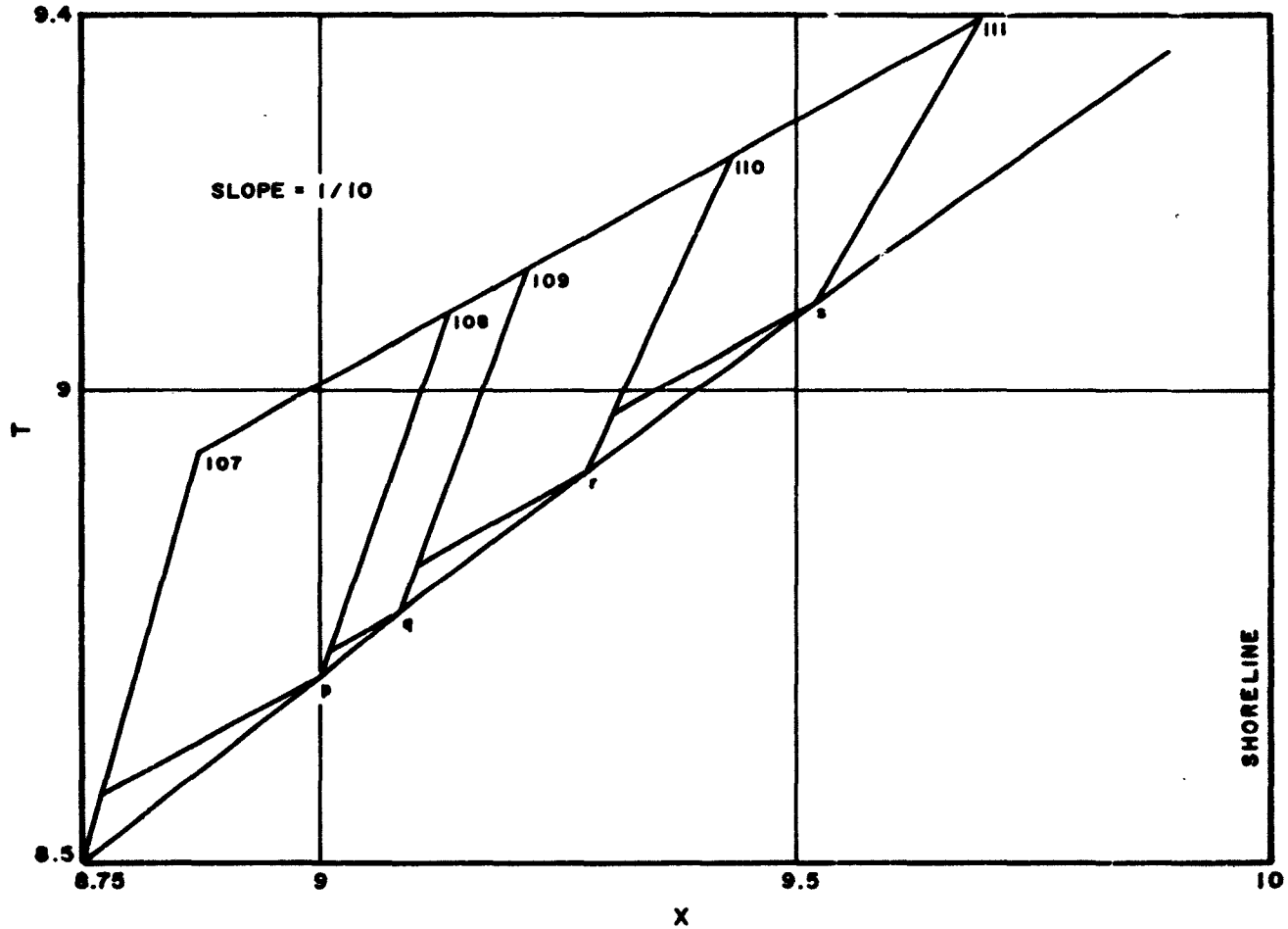

FIGURE VI-18
APPLICATION OF THE METHOD OF CHARACTERISTICS NEAR THE SHORELINE

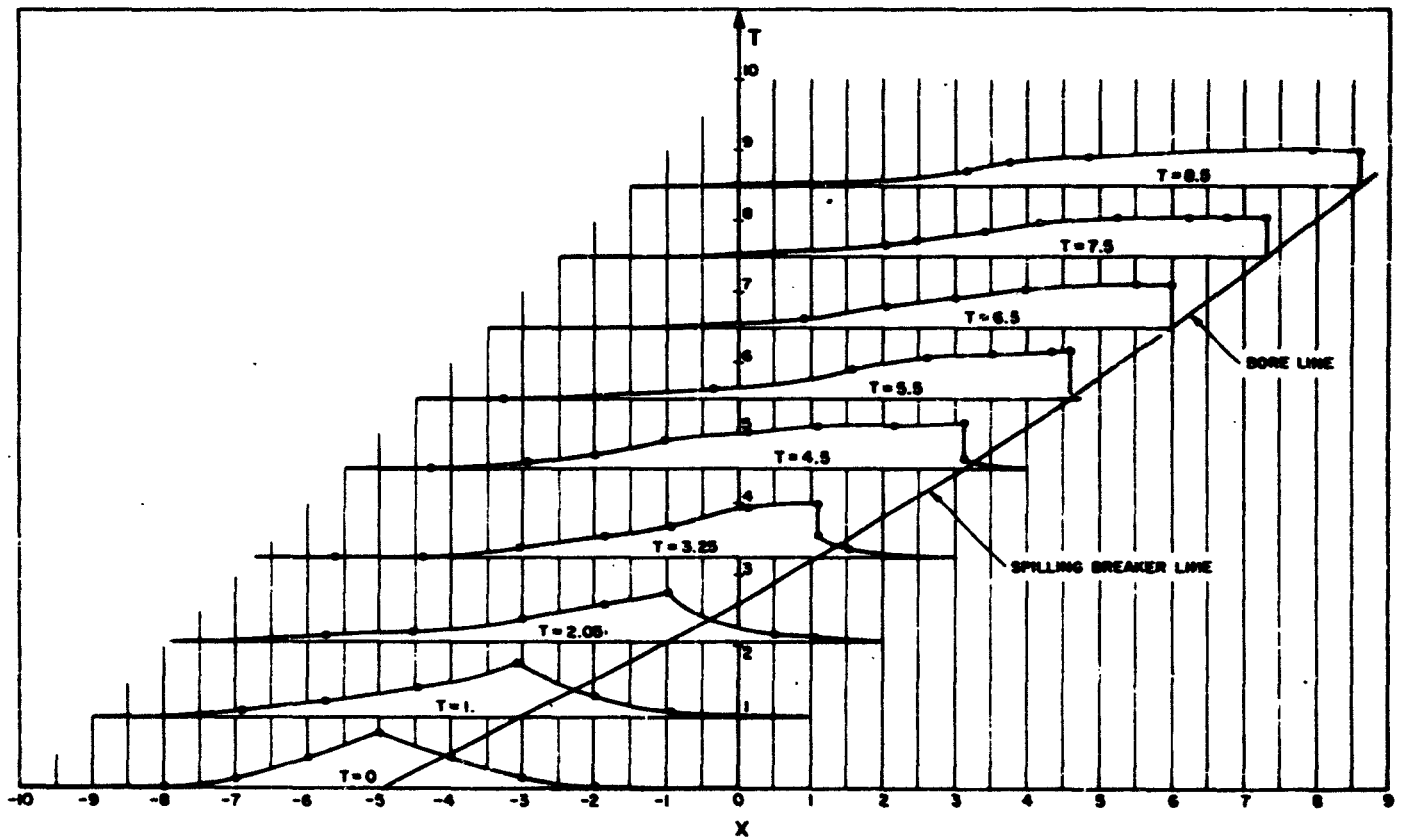

FIGURE VI-19
WAVE PROFILE VERSUS TIME AND DISTANCE

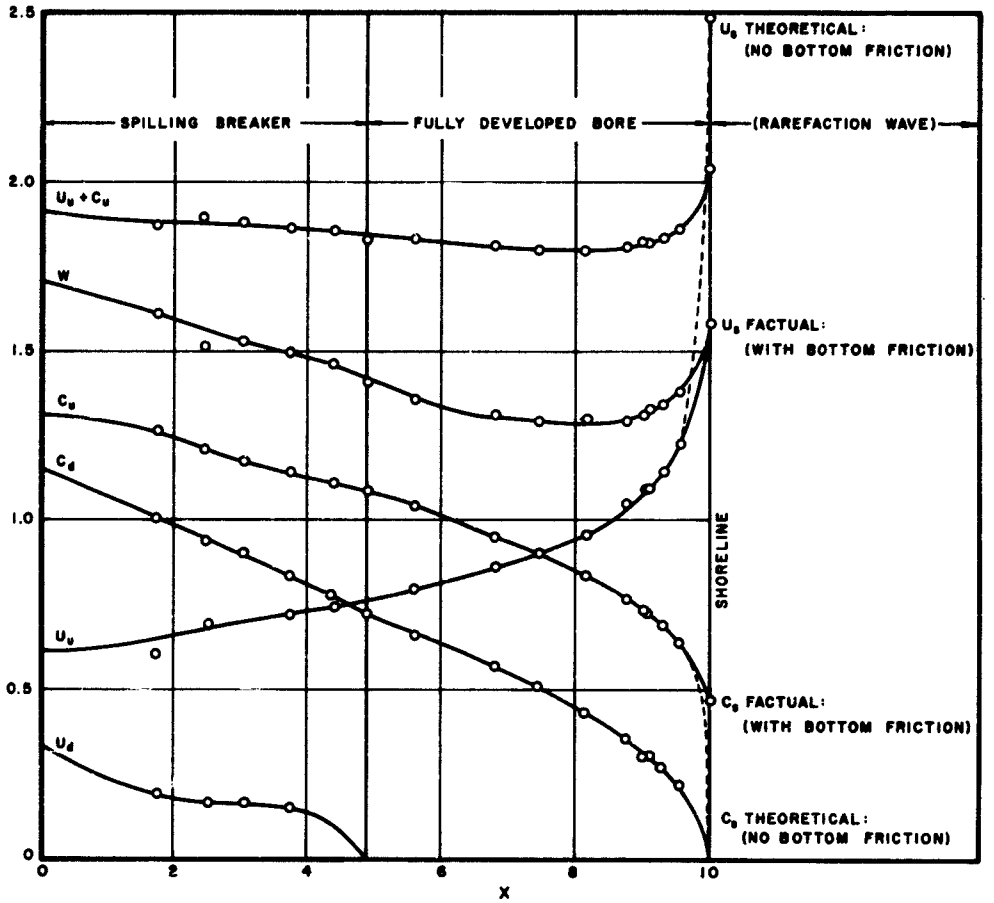

FIGURE VI-20
BORE CHARACTERISTICS VERSUS DISTANCE

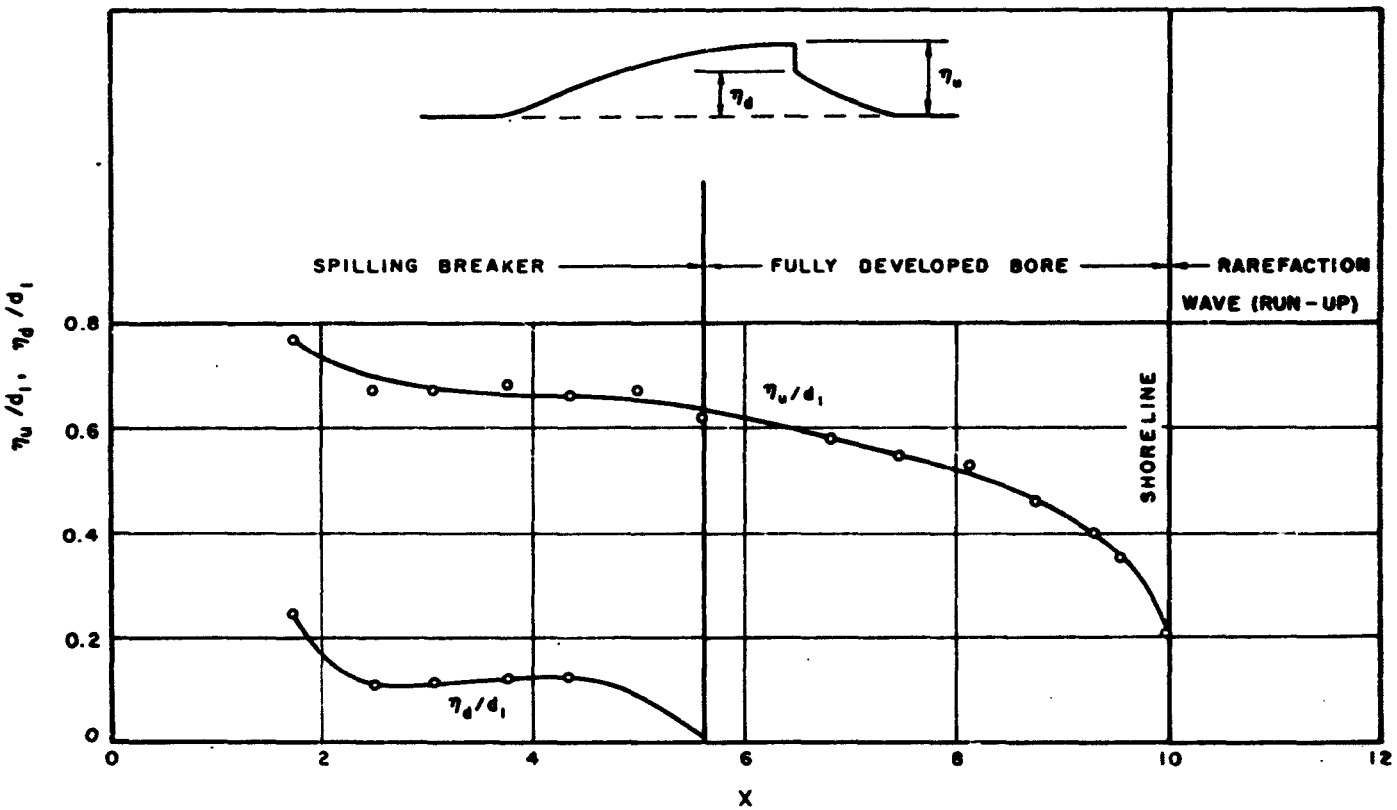

FIGURE VI-21
BORE CHARACTERISTICS VERSUS DISTANCE

TABLE VI-2

VALUES FOR U AND C (NUMBERS REFER TO THE POINTS OF FIGURE VI-17)

No.	U	C	No.	U	C	No.	U	C	No.	U	C	No.	U	C
1	.604	1.330	26	.380	1.188	51	.178	1.064	76	-.032	1.015	101	.613	1.087
2	.407	1.176	27	.400	1.181	52	.250	1.028	77	-.042	1.054	102	.618	1.068
3	.314	1.062	28	.630	1.313	53	.172	1.067	78	.131	1.041	103	.678	1.014
4	.076	1.020	29	.019	1.008	54	.383	1.190	79			104	.759	.933
5	.018	1.009	30	.059	1.028	55			80	.057	1.004	105	.815	.885
6	.352	1.205	31	.130	1.025	56	.141	.888	81	.203	1.005	106	.884	.828
7	.126	1.090	32	.084	.990	57	.148	.856	82	.129	.968	107	.984	.755
8	.083	1.017	33	.119	1.005	58	.198	1.038	83			108	1.035	.720
9	.046	.957	34	.153	.963	59	.134	.941	84			109		
10	.018	.991	35	.219	1.108	60	.185	.910	85	.125	1.043	110		
11	.066	.967	36	.219	1.083	61	.170	.889	86	.052	1.006	111	.047	1.141
12	.075	.996	37	.379	1.188	62	.155	.824	87	.106	1.052	112	.114	1.102
13	.031	1.043	38	.629	1.313	63	.177	.891	88			113	.307	1.002
14	.123	1.091	39	.304	1.175	64	.351	1.305	89	.033	1.016	114	.139	1.011
15	.353	1.204	40	.604	1.325	65	.438	1.248	90			115		
16	.659	1.302	41	.200	1.087	66	.437	1.228	91	.383	1.190	116	.116	.987
17	.474	1.142	42	.071	1.000	67	.512	1.165	92	.154	1.076	117	.114	.962
18	.237	1.100	43	.127	.947	68	.621	1.150	93	.106	1.052	118	.264	.938
19	.058	1.028	44	.134	.918	69	.607	1.111	94	.033	1.000	119	.168	.960
20	.408	1.178	45	.320	1.155	70	.041	.979	95			120		
21	.726	1.268	46	.102	.985	71	.006	1.030	96	.358	1.202	138	.199	.907
22	.397	1.180	47	.042	.986	72	.029	1.044	97	.130	1.088			
23	.219	1.108	48	.191	1.067	73	-.028	1.012	98	.082	1.064			
24	.479	1.142	49	.603	1.286	74	.003	1.032	99	-.007	1.020			
25	.647	1.305	50	.125	1.090	75	.031	1.091	100					

TABLE VI-3

BORE CHARACTERISTICS

No.	U_d	C_d	U_u	C_u	V	η_u/d_1	η_d/d_1	$\frac{1}{d_1}(\eta_u - \eta_d)$	$\frac{q}{d_1} = (1-sx)$	X	T
0											0
1	.604	1.330	.604	1.330	-	.769	.769	0	1.000	-4.32	.370
16	.659	1.302	.659	1.320	-	.695	.695	0	1.000	-3.60	.750
21	.726	1.268	.726	1.268	-	.607	.607	0	1.000	-2.90	1.100
25	.647	1.305	.647	1.305	-	.703	.703	0	1.000	-2.30	1.400
28	.630	1.313	.630	1.313	-	.724	.724	0	1.000	-1.65	1.72
38	.629	1.313	.629	1.313	-	.724	.724	0	1.000	-1.00	2.07
40	.304	1.175	.604	1.325	1.717	.380	.380	0	1.000	-0.30	2.40
45	-	-	-	-	-	-	-	-	-	-	2.80
49	-	-	-	-	-	-	-	-	-	-	3.20
58	.198	1.038	.602	1.266	1.609	.777	.252	.525	.825	1.75	3.60
59	.130	.940	.688	1.203	1.510	.677	.113	.564	.770	2.50	3.95
60	.169	.902	.705	1.172	1.526	.678	.118	.560	.695	3.05	4.45
61	.156	.868	.714	1.145	1.493	.686	.128	.558	.625	3.75	4.90
63	.158	.834	.741	1.109	1.460	.666	.132	.534	.563	4.35	5.35
j	0	.717	.740	1.089	1.400	.676	.004	.672	.510	5.00	5.70
k	0	.663	.794	1.034	1.353	.629	-.001	.629	.440	5.60	6.20
l	0	.565	.860	.949	1.309	.580	-.001	.580	.320	6.80	7.10
m	0	.505	-.901	.898	1.294	.551	0	.551	.255	7.45	7.60
n	0	.430	.954	.838	1.295	.517	0	.517	.185	8.15	8.15
o	0	.353	1.045	.766	1.290	.461	0	.461	.125	8.75	8.60
p	0	.316	1.090	.733	1.308	.437	0	.437	.100	9.00	8.695
q	0	.302	1.090	.725	1.329	.433	0	.433	.092	9.10	8.765
r	0	.268	1.144	.688	1.337	.401	0	.401	.072	9.27	8.912
s	0	.219	1.223	.635	1.374	.355	0	.355	.048	9.55	9.090

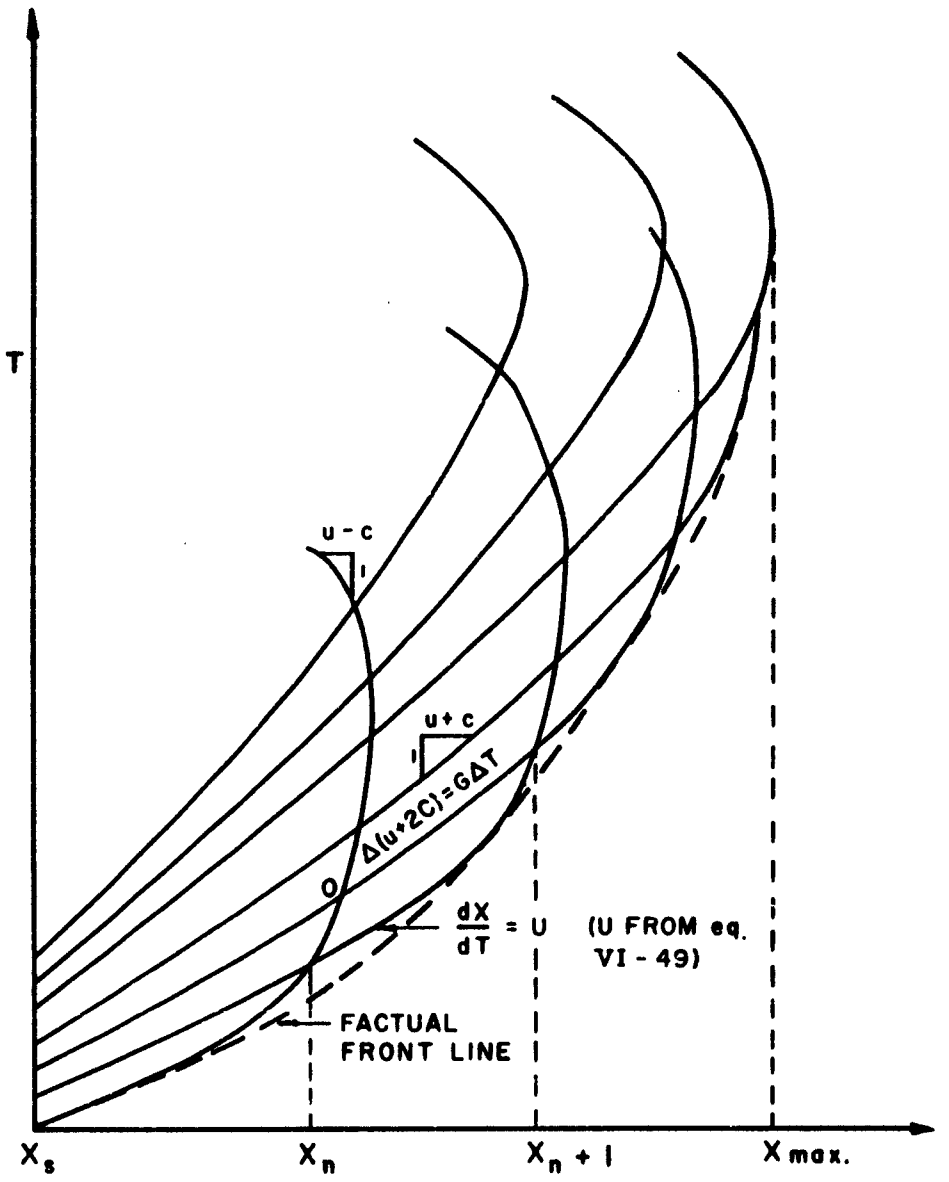

FIGURE VI-22
QUALITATIVE ASPECT OF THE METHOD OF CHARACTERISTICS FOR STUDYING SURGE OVER A DRY BED

It seems that the value for A is between the value proposed by Keulegan, namely A = 0.5, and the value chosen in this example, A = 0.34

9. CONCLUSION

A theoretical method has been developed for computing the wave run-up. The various steps of computation have been described, namely:

a. Input definition for possible maximum run-up

b. Wave deformation on a slope

c. Wave breaking inception

d. Bore traveling within the "limits" of the wave ($U_d \neq 0$).

e. Bore traveling outside the "limits" of the wave ($U_d = 0$).

f. Bore reaching the shoreline without bottom friction

g. Bore reaching the shoreline with bottom friction

h. The run-up on a dry bed with bottom friction, including the determination of the shape and height of the wave front.

It can therefore be said that a great step forward has been made in a field which, despite its importance, has had a relatively small number of theoretical studies. Most previous studies on wave run-up have been mainly limited to experimental studies on rather steep slopes in laboratories. Previous theoretical studies on the climb of a bore on a beach mainly covered topics e and f above. Practical considerations have shown that the bottom friction modified the theoretical results obtained in f.

Despite the present achievements, the problem deserves further investigation and refinement. A computer program has to be developed for analyzing rapidly and accurately the cases of waves traveling on various slopes. The friction coefficients can be determined by correlating the present theories with some experimental results. Then other cases can be investigated rapidly.

Finally the theory of run-up on a dry bed can be refined by further analytical and experimental investigation.

Among other topies to be investigated prior to writing the computer program is the choice of interval and characteristic numbers as a function of the error. Also a numerical method can be work out to calculate U and C for given values of X and T defining a fixed rectangular net as it has been proposed by Stoker for flood routing. This process will permit the path curvature term to be taken into account more easily.

REFERENCES

Birkhoff, G. (1949). Hydrodynamics . Dover, New York, p. 23

Earnshaw, S. (1845). Transactions. Cambridge Philosophical Society Vol. VIII.

Freeman, J.C., Jr. (1951). "The Solution of Nonlinear Meteorological Problems by the Method of Characteristics." Compendium of Meteorology, American Meteorological Society, pp. 421-433.

Ho, D.V. and R. E. Meyer (1962). "Climb of a Bore on a Beach." Technical Report No. 47, Brown Univeristy, Providence, R.I.

Keller, H. B., D. A. Levine, G. B. Whitham (1960). "Motion of a Bore Over a Sloping Beach." Journal of Fluid Mechanics, 7, pp. 302-316.

Laitone, E.V., (1961). Higher Approximation to Nonlinear Water Waves and the Limiting Heights of Cnoidal Solitary and Stokes Waves. I.E.R. Tech. Report 89 - 6. University of California, Berkeley.

Le Méhauté, B. (1962). "On Nonsaturated Breakers and the Wave Run-up." VIII Conf. on Coasting Engineering, Mexico.

Keulegan, G. H. (1949). "Wave Motion." Proc., IVth Hydraulics Conference, Iowa, John Wiley & Son, edited by H. Rouse, p. 756

McCowan (1891). "On the Solitary Wave." Phil. Mag., 32 (5), pp. 45-58.

Munk, W. H. (1949). "The Solitary Wave Theory and Its Application to Surf Problems." Annals of New York Academy of Science, Vol. 51., Art. 3, pp. 376-424.

Stoker, J. J. (1957). Water Waves. Interscience Publishers, Inc., New York, p. 291 and following.

Whitham, G.B. (1958). "On the Propagation of Shock Waves through Regions of Non-uniform Area of Flow." Journal of Fluid Mechanics, 4, pp. 337-360.

LIST OF SYMBOLS
APPENDIX VI

x		Horizontal coordinate positive towards the shoreline
z		Vertical coordinate positive upwards (Mid-water level $z = 0$)
t		Time
d		Depth (bottom: $z = -d$)
η		Vertical distance from the free surface to the mid-water level.
u		Horizontal water velocity
w		Vertical water velocity
c	$=$	$\sqrt{g(d+\eta)}$
g		Gravity acceleration
C_h		Chezy coefficient
f		Friction coefficient $= \frac{g}{C_h^2}$
G_*	$=$	$-gS - \frac{g^2}{C_h^2}\left(\frac{u}{c}\right)^2 + \frac{c^2}{3g^2}\frac{\delta^3(uc^2)}{\delta x^2 \delta t}$
S		Bottom slope
C_*		$\sqrt{g d_1}$
d_1		Depth at the origin
X	$=$	$\frac{x}{d_1}$: Dimensionless horizontal distance
T	$=$	$\frac{\sqrt{g d_1}\, t}{d_1}$: Dimensionless time
U	$=$	$\frac{u}{\sqrt{g d_1}}$: Dimensionless horizontal velocity
C	$=$	$\frac{c}{\sqrt{g d_1}}$: Dimensionless velocity for wave elements

$G = g G_*$: Dimensionless correcting term for characteristics

H Wave height of a solitary wave

V Solitary wave velocity ($\sqrt{g (d + H)}$)

Sub_u Related to the high side of the bore

Sub_d Related to the low side of the bore

Sub_s Related to the shoreline

Sub_b Related to the front of the wave

w Bore velocity

$W = \frac{w}{\sqrt{g d_1}}$: Dimensionless bore velocity

$Y = \frac{C_u}{C_d}$

$K = \frac{(U_o + 2C) - U_d + G \Delta T}{C_d}$

$\alpha = \frac{U_u}{C_d}$

$\beta = \frac{C_u}{C_d}$

R Vertical Run-up

$R_* = \frac{R}{d_1}$: Dimensionless vertical run-up

A Coefficient $\frac{U}{C}$ for the wave front

B Coefficient characterizing the length of the wave front.

APPENDIX VII

TWO-DIMENSIONAL NONLINEAR WAVE MOTION IN AN ESTUARY

By
John C. Freeman, Jr.
Larry Armijo
Mary Ann Noser

1. INTRODUCTION

The analysis of two-dimensional waves in an estuary has resulted in two studies:

a. The nonlinear motion of a single finite wave. This has yielded some new developments in wave analysis.

b. The presentation of a finite difference scheme, suitable for numerical machine computation, that allows for evaluation of two-dimensional wave motion by the method of wave derivatives. Although other approaches may exist, this was selected as the best and most economical computation method for the wave problem at hand.

2. NONLINEAR MOTION OF A THIN WAVE THROUGH A BAY

A moving wave is not a general two-dimensional disturbance over a 40 mile square. Indeed, even a wave with a period of a hundred seconds influences only about a mile and most indications are that the wave passes over an area in a finite time and leaves the given area relatively undisturbed after passage. This implies that the wave is a relatively thin long disturbance moving through a bay that is certainly undisturbed ahead of it and probably undisturbed behind it. Thus, a solitary wave may be regarded as a disturbance influencing only a narrow strip at any given time.

1. INTRODUCTION

The analysis of two-dimensional waves in an estuary has resulted in two studies:

a. The nonlinear motion of a single finite wave. This has yielded some new developments in wave analysis.

b. The presentation of a finite difference scheme, suitable for numerical machine computation, that allows for evaluation of two-dimensional wave motion by the method of wave derivatives. Although other approaches may exist, this was selected as the best and most economical computation method for the wave problem at hand.

2. NONLINEAR MOTION OF A THIN WAVE THROUGH A BAY

A moving wave is not a general two-dimensional disturbance over a 40 mile square. Indeed, even a wave with a period of a hundred seconds influences only about a mile and most indications are that the wave passes over an area in a finite time and leaves the given area relatively undisturbed after passage. This implies that the wave is a relatively thin long disturbance moving through a bay that is certainly undisturbed ahead of it and probably undisturbed behind it. Thus, a solitary wave may be regarded as a disturbance influencing only a narrow strip at any given time.

We write the equations of motion in shallow water in the following form:

$$\left.\begin{aligned} &\frac{\partial u}{\partial t} + u\frac{\partial u}{\partial x} + v\frac{\partial u}{\partial y} + 2c\frac{\partial c}{\partial x} = 2c_o\frac{\partial c_o}{\partial x} - E_x \\ &\frac{\partial v}{\partial t} + u\frac{\partial v}{\partial x} + v\frac{\partial v}{\partial y} + 2c\frac{\partial c}{\partial y} = 2c_o\frac{\partial c_o}{\partial y} - E_y \\ &2\left(\frac{\partial c}{\partial t} + u\frac{\partial c}{\partial x} + v\frac{\partial c}{\partial y}\right) + c\left(\frac{\partial u}{\partial x} + \frac{\partial v}{\partial y}\right) = 0 \end{aligned}\right\} \qquad \text{(VII-1)}$$

In order to discuss the problem of leaving the fluid undisturbed, we consider a one-dimensional problem.

$$\begin{aligned} &\frac{\partial u}{\partial t} + u\frac{\partial u}{\partial x} + 2c\frac{\partial c}{\partial x} = 2c_o\frac{\partial c_o}{\partial x} - E_x \\ &2\left(\frac{\partial c}{\partial t} + u\frac{\partial c}{\partial x}\right) + c\frac{\partial u}{\partial x} = 0 \end{aligned} \qquad \text{(VII-2)}$$

This give us $\frac{d(u-2c)}{dt} = 2C_o\frac{\partial C_o}{\partial x} - E_x$ along $\frac{dx}{dt} = u + c$

which is the way we follow the wave

$$\frac{d(u-2c)}{dt} = +2C_o\frac{\partial C_o}{\partial x} - E_x \quad \text{along} \quad \frac{dx}{dt} = u - c$$

The wave moves along the x axis with a speed of the order of c so that $\frac{dx}{dt} = u - c$ moves through the wave with a speed of the order of -2c. This means that the line $\frac{dx}{dt} = u - c$ is almost parallel to the x axis and we can consider $\frac{d(u-2c)}{dx} = \frac{dt}{dx}\frac{d(u-2c)}{dt}$. If we neglect friction, $\frac{d(u-2c)}{dx} = \frac{Co}{u-c}\frac{\partial Co}{\partial x}$. Since $\frac{Co}{u-c} \approx -1$ and $\frac{dx}{dt} = \frac{dx}{dt} = (u - c)$ is almost parallel to t = zero,

$$\frac{d(u-2c)}{dx} = \frac{\partial(u-2c)}{\partial x} = \frac{\partial(-2\,Co)}{\partial x}$$

This tells us that a good approximation is

$$(u - 2c)\ (x,\ t) = -2\ Co\ (x).$$

This approximation includes as a result that the water is undisturbed after the last characteristic $\frac{dx}{dt} = u + c$ passes a point. Note that this says $u - c = Co - \frac{u}{2}$ so that $\frac{Co}{-Co - \frac{u}{2}}$

$$\approx -1 + \frac{u}{2Co}$$

The thin wave and the observed fact that most of the motion and wave height changes occur along a normal to the wave suggests the desirability of a system in which a normal to the wave is used as a coordinate system and in which the largest fluid motions are parallel to the wave so that v $\frac{\delta u}{\delta y}$, $\frac{\delta \eta}{\delta y}$, $\frac{\delta c}{\delta y}$ can be considered to the first order only, u and c will be considered to higher order.

Since changes in the y-direction in the ordinary flow would move through the wave much faster than along it (See Fig. VII-1) it is assumed that the chief contribution to v would be the turning of the wave front as you move parallel to it.

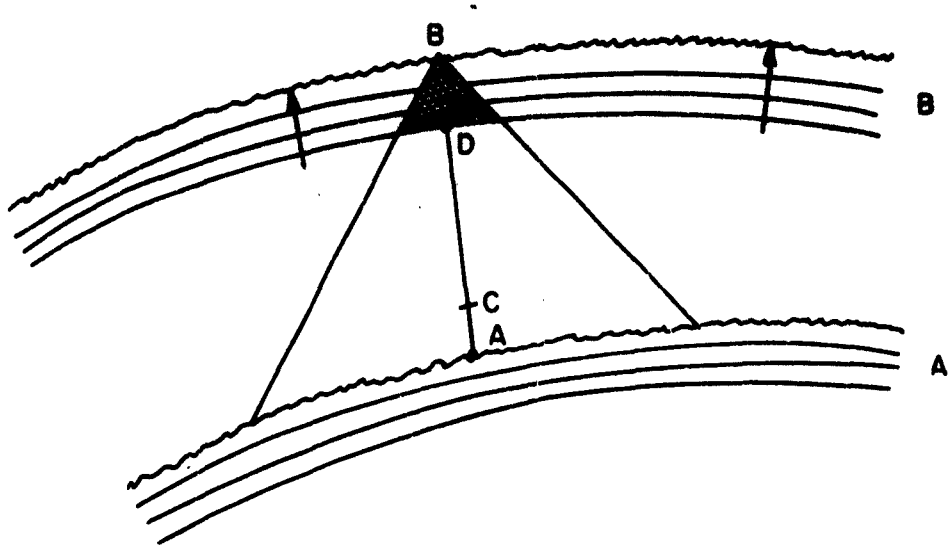

FIGURE VII-1
BASIC PRINCIPLE OF CALCULATION

If the wave travels from A to B, a disturbance at A could have only affected the wave in the shaded area and that only while the wave travels to C . The shaded area is determined completely by condition between D and B in the time it takes to travel from D to B . These considerations lead to the approximation that

$$v\,(y - y_o) = u(y - y_o)\;\theta(y - y_o)$$

or $(u \sin(\theta - \theta_o)$ in extreme cases).

The term $c\,\frac{\partial v}{\partial y}$ in Eq. VII-1 can then be written $c\,\frac{\partial}{\partial y}(u\theta)$.

We will ultimately find that W (the speed of a forward advancing bore) will control our wave and that

$$\frac{\partial \theta}{\partial t} = \frac{\partial V}{\partial y}\,,\quad V = f(u_b, c_b, c_{ob})$$

which we will show later.

This leaves us with the following equation for the motion of a wave with a leading bore moving through a shallow bay in a coordinate system with x normal to the wave.

$$\frac{\partial u}{\partial t} + u\frac{\partial u}{\partial x} + 2c\frac{\partial c}{\partial x} = 2c_o\frac{\partial c_o}{\partial x} - \frac{k g^{-\frac{1}{3}} u|u|}{c^{\frac{2}{3}}}$$

$$2\left(\frac{\partial c}{\partial t} + u\frac{\partial c}{\partial x} + v\frac{\partial c}{\partial y}\right) + c\frac{\partial u}{\partial x} + c\frac{\partial}{\partial y}(u\theta) = 0$$

$$\frac{\partial \theta}{\partial t} = \frac{\partial V}{\partial t}\ ;\ V = f(u_b, c_b, c_{ob})\ ;\ c_{ob} = c_o(x_b, y_b, t_b)$$

x_b, y_b, t_b are coordinates of a leading bore.

This give us

$$\frac{d}{dt}(u+2c) = 2c_o\frac{\partial c_o}{\partial x} - c\frac{\partial}{\partial y}(u\theta) - \frac{k g^{-\frac{1}{3}} u|u|}{c^{\frac{2}{3}}}$$

along $\frac{dx}{dt} = u + c$

We are also given as an approximation that

$$u - 2c = -2c_o$$

or

$$u = 2(c - c_o)$$

So we have

$$\frac{d}{dt}(4c - 2c_o) = 2c_o\frac{\partial c_o}{\partial x} - c\frac{\partial}{\partial y}2(c-c_o)\theta - 4\frac{k g^{-\frac{1}{3}}(c-c_o)|c-c_o|}{c^{\frac{2}{3}}}$$

along

$$\frac{dx}{dt} = 3c - 2c_o$$

This can be written

$$\frac{d(3c-2c_o)}{dt} = \left(-\frac{15}{4}c + 4c_o\right)\frac{\partial c_o}{\partial x} - \frac{3c}{2}\frac{\partial}{\partial y}(c-c_o)\theta - \frac{3k g^{-1/3}(c-c_o)|c-c_o|}{c^{2/3}}$$

along $\frac{dx}{dt} = 3c - 2c_0$ Note that:

$$c = \frac{(3c-2c_0)+2c_0}{3} \quad \text{and} \quad c - c_0 = \frac{(3c-2c_0)-c_0}{3}$$

are handy equations to use with this differential expression.

We can rewrite this expression setting $\epsilon = 3c - 2c_0$ so that

1. $-\frac{15}{4}c + 4c_0 = -\frac{5}{4}c - \frac{10}{4}c_0 + 4c_0 = -\frac{5}{4}c + \frac{3}{2}c_0$
2. $\frac{3}{2}c = \frac{\epsilon}{2} + c_0$
3. $(c-c_0)\,|c-c_0| = (\frac{\epsilon - c_0}{3})^2$
4. $c^{2/3} = (\frac{\epsilon + 2c_0}{3})^{2/3}$

The resulting statement of the problem is as follows:

$$\frac{d\epsilon}{dt} = (-\frac{5}{4}c + \frac{3}{2}c_0)\frac{\partial c_0}{\partial x} - \frac{(\frac{\epsilon}{2} - c_0)}{3}\frac{\partial}{\partial y}\theta(\epsilon - c_0)$$

$$- \frac{kg^{-1/3}}{3} \frac{(\epsilon - c_0)\,|\epsilon - c_0|}{(\frac{\epsilon + 2c_0}{3})^{2/3}}$$

along $\frac{dx}{dt} = \epsilon$

It is obvious from the structure of this set of equations that if a system in which we have large values of ϵ following on smaller values, that the larger values will overtake the smaller and a jump (or a bore) will form. Thus we are most interested in the wave with a leading bore.

We calculate the conditions at and the speed of this bore with the equations of conservation of mass and of momentum. Consider the bore as stationary with the fluid moving through it at speed -V.

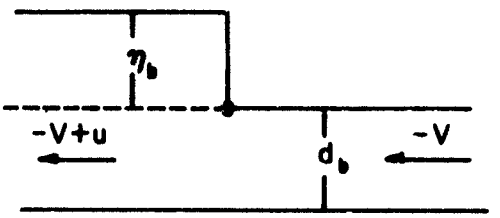

FIGURE VII-2
BORE NOTATION

Continuity of mass tells us $-V\, d_b = (-V+u)(d_b+\eta_b)$.

From our previously given equations, we find

$$V c_o^2 = \left[-V + 2(c-c_o)\right] c^2, \qquad V = \frac{2c^2(c-c_o)}{(c^2-c_o^2)} = \frac{2c^2}{c+c_o}$$

$$V(c^2-c_o^2) = 2c^2(c-c_o),$$

or the speed of the bore $V = \frac{2c^2}{c+c_o}$

We express this in terms of ϵ:

$$c = \frac{\epsilon}{3} + \frac{2}{3}c_o \; ; \; c + c_o = \frac{\epsilon}{3} + \frac{5}{3}c_o$$
$$V = \frac{2(\frac{\epsilon}{3} + \frac{2}{3}c_o)^2}{\frac{\epsilon}{3} + \frac{5}{3}c_o} = \frac{2}{3}\frac{(\epsilon+2c_o)^2}{\epsilon+5c_o} \qquad \text{(VII-3)}$$

It is inherent in the physics of the problem that $\epsilon - V \geq 0$. If $c - V = 0$ or nearly so and there is an indication c_o changes so that $\frac{d\epsilon - V}{dt} < 0$ then we must adjust ϵ so that $d(\epsilon - V) = 0$. (This usually occurs with decreasing c_o.) From Eq. (VII-3), $\epsilon_b > W$ except for $c_b = c_o$. There is a following value of $\epsilon < \epsilon_b$ for which we can say $\epsilon = V$. This value of ϵ will

be moving at the same speed as the bore and the values between it and the bore will be trapped unless the bore slows down.

Over a large part of the course of a wave, you might expect $c \approx c_0$. We write:

$$V = \frac{2}{3}\left[\frac{c^2+5cc_0}{c+5c_0} + \frac{4c_0^2-cc_0}{c+5c_0}\right]$$

$$V = \frac{2}{3}c + \frac{2}{3}c_0\,\frac{4c_0-c}{c+5c_0}$$

and get as an approximation:

$$V \approx \frac{2}{3}c + \frac{1}{3}c_0$$

We are now in a position to compute the wave and the bore.

$$\frac{dc}{dt} = -\frac{5}{4}\frac{dc_0}{dt} + \frac{3}{2}c_0\frac{\partial c_0}{\partial x} - \frac{\frac{c}{2}-c_0}{3}\frac{\partial}{\partial y}\theta(c-c_0)$$

$$-\frac{kg^{-1/3}}{3}\,\frac{(c-c_0)\,|c-c_0|}{\left(\frac{c+2c_0}{3}\right)^{2/3}}$$

In order to speed up computation, we now make two assumptions. One is that we can recognize when $(c-c_0)$ is negative or positive so that we can simplify the last term in the equation; the other and less justified assumption is that $(c-c_0)$ has a weak dependence on y so that the second term can be written

$$\frac{c_0}{6}(c-c_0)\frac{\partial\theta}{\partial y} - \frac{(c-c_0)^2}{6}\frac{\partial\theta}{\partial y}$$

We now set $$\frac{d'}{dt} = \frac{\partial}{\partial t} + (c-c_0)\frac{\partial}{\partial x}$$

and we have $$\frac{dc}{dt} = \frac{1}{4}\frac{dc_0}{dt} - \frac{3}{2}\frac{d'c_0}{dt} +$$

$$\frac{c_0(c-c_0)}{6}\frac{\partial\theta}{\partial y} - \frac{(c-c_0)^2}{6}\left[\frac{\partial\theta}{\partial y} + \frac{2(3)^{2/3}kg^{-1/3}}{(c+2c_0)^{2/3}}\right]$$

be moving at the same speed as the bore and the values between it and the bore will be trapped unless the bore slows down.

Over a large part of the course of a wave, you might expect $c \approx c_0$. We write:

$$V = \frac{2}{3}\left[\frac{c^2+5cc_0}{c+5c_0} + \frac{4c_0^2-cc_0}{c+5c_0}\right]$$

$$V = \frac{2}{3}c + \frac{2}{3}c_0\,\frac{4c_0-c}{c+5c_0}$$

and get as an approximation:

$$V \approx \frac{2}{3}c + \frac{1}{3}c_0$$

We are now in a position to compute the wave and the bore.

$$\frac{dc}{dt} = -\frac{5}{4}\frac{dc_0}{dt} + \frac{3}{2}c_0\frac{\partial c_0}{\partial x} - \frac{\frac{c}{2}-c_0}{3}\frac{\partial}{\partial y}\theta(c-c_0)$$

$$-\frac{kg^{-1/3}}{3}\,\frac{(c-c_0)|c-c_0|}{\left(\frac{c+2c_0}{3}\right)^{2/3}}$$

In order to speed up computation, we now make two assumptions. One is that we can recognize when $(c-c_0)$ is negative or positive so that we can simplify the last term in the equation; the other and less justified assumption is that $(c-c_0)$ has a weak dependence on y so that the second term can be written

$$\frac{c_0}{6}(c-c_0)\frac{\partial\theta}{\partial y} - \frac{(c-c_0)^2}{6}\frac{\partial\theta}{\partial y}$$

We now set $$\frac{d'}{dt} = \frac{\partial}{\partial t} + (c-c_0)\frac{\partial}{\partial x}$$

and we have $$\frac{dc}{dt} = \frac{1}{4}\frac{dc_0}{dt} - \frac{3}{2}\frac{d'c_0}{dt} +$$

$$\frac{c_0(c-c_0)}{6}\frac{\partial\theta}{\partial y} - \frac{(c-c_0)^2}{6}\left[\frac{\partial\theta}{\partial y} + \frac{2(3)^{2/3}kg^{-1/3}}{(c+2c_0)^{2/3}}\right]$$

Also we recall:

$$V_b = \frac{2}{3} c_b + \frac{2}{3} c_{ob} \frac{4c_{ob} - c_b}{c_b + 5c_{ob}}$$

Thus we can see that the total computation can be done in terms of c_i, c_o and $\frac{\partial \theta}{\partial y}$.

Thus a set of nomograms is indicated. These should give:

a. $c - c_o$

b. $\frac{c_o (c - c_o)}{6}$

c. $\frac{(c - c_o)^2}{6}$

d. $\frac{2(3)^{\frac{2}{3}} \, kg^{-\frac{1}{3}}}{(c + 2c_o)^{\frac{2}{3}}}$

e. $\frac{2}{3} c_o \frac{4c_o - c}{c + 5c_o} + \frac{2}{3} c = V$

f. $\frac{\partial \theta}{\partial y}$

Some of these quantities should be expressed as numbers and others should be shown as the distance traveled in a time increment.

The nomogram used for computation is included in Fig. VII-1. A sample approximate computation for Chesapeake Bay is included in Fig. VII-2.

3. USE OF THE NOMOGRAM

This nomogram is designed to compute the travel of a wave at speed c on the Coast and Geodetic chart No. C & GS 70-A for Chesapeake Bay near Norfolk. The travel is for 500 seconds. The

value of C_o is indicated by the depth d on the chart and it is assumed that values of c are written on the chart. The wave front traveling at speed V is the basis of Fig. VII-2. This is very much like a wave refraction diagram.

The use of this theory and nomogram should yield interesting results on two dimensional wave travel. The next section gives a more general development.

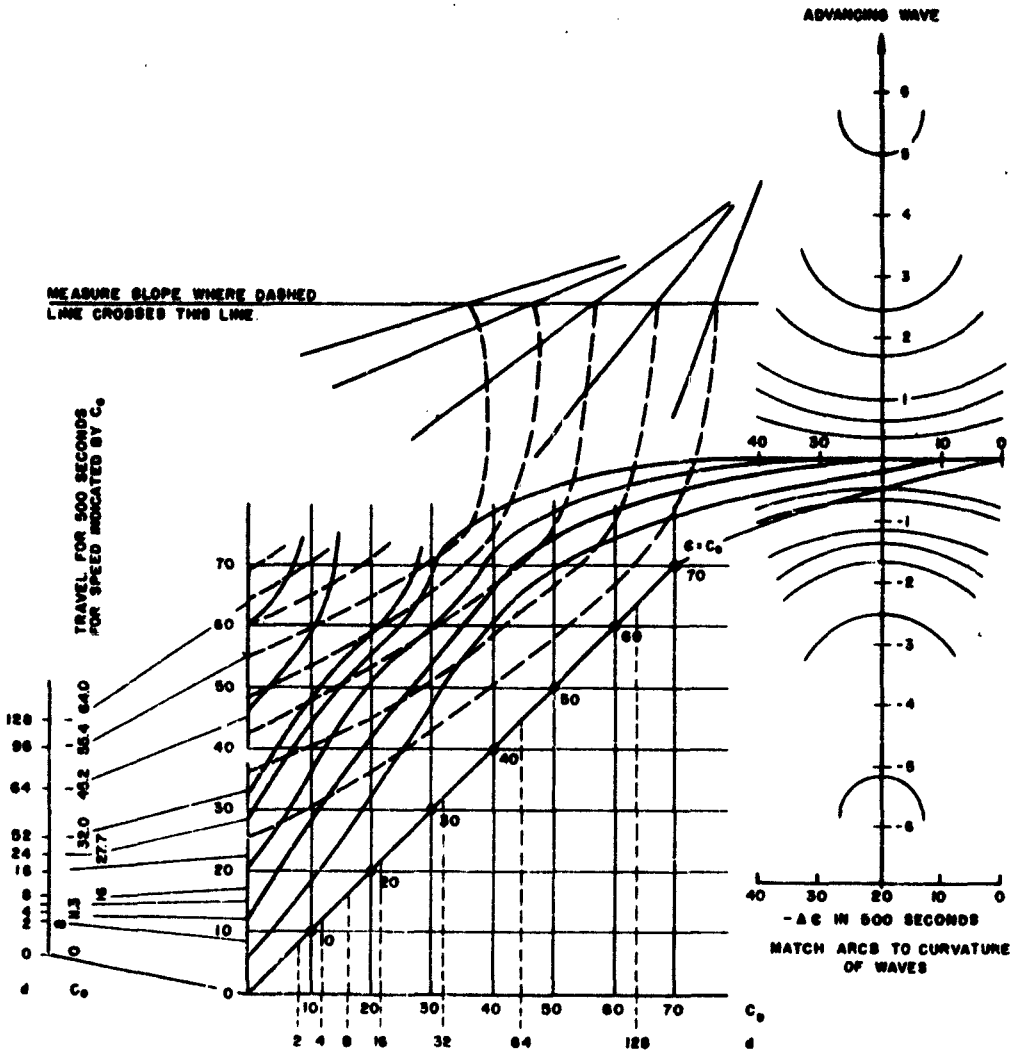

To find $(-\Delta C)$ enter nomogram with C and C_o.

1) Follow solid line to intercept on axis $\partial\theta/\partial y = 0$.
2) Follow dashed line to find slope.
3) Draw line in $(-\Delta C, \partial\theta/\partial y)$ plane.
4) Match arcs to find $\partial\theta/\partial y$.
5) Read $(-\Delta C)$.

FIGURE VII-3

NOMOGRAPH FOR TWO-DIMENSIONAL NONLINEAR LONG WAVES

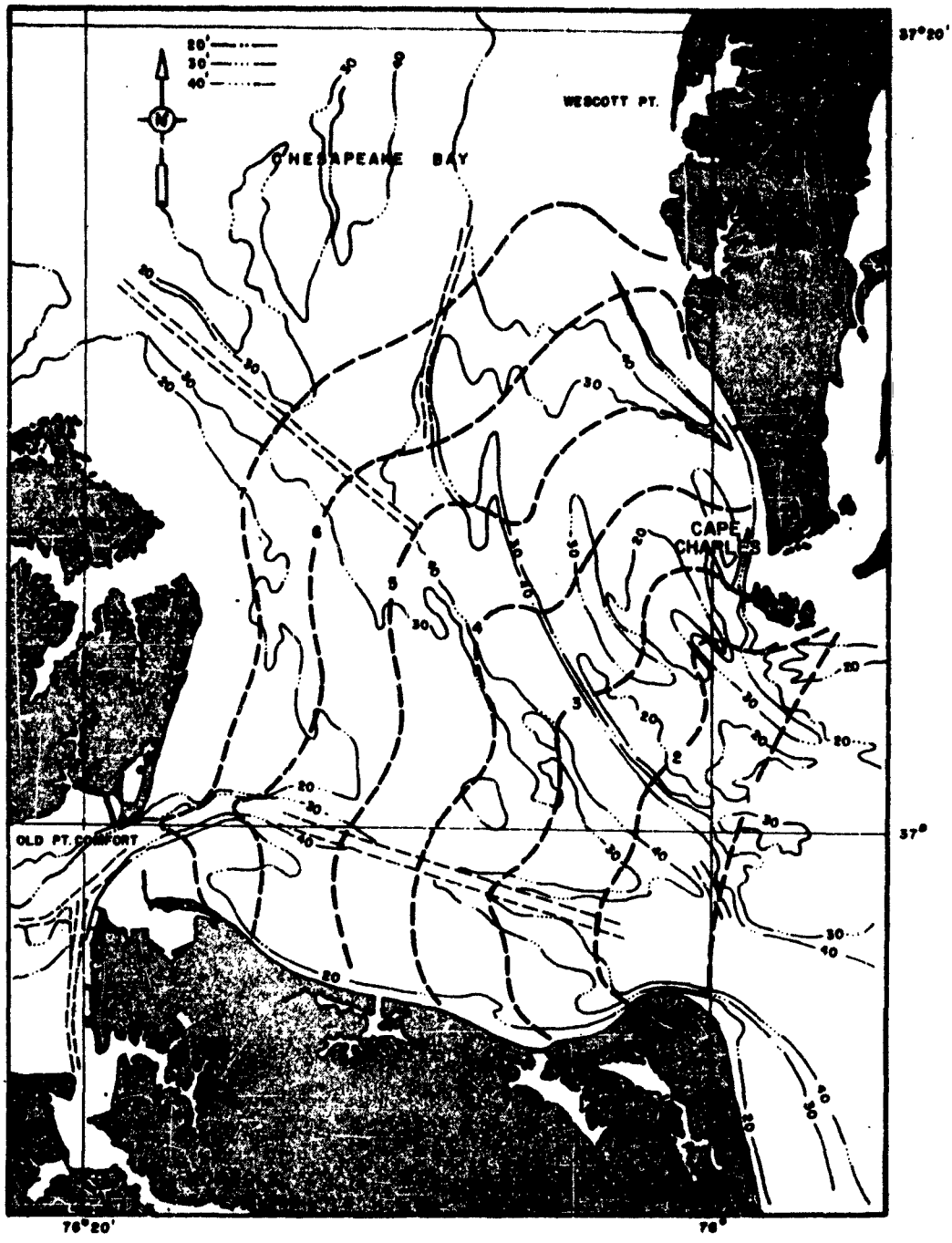

FIGURE VII-4

LEADING EDGE OF THE BORE POSITIONS EVERY 333 SECONDS IN THE LOWER CHESAPEAKE BAY

4. A NUMERICAL PROCEDURE FOR OBTAINING AN APPROXIMATE SOLUTION FOR THE TWO-DIMENSIONAL TIME WATER WAVE PROBLEM

The following is an approximate method for following the progress of a solitary wave through an estuary or bay. The method suggested is a slight modification of " The Method of Wave Derivatives," proposed by Freeman and Baer (1957)* . The notation used here is very much the same as that used in the above reference except that variable depth and friction effects are taken into account while Coriolis and wind effects are ignored. The difference equations are stated in terms of a fixed space grid, but only those portions of the grid in which the effects of a solitary wave will be noticeable are used in the computation. The entire procedure is motivated by physical considerations and the need to obtain reasonable results in a limited amount of time. Consequently, the procedure is not presented with an appropriate analysis of stability. We apologize in advance for the rather glaring lack of mathematical rigor in this discussion.

Let D be a bounded domain in the first quadrant of the x, y plane. Let D^* be a domain contained in D such that the distance from any point P in D^* to the boundary of D is greater than some fixed number $\sigma > 0$.

---

* Freeman, John C., Jr. and Ledolph Baer. "The Method of Wave Derivatives." Transactions, American Geophysical Union, Vol. 38, No. 4, August 1957, pp. 483-494.

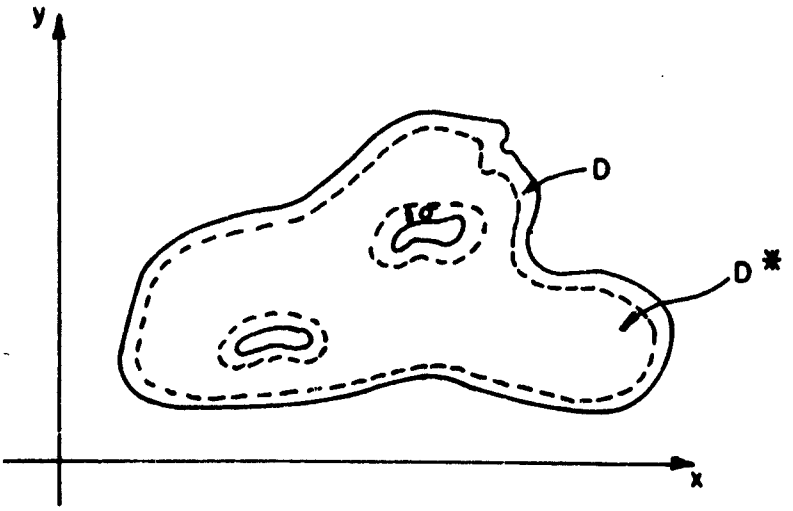

FIGURE VII-5
NOTATION FOR A NUMERICAL PROCEDURE
FOR NONLINEAR LONG WAVES

Let (x_i, y_j) be a square grid on the x, y plane of mesh width δ, i. e.

$$\left.\begin{aligned} x_i &= \delta_i \\ y_i &= \delta_i \end{aligned}\right\} \quad i, j = 0, 1, 2, \ldots .$$

We are concerned with the system of partial differential equations

$$\left\{\begin{aligned} &\frac{\partial u}{\partial t} + u\frac{\partial u}{\partial x} + v\frac{\partial u}{\partial y} + 2c\frac{\partial c}{\partial x} = g\frac{\partial d}{\partial x} - E_x \\ &\frac{\partial v}{\partial t} + u\frac{\partial v}{\partial x} + v\frac{\partial v}{\partial y} + 2c\frac{\partial c}{\partial y} = g\frac{\partial d}{\partial y} - E_y \\ &2\left(\frac{\partial c}{\partial t} + u\frac{\partial c}{\partial x} + v\frac{\partial c}{\partial y}\right) + c\left(\frac{\partial u}{\partial x} + \frac{\partial v}{\partial y}\right) = 0 \end{aligned}\right\} \quad (x,y) \in D,\ t > 0, \qquad \text{(VII-4)}$$

where u and v are the x and y components of the fluid velocity, d(x, y) is the depth of the basin represented by the domain D from a given reference level (e.g. sea level), c is the wave velocity, i.e.

$$c = \sqrt{gh} \tag{VII-5}$$

where

$$h(x,y,t) = d(x,y) + \eta(x,y,t)$$

$\eta(x, y, t)$ being the displacement of the free surface relative to the reference level. The quantities E_x and E_y are, respectively, the x and y components of the internal friction forces per unit mass. These are assumed to be of the forms

$$\left.\begin{aligned} E_x &= \frac{kg^{-1/3}\, u\sqrt{u^2+v^2}}{c^{2/3}}, \\ E_y &= \frac{kg^{-1/3}\, v\sqrt{u^2+v^2}}{c^{2/3}} \end{aligned}\right\} \tag{VII-6}$$

The values $u(x, y, 0)$, $v(x, y, 0)$, $d(x, y)$ and $(x, y, 0)$ are assumed to be known in D. The domain D^* or equivalently, the quantity σ, is to be determined so that the quantity h is bounded away from zero. For example, if an upper bound

$$M = \sup_{\substack{(x,y)\in D \\ 0\le t\le T}} |\eta(x,y,t)|$$

is known, then the domain D^* could be determined by the requirement that if $(x, y) \in D^*$, then

$$d(x,y) - M > e > 0,$$

where ϵ is some pre-assigned positive number.

By the methods of [1] , the system VII-1 may be replaced by the system

$$\left.\begin{aligned}
&\frac{D_1 A_1}{dt} + \frac{D_2 A_2}{dt} = 2g \frac{\delta d}{\delta x} - 2E_x, \\
&\frac{D_3 A_3}{dt} + \frac{D_4 A_4}{dt} = 2g \frac{\delta d}{\delta x} - 2E_x, \\
&\frac{D_1 A_1}{dt} + \frac{D_3 A_3}{dt} = 2g \left(\frac{\delta d}{\delta x} + \frac{\delta d}{\delta y}\right) - 2 (E_x + E_y), \\
&\frac{D_2 A_2}{dt} + \frac{D_4 A_4}{dt} = 2g \left(\frac{\delta d}{\delta x} - \frac{\delta d}{\delta y}\right) - 2 (E_x + E_y),
\end{aligned}\right\} \qquad \text{(VII-7)}$$

where

$$\left.\begin{aligned}
\frac{D_1}{dt} &= \frac{\delta}{\delta t} + (u+c) \frac{\delta}{\delta x} + (v+c) \frac{\delta}{\delta y}, \\
\frac{D_2}{dt} &= \frac{\delta}{\delta t} + (u+c) \frac{\delta}{\delta x} + (v-c) \frac{\delta}{\delta y}, \\
\frac{D_3}{dt} &= \frac{\delta}{\delta t} + (u-c) \frac{\delta}{\delta x} + (v-c) \frac{\delta}{\delta y}, \\
\frac{D_4}{dt} &= \frac{\delta}{\delta t} + (u-c) \frac{\delta}{\delta x} + (v+c) \frac{\delta}{\delta y},
\end{aligned}\right\} \qquad \text{(VII-8)}$$

and

$$\left.\begin{aligned}
A_1 &= u + v + 2c, \\
A_2 &= u - v + 2c, \\
A_3 &= u + v - 2c, \\
A_4 &= u - v - 2c,
\end{aligned}\right\} \qquad \text{(VII-9)}$$

The operators $\frac{D_i}{dt}$ are called "wave derivatives" and the method is a generalization of the familiar method of characteristics

for the one dimensional time dependent problem.

We will have use for the following results obtained in Freeman and Baer

$$\left.\begin{aligned} u &= \frac{(A_1 + A_3) + (A_2 + A_4)}{4}, \\ v &= \frac{(A_1 + A_3) - (A_2 + A_4)}{4}, \\ 2c &= \frac{(A_1 + A_2) - (A_3 + A_4)}{4}. \end{aligned}\right\} \qquad \text{(VII-10)}$$

$$\left.\begin{aligned} A_1 &= \frac{(A_1 + A_3)}{4} + \frac{(A_1 + A_2) - (A_3 + A_4)}{4}, \\ A_2 &= \frac{(A_2 + A_4)}{2} + \frac{(A_1 + A_2) - (A_3 + A_4)}{4}, \\ A_3 &= \frac{(A_1 + A_3)}{2} - \frac{(A_1 + A_2) - (A_3 + A_4)}{4}, \\ A_4 &= \frac{(A_2 + A_4)}{2} - \frac{(A_1 + A_2) - (A_3 + A_4)}{4}, \end{aligned}\right\} \qquad \text{(VII-11)}$$

We will replace the system (VII-8) by a system of difference equations and will define subregions $R(n \Delta t)$, $n = 0, 1, \ldots, M$, $M \Delta t = T$, of the domain D^* in which our computations will take place.

The region $R(0)$ will be defined by our initial conditions which will describe a solitary wave. We will assume that for points (x, y) outside of or on the boundary of the region $R(0)$,

$$\begin{cases} u(x,y,0) = v(x,y,0) = 0 \\ \eta(x,y,0) = 0 \end{cases}$$

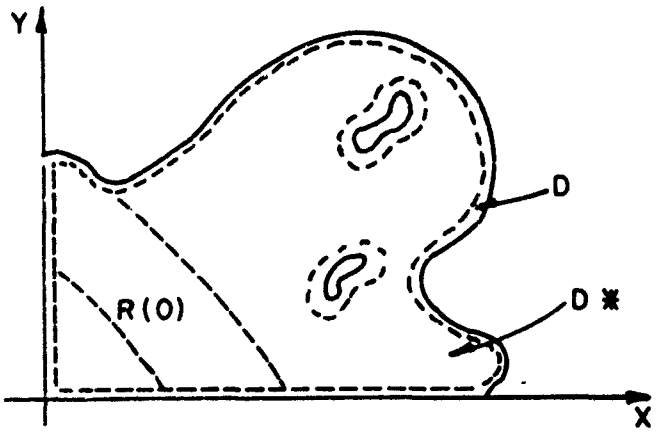

FIGURE VII-6
NOTATION FOR A NUMERICAL PROCEDURE
FOR NONLINEAR LONG WAVES

We define R(0) to be the set of all those points of our space grid which are contained in R(0) . We define $\overset{*}{R}(0)$ to be all those points of R(0) which are at a vertex of a square contained entirely in R(0) . Analagous definitions will be assumed for other regions in the x, y plane.

Let $P_{ij} = (x_i, y_j)$ and let

$$\left.\begin{aligned} V_1(u,v,c) &= (u+c, v+c), \\ V_2(u,v,c) &= (u+c, v-c), \\ V_3(u,v,c) &= (u-c, v-c), \\ V_4(u,v,c) &= (u-c, v+c), \end{aligned}\right\} \qquad \text{(VII-12)}$$

Also let

$$\left.\begin{aligned} \tilde{u}^0_{ij} &= u(x_i, y_j, 0), \\ \tilde{v}^0_{ij} &= v(x_i, y_j, 0), \\ \tilde{\eta}^0_{ij} &= \eta(x_i, y_j, 0), \end{aligned}\right\} \qquad \text{(VII-13)}$$

for points $(x_i, y_j) \in \overset{*}{R}(0)$. For all other points of the lattice in D^*, define all of these quantities to be equal to zero. Extend the values of $\tilde{u}^0_{ij}, \tilde{v}^0_{ij}, \tilde{\eta}^0_{ij}$ to all points of the piecewise rectangular region determined by $\overset{*}{R}(0)$ by linear interpolation. The extended functions $\tilde{u}^0(x,y), \tilde{v}^0(x,y), \tilde{\eta}^0(x,y)$ will then be continuous on the piecewise rectangular region determined by $\overset{*}{R}(0)$.

Define $\dot{R}(\Delta t)$ to be all those points of P_{ij} of $\dot{D}^*$ which satisfy the requirements that the points

$$P^{*\ell}_{ij} = P_{ij} - V_\ell(\tilde{u}^0_{ij}, \tilde{v}^0_{ij}, \tilde{c}^0_{ij})\Delta t, \quad \ell = 1, \ldots\ldots\ldots, 4, \qquad \text{(VII-14)}$$

are in the piecewise rectangular region determined by $\overset{*}{R}(0)$. Define $R^*(\Delta t)$ to be the set of all points of $\dot{R}(\Delta t)$ which are at the vertex of a square contained entirely in D^*

For those points $P_{ij} \in R^*(\Delta t)$ we can solve the system of difference equations

$$\left.\begin{aligned}
\tilde{A}'_{1ij} + \tilde{A}'_{2ij} &= \Delta t \left[\alpha_{ij} - 2E_x(\tilde{u}^\circ_{ij}, \tilde{v}^\circ_{ij}, \tilde{c}^\circ_{ij})\right] + \tilde{A}^\circ_1(P^{*1}_{ij}) + \tilde{A}^\circ_2(P^{*2}_{ij}), \\
\tilde{A}'_{3ij} + \tilde{A}'_{4ij} &= \Delta t \left[\alpha_{ij} - 2E_x(\tilde{u}^\circ_{ij}, \tilde{v}^\circ_{ij}, \tilde{c}^\circ_{ij})\right] + \tilde{A}^\circ_3(P^{*3}_{ij}) + \tilde{A}^\circ_4(P^{*4}_{ij}), \\
\tilde{A}'_{1ij} + \tilde{A}'_{3ij} &= \Delta t \left[(\alpha_{ij} + \beta_{ij}) - 2\left\{E_x(\tilde{u}^\circ_{ij}, \tilde{v}^\circ_{ij}, \tilde{c}^\circ_{ij}) + E_y(\tilde{u}^\circ_{ij}, \tilde{v}^\circ_{ij}, \tilde{c}^\circ_{ij})\right\}\right] + \tilde{A}^\circ_1(P^{*1}_{ij}) + \tilde{A}^\circ_3(P^{*3}_{ij}), \\
\tilde{A}'_{2ij} + \tilde{A}'_{4ij} &= \Delta t \left[(\alpha_{ij} - \beta_{ij}) - 2\left\{E_x(\tilde{u}^\circ_{ij}, \tilde{v}^\circ_{ij}, \tilde{c}^\circ_{ij}) - E_y(\tilde{u}^\circ_{ij}, \tilde{v}^\circ_{ij}, \tilde{c}^\circ_{ij})\right\}\right] + \tilde{A}^\circ_2(P^{*2}_{ij}) + \tilde{A}^\circ_4(P^{*4}_{ij}),
\end{aligned}\right\} \quad \text{(VII-15)}$$

where

$$\left.\begin{aligned}
\alpha_{ij} &= 2g\,\frac{\delta d(P_{ij})}{\delta x}, \\
\beta_{ij} &= 2g\,\frac{\delta d(P_{ij})}{\delta y}, \\
\tilde{A}^\circ_{1ij} &= \tilde{u}^\circ_{ij} + \tilde{v}^\circ_{ij} + 2\tilde{c}^\circ_{ij}, \\
\tilde{A}^\circ_{2ij} &= \tilde{u}^\circ_{ij} - \tilde{v}^\circ_{ij} + 2\tilde{c}^\circ_{ij}, \\
\tilde{A}^\circ_{3ij} &= \tilde{u}^\circ_{ij} + \tilde{v}^\circ_{ij} - 2\tilde{c}^\circ_{ij}, \\
\tilde{A}^\circ_{4ij} &= \tilde{u}^\circ_{ij} - \tilde{v}^\circ_{ij} - 2\tilde{c}^\circ_{ij},
\end{aligned}\right\} \quad \text{(VII-16)}$$

and the quantities $\tilde{A}^\circ_\ell(P)$ are the continuous extensions of $\tilde{A}^\circ_{\ell ij}$ to the piecewise rectangular region determined by $R^*(0)$. The quantities $\tilde{u}'_{ij}$, $\tilde{v}'_{ij}$, $\tilde{c}'_{ij}$, and $\tilde{A}'_{1ij}, \tilde{A}'_{2ij}, \tilde{A}'_{3ij}, \tilde{A}'_{4ij}$ may now be respectively determined from Eqs. (VII-10) and (VII-11) and all of these can be extended by linear interpolation to functions $\tilde{u}'(P), \tilde{v}'(P), \tilde{c}'(P), \tilde{A}'_1(P), \tilde{A}'_2(P), \tilde{A}'_3(P), \tilde{A}'_4(P)$ continuous on the piecewise rectangular region determined by $R^*(\Delta t)$

The general algorithm for continuing our computations is now obvious, but we will state it for the sake of completeness.

Assume that the quantities $\tilde{u}^k_{ij}, \ldots\ldots\ldots\ldots, \tilde{A}^k_{4ij}$ have been found for points in the region $R^*(k\Delta t)$ and have been extended by linear interpolation to the functions $\tilde{u}^k_{ij}(P), \ldots\ldots\ldots\ldots, \tilde{A}^k_{4ij}(P)$ continuous on the piecewise rectangular region determined by $R^*(k\Delta t)$. For points P_{ij} of D^* which are not in $R^*(k\Delta t)$, the values $\tilde{u}^k_{ij}, \ldots\ldots, \tilde{A}^k_{4ij}$ are to be obtained by setting $\tilde{u}^k_{ij} = \tilde{v}^k_{ij} = \tilde{n}^k_{ij} = 0$. Define $\dot{R}\left((k+1)\Delta t\right)$ to be all those points P_{ij} of D^* which satisfy the requirements that the points

$$P^*_{ij\ell} = P_{ij} - V_\ell\,(\tilde{u}^k_{ij}, \tilde{v}^k_{ij}, \tilde{c}^k_{ij})\,\Delta t, \ell = 1, \ldots, 4, \qquad \text{(VII-17)}$$

are in the piecewise rectangular region determined by $\overset{*}{R}(k\Delta t)$. Define $\overset{*}{R}\left((k+1)\Delta t\right)$ to be the set of all those points of $\dot{R}\left((k+1)\Delta t\right)$ which are at a vertex of a square contained entirely in D^*.

For those points $P_{ij} \in R^*(k+1)\Delta t)$ we can solve the system of difference equations

$$\begin{aligned}
&\tilde{A}^{k+1}_{1ij} + \tilde{A}^{k+1}_{2ij} = \Delta t\left[\alpha_{ij} - 2E_x(\tilde{u}^k_{ij}, \tilde{v}^k_{ij}, \tilde{c}^k_{ij})\right] + \tilde{A}^k_1(P^{*1}_{ij}) + \tilde{A}^k_2(P^{*2}_{ij}),\\
&\tilde{A}^{k+1}_{3ij} + \tilde{A}^{k+1}_{4ij} = \Delta t\left[\alpha_{ij} - 2E_x(\tilde{u}^k_{ij}, \tilde{v}^k_{ij}, \tilde{c}^k_{ij})\right] + \tilde{A}^k_3(P^{*3}_{ij}) + \tilde{A}^k_4(P^{*4}_{ij}),\\
&\tilde{A}^{k+1}_{1ij} + \tilde{A}^{k+1}_{3ij} = \Delta t\left[(\alpha_{ij} + \beta_{ij}) - 2\left\{E_x(\tilde{u}^k_{ij}, \tilde{v}^k_{ij}, \tilde{c}^k_{ij})\right.\right.\\
&\left.\left. + E_y(\tilde{u}^k_{ij}, \tilde{v}^k_{ij}, \tilde{c}^k_{ij})\right\}\right] + \tilde{A}^k_1(P^{*1}_{ij}) + \tilde{A}^k_3(P^{*3}_{ij}),\\
&\tilde{A}^{k+1}_{2ij} + \tilde{A}^{k+1}_{4ij} = \Delta t\left[(\alpha_{ij} - \beta_{ij}) - 2\left\{E_x(\tilde{u}^k_{ij}, \tilde{v}^k_{ij}, \tilde{c}^k_{ij})\right.\right.\\
&\left.\left. - E_y(\tilde{u}^k_{ij}, \tilde{v}^k_{ij}, \tilde{c}^k_{ij})\right\}\right] + \tilde{A}^k_2(P^{*2}_{ij}) + \tilde{A}^k_4(P^{*4}_{ij}).
\end{aligned} \qquad \text{(VII-18)}$$

The quantities $\tilde{u}_{ij}^{k+1}, \ldots, \tilde{A}_{4ij}^{k+1}$ can now be determined from Eq. (VII-10) and Eq. (VII-11) and all of these can be extended by linear interpolation to functions $\tilde{u}^{(k+1)}(P), \ldots, \tilde{A}_4^{(k+1)}(P)$ continuous on the piecewise rectangular region determined by $\overset{*}{R}\left((k+1)\Delta t\right)$ The algorithm is now completely defined and the computations are iterated M times until the final time $M\Delta t = T$ is obtained.

LIST OF SYMBOLS

x, y	horizontal coordinates
u	particle velocity along the x-axis
v	Particle velocity along the y-axis
t	time variable
c	$\sqrt{g\,(d+\eta)}$
g	gravity acceleration
d	water depth
η	free surface elevation around the still water level
h	$d+\eta$
c_o	$\sqrt{g\,d}$
E_x	friction force component in the x direction
E_y	friction force component in the y direction
θ	angle of a nearby u vector with the u vector with which we are working
V	bore velocity
sub $_b$	relative to the bore characteristics
h	friction coefficient
ϵ	$3c - 2c_o$
e	preassigned positive number
D_i, D_t	wave derivatives operator
A	$u \mp v \mp 2c$
n	integer
D^*	domain
R	subregion of domain D^*

National Engineering Science Co., Pasadena, California. INVESTIGATION OF LONG WAVES AND THEIR EFFECTS ON THE COASTAL AND HARBOR ENVIRONMENT OF THE LOWER CHESAPEAKE BAY, by NESCO Staff, Vol. II UNCLASSIFIED, NESCO Tech. Rept. No. SN-93, Contract No. DA-49-146-XZ-151.

Appendix I: Long Waves Generated by Nuclear Explosions. Type of Waves and Initial Decay in Deep Water.
Appendix II: Water Waves Produced by Explosions.
Appendix III: Surface Waves Generated by Disturbance on Sea Bed in Constant Depth Open Sea
Appendix IV: The Principle of Superposition and the Theory of Cauchy-Poisson.
Appendix V: Long Waves and Breakers Over the Continental Shelf.
Appendix VI: The Wave Run-up by the Method of Characteristics.
Appendix VII: Two-Dimensional Nonlinear Wave Motion in an Estuary.

UNCLASSIFIED

1. Hydrodynamics of Waves
2. Underwater Explosion
3. Tsunami Waves
4. Wave Run-up

I. Wilson, Basil W.
II. Armijo, L. and Noser, M. A.
III. Hendrickson, J. A.
IV. Le Mehaute, B.
V. Le Mehaute, B.
VI. Le Mehaute, B.
VII. Freeman, J. C., Armijo, L., Noser, M. A.

UNCLASSIFIED

National Engineering Science Co., Pasadena, California. INVESTIGATION OF LONG WAVES AND THEIR EFFECTS ON THE COASTAL AND HARBOR ENVIRONMENT OF THE LOWER CHESAPEAKE BAY, by NESCO Staff, Vol. II UNCLASSIFIED, NESCO Tech. Rept. No. SN-93, Contract No. DA-49-146-XZ-151.

Appendix I: Long Waves Generated by Nuclear Explosions. Type of Waves and Initial Decay in Deep Water.
Appendix II: Water Waves Produced by Explosions.
Appendix III: Surface Waves Generated by Disturbance on Sea Bed in Constant Depth Open Sea
Appendix IV: The Principle of Superposition and the Theory of Cauchy-Poisson.
Appendix V: Long Waves and Breakers Over the Continental Shelf.
Appendix VI: The Wave Run-up by the Method of Characteristics.
Appendix VII: Two-Dimensional Nonlinear Wave Motion in an Estuary.

UNCLASSIFIED

1. Hydrodynamics of Waves
2. Underwater Explosion
3. Tsunami Waves
4. Wave Run-up

I. Wilson, Basil W.
II. Armijo, L. and Noser, M. A.
III. Hendrickson, J. A.
IV. Le Mehaute, B.
V. Le Mehaute, B.
VI. Le Mehaute, B.
VII. Freeman, J. C., Armijo, L., Noser, M. A.

UNCLASSIFIED

National Engineering Science Co., Pasadena, California. INVESTIGATION OF LONG WAVES AND THEIR EFFECTS ON THE COASTAL AND HARBOR ENVIRONMENT OF THE LOWER CHESAPEAKE BAY, by NESCO Staff, Vol. II UNCLASSIFIED, NESCO Tech. Rept. No. SN-93, Contract No. DA-49-146-XZ-151.

Appendix I: Long Waves Generated by Nuclear Explosions. Type of Waves and Initial Decay in Deep Water.
Appendix II: Water Waves Produced by Explosions.
Appendix III: Surface Waves Generated by Disturbance on Sea Bed in Constant Depth Open Sea
Appendix IV: The Principle of Superposition and the Theory of Cauchy-Poisson.
Appendix V: Long Waves and Breakers Over the Continental Shelf.
Appendix VI: The Wave Run-up by the Method of Characteristics.
Appendix VII: Two-Dimensional Nonlinear Wave Motion in an Estuary.

UNCLASSIFIED

1. Hydrodynamics of Waves
2. Underwater Explosion
3. Tsunami Waves
4. Wave Run-up

I. Wilson, Basil W.
II. Armijo, L. and Noser, M. A.
III. Hendrickson, J. A.
IV. Le Mehaute, B.
V. Le Mehaute, B.
VI. Le Mehaute, B.
VII. Freeman, J. C., Armijo, L., Noser, M. A.

UNCLASSIFIED